The role of primary cilia and sonic hedgehog signalling in adrenal development function.

Cogger, Kathryn

THE ROLE OF PRIMARY CILIA AND SONIC HEDGEHOG SIGNALLING IN ADRENAL DEVELOPMENT AND FUNCTION

Kathryn Cogger

A thesis submitted to Queen Mary, University of London for the degree of Doctor of Philosophy

August 2012

Centre for Endocrinology
William Harvey Research Institute
Barts and The London School of Medicine and Dentistry
Queen Mary University of London

ABSTRACT

Primary cilia are sensory organelles found on most vertebrate cells during interphase. They play key roles in development, cell signalling and cancer, and are involved in signal transduction pathways such as Hh and Wnt signalling. The adrenal cortex produces steroid hormones essential for controlling homeostasis and mediating the stress response. Signalling pathways involved in the process of its development and differentiation are still being identified but include Hh and Wnt, and adrenal development is thus likely to require cilia.

I have demonstrated that inhibiting cilia formation, using siRNA targeted to different ciliary components, results in reduced differentiation of the human adrenal carcinoma cell line H295R towards a zona glomerulosa (zG)-like phenotype. These data suggest that primary cilia play a key role in adrenal differentiation, but which signalling pathways are involved still remains unclear. I have also discovered that adrenals from Bardet-Biedl syndrome (BBS) mice, the most prominently studied ciliopathy, have thin capsules, the proposed adrenal stem cell niche, and abnormal histology, while zebrafish embryos injected with morpholinos targeting BBS genes show delayed and reduced expression of ff1b, a marker of interrenal tissue. These data further suggest a role for primary cilia in adrenal development and maintenance.

These studies are the foundation for elucidating the role of primary cilia in the development and function of the adrenal gland, and furthering our understanding of adrenocortical development. This promises to lead to improved management of adrenal dysfunction, and demonstrating that adrenal defects are a characteristic of ciliopathies will potentially inform new strategies for patient care.

ACKNOWLEDGEMENTS

First and foremost I would like to thank my supervisor Dr Peter King for his guidance, support and advice during the course of my PhD. I am especially grateful for the benefit of his experience and suggestions in the preparation of this thesis.

I would like to thank Dr Paul Chapple for his help and encouragement throughout my PhD, and Dr Leonardo Guasti for his expertise in laboratory techniques. My gratitude also extends to my panel of advisors, Dr Martin Knight and Professor Mike Philpott, for their useful and valuable suggestions about the project.

I thank Dr Vincent Marion and Professor Phil Beales for providing the BBS knockout mice, and Dr Rachel Ashworth and Dr Caroline Brennan for their assistance with the collection of zebrafish data. I would also like to acknowledge Dr Wesley Harrison for his help with the FACS analysis, and the Queen Mary Genome Centre for their sequencing and Taqman qPCR services.

Thank you to all my colleagues in the department of Endocrinology for making it a fun and enjoyable place to work, and for the unforgettable memories over the last four years.

The work of this thesis would not have been possible without the generous financial support of the Medical Research Council, to whom I am most grateful.

Finally I would like to thank my friends for their patience and constant encouragement, and my family for their unconditional love and for being so incredibly supportive. I am particularly appreciative for the help and hard work of my parents over the last 26 years, and I hope that I can make them proud.

STATEMENT OF ORIGINALITY

I hereby certify that I am the sole author of this thesis and that to the best of my knowledge, my thesis does not infringe upon anyone's copyright nor violate any proprietary rights and that any ideas, techniques, quotations, or any other material from the work of other people included in my thesis, published or otherwise, are fully acknowledged in accordance with the standard referencing practices. All data was generated by myself except where stated. This thesis has not been submitted for a higher degree to any other University or Institution.

TABLE OF CONTENTS

CHAPTER 1: INTRODUCTION 18

1.1 The Adrenal Gland 19

1.1.1 Steroidogenesis 20

1.1.2 The stress system, HPA axis, and RAA system 21

1.1.3 Cortisol, aldosterone and adrenal androgens 26

1.2 Development of the adrenal glands 27

1.2.1 Organogenesis and zonation 27

1.2.2 Signalling pathways 29

1.2.3 Adrenocortical stem/progenitor cells 34

1.2.4 Adrenal dysregulation 36

1.3 Adrenal cell lines 39

1.4 Shh signalling 41

1.4.1 Hh proteins 41

1.4.2 Signalling components 42

1.4.3 Agonists and Antagonists 45

1.4.4 Hh signalling in the adrenal 45

1.5 Primary Cilia 47

1.5.1 IFT 49

1.5.2 Signalling pathways 50

1.6 Nonmotile Ciliopathies 51

1.6.1 Bardet-Biedl Syndrome 52

1.7 Zebrafish 53

1.7.1 Corticosteroids 54

1.7.2 Signalling pathways and transcription factors 55
1.7.3 Hh signalling and primary cilia 57
1.8 Aims of the project 59
CHAPTER 2: MATERIALS AND METHODS 60
2.1 Cell culture 61
2.1.1 Trypsinisation 61
2.1.2 Freezing down cells 61
2.1.3 Counting cells – Haemocytometer 62
2.2 Differentiation 63
2.3 RNA Extraction 63
2.3.1 DNase treatment 63
2.3.2 Phenol extraction 64
2.3.3 RNA precipitation 64
2.4 First strand cDNA synthesis 64
2.5 Polymerase chain reaction 65
2.5.1 Gel electrophoresis 66
2.5.2 Primers, probes and siRNA sequences 67
2.5.3 Gel purification 69
2.6 Real-time qPCR 70
2.6.1 $SYBR_{GREEN}$ I 70
2.6.2 Taqman 72
2.7 Transfections 73
2.7.1 siRNA transfections 73
2.7.2 Dual-Luciferase reporter transfections 74
2.8 Dual-Luciferase reporter assay 74

2.9 Shh Light II luciferase reporter assay 75
2.10 Enzyme-Linked Immunosorbent Assay (ELISA) 76
2.10.1 Aldosterone and Cortisol 76
2.10.2 Corticosterone 76
2.11 Cytotoxicity assays 77
2.11.1 Lactate dehydrogenase (LDH) 77
2.11.2 Fluorescence-activated cell sorting (FACS) 78
2.12 Protein Analysis 78
2.12.1 Western Blot 78
2.13 Cytology 79
2.13.1 Fixation 79
2.13.2 Immunofluorescence 80
2.13.3 Counting and measuring cilia 80
2.13.4 3βHSD Assay 81
2.14 Histology 81
2.14.1 Paraffin embedding 81
2.14.2 Sectioning and Mounting 82
2.14.3 Deparaffinisation 82
2.14.4 Haematoxylin & Eosin staining 82
2.14.5 DAPI staining to quantify capsule density 83
2.14.6 Immunoperoxidase staining 83
2.15 Zebrafish 84
2.15.1 Microinjection 84
2.15.2 Immunofluorescence 85
2.15.3 Counting and measuring cilia 86

2.15.4 Whole mount ISH 86
2.16 Data Analysis 87
CHAPTER 3: ESTABLISHING AN *IN VITRO* SYSTEM 88
3.1 Aims 89
3.2 H295R cells express components of the Hh pathway and have primary cilia 89
3.3 Hh pathway agonists and antagonists 92
3.4 Differentiation of H295R cells 100
3.5 Discussion 103
CHAPTER 4: THE ROLE OF PRIMARY CILIA IN THE DIFFERENTIATION OF H295R CELLS 110
4.1 Aims 111
4.2 The effects of siRNA on ciliation 111
4.3 Cilia are required for zG-like differentiation 114
4.4 The effects of ShhN on differentiation 118
4.5 Wnt signalling 123
4.6 Discussion 126
CHAPTER 5: *IN VIVO* MODELS 134
5.1 Aims 135
5.2 Part A - BBS Mice 135
5.2.1 BBS adrenals have reduced capsule density 135
5.2.2 BBS12 null mice have increased serum corticosterone following synacthen testing compared to wild-type mice 141
5.3 Part B - Zebrafish 142
5.3.1 Survival and initial observations 142
5.3.2 Specific morpholino phenotypes 143

5.3.3 Ff1b expression 148

5.4 Discussion 152

CHAPTER 6: GENERAL DISCUSSION 158

REFERENCES 163

TABLE OF FIGURES

CHAPTER 1: INTRODUCTION

Figure 1.1.1 – The human adrenal gland 20

Figure 1.1.2 – Human adrenal steroidogenesis 21

Figure 1.1.3 – The Stress System 25

Figure 1.2.1 – Adrenal development 29

Figure 1.2.2 – The Wnt signalling pathway 33

Figure 1.4.1 – Schematic diagram of the mammalian Hh pathway 44

Figure 1.4.2 – Primary cilia and Hh signalling 45

Figure 1.5.1 – Schematic representation of a primary cilium 48

Figure 1.7.1 – Schematic diagram depicting interrenal development in the zebrafish 57

CHAPTER 2: MATERIALS AND METHODS

Figure 2.1.1 – Haemocytometer Grid 62

CHAPTER 3: ESTABLISHING AN *IN VITRO* SYSTEM

Figure 3.2.1 – H295R cells express components of the Hh pathway 90

Figure 3.2.2 – H295R cells can form primary cilia 92

Figure 3.3.1 – Shh Light II luciferase assay 94

Figure 3.3.2 – Gli1 mRNA expression 95

Figure 3.3.3 – Cytotoxicity of Hh pathway agonists and antagonists 98

Figure 3.4.1 – Differentiation of H295R cells 102

CHAPTER 4: THE ROLE OF PRIMARY CILIA IN THE DIFFERENTIATION OF H295R CELLS

Figure 4.2.1 – Knockdown of ciliary components in H295R cells 113

Figure 4.2.2 – The effects of siRNA on ciliation 114

Figure 4.3.1 – The effects of siRNA on differentiation 117

Figure 4.4.1 – Gli1 mRNA expression in differentiating H295R cells 118

Figure 4.4.2 – The effects of ShhN on differentiation 120
Figure 4.4.3 – AT1 promoter activity and mRNA expression 122
Figure 4.4.4 – CYP11B2 luciferase assay 123
Figure 4.5.1 – Wnt signalling in H295R cells 125

CHAPTER 5: *IN VIVO* MODELS

Figure 5.2.1 – CYP11A1 and CYP11B1 expression in BBS adrenals 136
Figure 5.2.2 – Adrenal histology 138
Figure 5.2.3 – Capsule density of BBS adrenals 139
Figure 5.2.4 – Corticosterone ELISA 141
Figure 5.3.1 – Initial observations and survival rate 143
Figure 5.3.2 – Classification of morpholino phenotypes 144
Figure 5.3.3 – The effects of morpholinos on ciliation 147
Figure 5.3.4 – The effects of morpholinos on ff1b expression 150

TABLE OF TABLES

CHAPTER 2: MATERIALS AND METHODS

Table 2.5.1 – Sequences.....67
Table 2.7.1 – Quantities used for transfection 73
Table 2.12.1 – Antibodies used for western blotting 79
Table 2.13.1 – Antibodies used for immunofluorescence 80
Table 2.14.1 – Antibodies used in immunoperoxidase staining 84
Table 2.15.1 – Morpholino sequences.....85
Table 2.15.2 – Antibodies used for zebrafish immunofluorescence 86

LIST OF ABBREVIATIONS

11β-HSD1	11β-hydroxysteroid dehydrogenase type 1
11β-HSD2	11β-hydroxysteroid dehydrogenase type 2
3βHSD	3β-hydroxysteroid dehydrogenase
ACAs	Adrenocortical adenomas
ACCs	Adrenocortical carcinomas
ACE	Angiotensin-converting enzyme
ACTH	Adrenocorticotropic hormone
ACTs	Adrenocortical tumours
AHC	Adrenal hypoplasia congenital
ALMS	Alstrom syndrome
AngII	Angiotensin II
ANOVA	Analysis of variance
APC	Adenomatous polyposis coli
ARL	ADP-ribosylation factor-like protein
AT1	Angiotensin II receptor type 1
AT1b	Rat angiotensin II receptor type 1
ATP	Adenosine triphosphate
AVP	Arginine vasopressin
b5	Cytochrome b5
BBS	Bardet-Biedl syndrome
Boc	Brother of Cdo
CaMK	Calmodulin dependent protein kinases
cAMP	Cyclic adenosine monophosphate
Cdo	CAM-related/down-regulated by oncogenes
CEP290	Centrosomal protein of 290 kDa
Ci	*Cubitus interruptus*
Cited2	CREB-binding protein/p300-interacting transactivator, with ED-rich tail, 2
CK1	Casein kinase 1
CRH	Corticotrophin-releasing hormone
CSCs	Cancer stem cells
ctrl	Control
CYP11A1	Cytochrome P450 side chain cleavage/$P450_{SCC}$
CYP11B1	11β-hydroxylase
CYP11B2	Aldosterone synthase
CYP17	Cytochrome P450 17α hydroxylase/17,20 lyase
CYP21	21α-hydroxylase
Daam1	Dishevelled associated activator of morphogenesis 1
DAB	3, 3'-diaminobenzidine
DAG	1,2-diacylglycerol

DAPI	4’,6-diamidino-2-phenylindole
Dax1	Dosage-sensitive sex-reversal adrenal hypoplasia congenita on the X chromosome, gene 1
DHEA	Dehydroepiandrosterone
DHEAS	Dehydroepiandrosterone sulphate
Dhh	Desert hedgehog
DIG	Digoxigenin
DMEM	Dulbecco’s modified eagles medium
DMSO	Dimethyl sulfoxide
DNA	Deoxyribonucleic acid
dNTPs	Deoxynucleoside triphosphates
DOC	11-deoxycoticosterone
DPBS	Dulbecco’s phosphate buffered saline
dpf	Days post fertilisation
Dsh	Dishevelled
DTT	Dithiothreitol
E9	Embryonic day 9
EDTA	Ethylenediaminetetraacetic acid
ELISA	Enzyme-linked immunosorbent assay
ENaC	Epithelial sodium channel
Erk1/2	Extracellular-signal-regulated kinase 1/2
EVC	Ellis Van Creveld
Ewk4	Embryonic week 4
FACS	Fluorescence-activated cell sorting
FAM	6-carboxyfluorescein
FBS	Foetal bovine serum
ff1b	Fushi tarazu-F1 β
ff1d	Fushi tarazu-F1 δ
FGD	Familial glucocorticoid deficiency
FRET	Fluorescence resonance energy transfer
FSH	Follicle-stimulating hormone
Fsk	Forskolin
Fz	Frizzled
Gas1	Growth arrest-specific protein 1
GFP	Green fluorescent protein
Gli	Glioma-associated, krupple family member
GliA	Gli activator
GliR	Gli repressor
GnRH	Gonadotropin-releasing hormone
GOI	Gene of interest
GPCR	G-protein coupled receptor
GR	Glucocorticoid receptor
GRE	Glucocorticoid-response elements

GSK3β	Glycogen synthase kinase 3β
HDL	High-density lipoprotein
HEPES	4-(2-hydroxyethyl)-1-piperazineethanesulfonic acid
Hh	Hedgehog
Hh-C	Hedgehog carboxy terminal fragment
Hh-N	Hedgehog amino terminal fragment
HPA	Hypothalamic-pituitary-adrenal
hpf	Hours post fertilisation
HRP	Horseradish peroxidase
hsp90	Heat shock protein 90
IFN-γ	Interferon-γ
IFT	Intraflagellar transport
IGF2	Insulin-like growth factor 2
Ihh	Indian hedgehog
IL-12	Interleukin-12
Ins(1,4,5)*P*3	Inositol 1,4,5-trisphosphate
ITS	Insulin, transferrin and sodium selenite
JATD	Jeune asphyxiating thoracic dystrophy
JBTS	Joubert syndrome
JNK	Jun N-terminal kinase
Kif7	Kinesin family member 7
KO	Knockout
LAF_1	Long after far-red light 1
LCA	Leber congenital amaurosis
LDH	Lactate dehydrogenase
LEF	Lymphoid enhancer-binding factor
LH	Leutinising hormone
LRP5/6	Low-density-lipoprotein-related protein5/6
MC2R	Melanocortin receptor 2
Mek1/2	Mitogen-activated protein kinase kinase 1/2
MIP	Maximum intensity projection
MKS	Meckel syndrome
MMLV	Moloney murine leukemia virus
MO	Morpholino
MOPS	3-(N-morpholino)propanesulfonic acid
MR	Mineralocorticoid receptor
MRAP	Melanocortin receptor accessory protein
MZovl	Maternal zygotic oval
NAD^+	Nicotinamide adenine dinucleotide
NBT	Nitroblue Tetrazolium
NPHP	Nephronophthisis
NTC	No template control
OD	Optical density

OFD 1	Oral-facial-digital type 1
P5	5 days postpartum
PBS	Phosphate buffered saline
PC2	Polycystin 2
PCP	Planar cell polarity
PCR	Polymerase chain reaction
PDGF	Platelet derived growth factor
PDGFRα	Platelet derived growth factor receptor α
PFA	Paraformaldehyde
PI	Propidium iodide
PI3C	Phosphoinositidase C
PKA	Protein kinase A
PKC	Protein kinase C
PKD	Polycystic kidney disease
POMC	Pro-opiomelanocortin
POR	NADPH cytochrome P450 oxidoreductase
PREF1	Preadipocyte factor 1
Ptch	Patched
PtdIns(4,5)*P*2	Phosphatidylinositol 4,5-bisphosphate
PTU	Propylthiouracil
qPCR	Quantitative polymerase chain reaction
RAA	Renin-angiotensin-aldosterone
RNA	Ribonucleic acid
RND	Resistance, nodulation, cell division
ROCK	Rho-associated kinase
SAG	Smoothened agonist
Sant1	Smoothened antagonist 1
SCID	Severe combined immunodeficiency
SDS PAGE	Sodium dodecyl sulfate polyacrylamide gel electrophoresis
SERKAL	Sex reversion, kidneys, adrenal and lung dysgenesis
SF-1	Steroidogenic factor-1
Shh	Sonic hedgehog
ShhN	Recombinant mouse sonic hedgehog N-terminus
siRNA	Small interfering RNA
Smo	Smoothened
SNLS	Senior-Loken syndrome
SPOP	Speckle-type PDZ protein
SSC	Sodium saline citrate
StAR	Steroidogenic acute regulatory protein
SuFu	Suppressor of fused
SULT2A1	Sulphonyltransferase
TAE	Tris-acetate-ethylenediamenetetraacetic acid
TAMRA	Tetramethylrhodamine

Taq	*Thermus aquaticus*
TCF	T-cell factor
TESPA	3-triethoxysilylpropylamine
TNF-α	Tumour necrosis factor-α
TPR	Tetratricopeptide repeats
UT	Untreated
Wnt	Wingless-related mouse mammary tumour virus integration site
WT	Wild-type
WT1	Wilms' tumour 1
zF	Zona fasciculata
zG	Zona glomerulosa
zR	Zona reticularis
zU	Undifferentiated zone
β-cat	β-catenin
βNAD	β nicotinamide adenine dinucleotide hydrate
βTrCP	β-transducing repeat-containing protein

CHAPTER 1: INTRODUCTION

1.1 The Adrenal Gland

The adrenal gland is a bilateral organ that sits on top of the kidneys and produces hormones essential to maintain everyday life. It has an outer cortex and inner medulla which are embryonically distinct tissues. The cortex is established from intermediate mesoderm, while the medulla arises from neuroectoderm.

The adrenal cortex, and its homologues, are essential for mediating the stress response and maintaining homeostasis, which they achieve by the production of steroid hormones. In humans, the cortex has 3 distinct concentric zones, named from outer to inner as the zona glomerulosa (zG), zona fasciculata (zF) and zona reticularis (zR) (Arnold, 1866; Rainey et al, 2004), and is surrounded by a mesenchymal capsule (Figure 1.1.1).

The zG and zF produce mineralocorticoids and glucocorticoids respectively, while the zR produces adrenal androgens in humans and primates. These zones can be characterised by their expression of specific steroidogenic enzymes required for the production of adrenal steroid hormones, by their responsiveness to specific peptide hormones (Keegan & Hammer, 2002), and are distinguishable morphologically and ultrastructurally (Vinson, 2003). The medulla is the innermost part of the adrenal gland, and forms part of the sympathetic nervous system, producing catecholamines that control heart rate and blood pressure during stress (Kempna & Fluck, 2008). Adrenal failure or insufficiency can lead to disrupted electrolyte balance, impaired carbohydrate metabolism, and in the most severe cases hypoglycaemic coma, and even death (Kempna & Fluck, 2008).

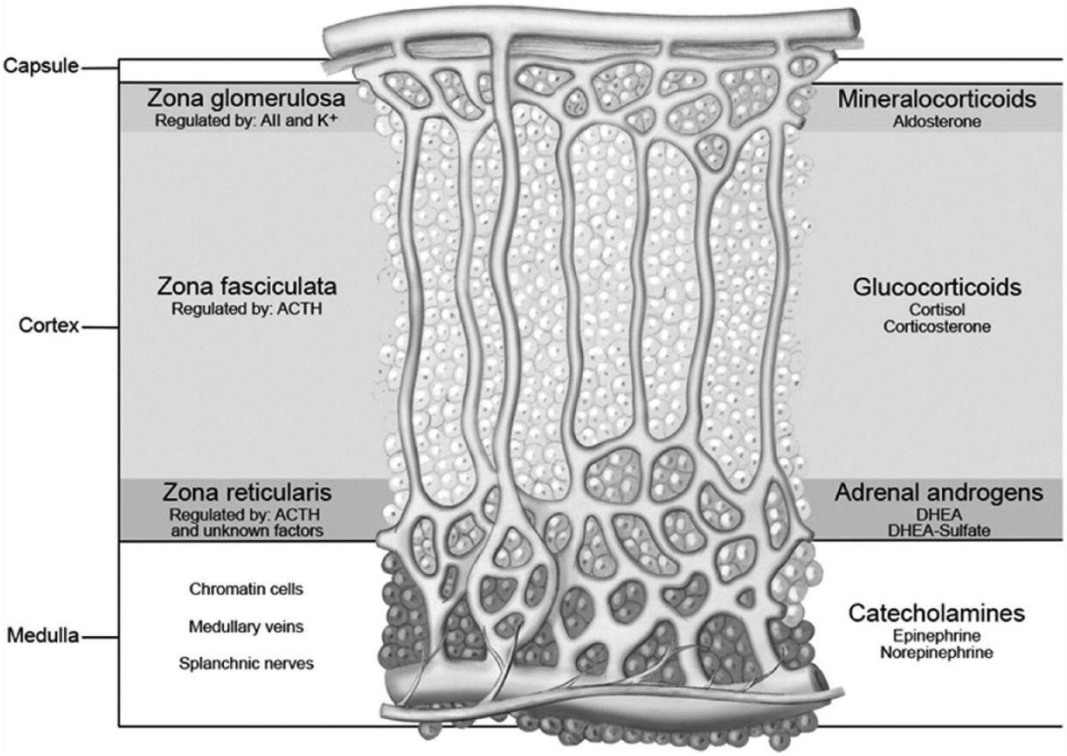

Figure 1.1.1 – The human adrenal gland (Wang & Rainey, 2012)
Diagram depicting the zones of the human adrenal gland and the steroid hormones they produce. AII; angiotensin II, ACTH; adrenocorticotropic hormone, DHEA; dehydroepiandrosterone.

1.1.1 Steroidogenesis

Steroidogenesis is a complex cascade of sequential enzymatic steps, starting with the principal precursor cholesterol, and resulting in the production of aldosterone, cortisol, and DHEA (dehydroepiandrosterone) in primates (Figure 1.1.2). The majority of steroidogenic cholesterol is obtained from high-density lipoproteins (HDLs) in the circulating blood plasma (Yaguchi et al, 1998), with only about 20% being synthesised de novo from acetate (Borkowski et al, 1967). HDL receptors have been shown to be expressed in the steroidogenic cells of human adrenal tissue (Liu et al, 2000).

Cholesterol is carried across the mitochondrial membrane by the transporter protein StAR (steroidogenic acute regulatory protein). This is the rate-limiting step of steroidogenesis and is closely followed by the conversion of cholesterol to pregnenolone, catalysed by the enzyme cytochrome P450 side chain cleavage (P450scc or CYP11A1). Pregnenolone is then transported from the mitochondria to the smooth endoplasmic reticulum, where the intermediate enzymatic steps occur. The final steps of steroid synthesis take place back in the mitochondria, where aldosterone synthase

(CYP11B2) and 11β-hydroxylase (CYP11B1) are located. CYP11B2 is required for the end point reaction resulting in aldosterone production in the zG, whereas CYP11B1 is involved in the hydroxylation of 11-deoxycortisol to produce cortisol in the zF (Gazdar et al, 1990; Simpson et al, 1992). As CYP11B1 is only expressed in the zF, and CYP11B2 in the zG, antibodies for these two enzymes can be used to visualise functional adrenal zonation (Ogishima et al, 1992). The expression of their mRNAs, or detection of the proteins themselves, can also be used to determine zonal identity.

As well as CYP11B1, CYP17 (cytochrome P450 c17) activity is essential for cortisol production in primates. CYP17 has both 17α-hydroxylase and 17,20 lyase activities. 17α-hydroxylase activity in the zF allows cortisol to be produced, while combining both 17α-hydroxylase and 17,20 lyase activities in the zR allows the synthesis of C_{19} androgens (Miller et al, 1997; Rainey et al, 2004; Staels et al, 1993). In rodents however, corticosterone is produced instead of cortisol and there are no adrenal androgens, as adult murine adrenals lack the enzyme CYP17, and therefore do not have a functional zR.

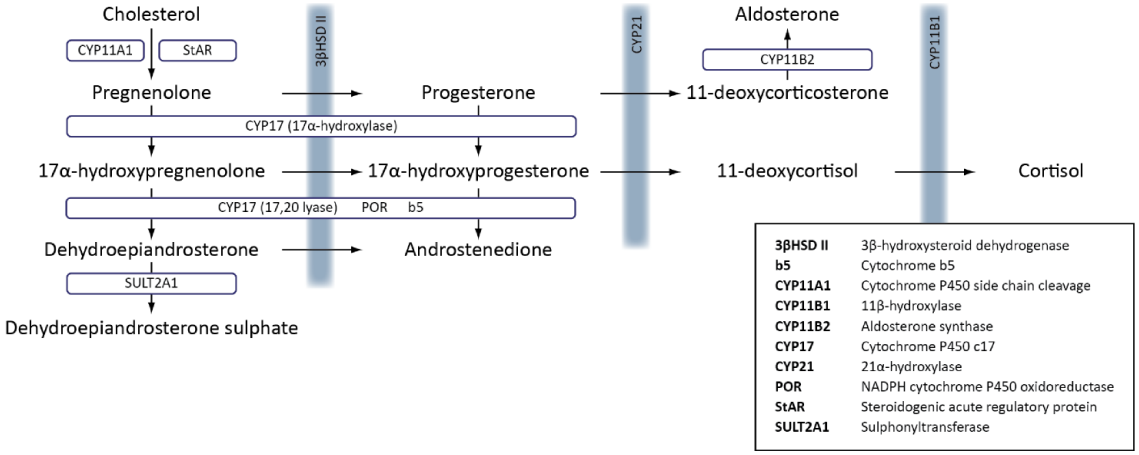

Figure 1.1.2 – Human adrenal steroidogenesis (Gazdar et al, 1990; Oskarsson et al, 2006; Rainey et al, 2002; Samandari et al, 2007)

1.1.2 The stress system, HPA axis, and RAA system

The stress response, first described by Hans Selye in 1936 (Selye, 1998), involves changes in behaviour, autonomic function, hormone secretion, and activation of the hypothalamic-pituitary-adrenal (HPA) axis and the renin-angiotensin-aldosterone

(RAA) system regardless of the type of stressor (Figure 1.1.3). It is designed to increase our chances of survival, but can be adapted over time with conditioning to either reinforce fears (stressors), or desensitise them.

Upon activation of the HPA axis, parvocellular neurons of the hypothalamic paraventricular nucleus synthesise and secrete corticotrophin-releasing hormone (CRH) and arginine vasopressin (AVP) into the hypophysial portal circulation (Carrasco & Van de Kar, 2003; Chrousos, 1995; Sapolsky et al, 2000; Van de Kar & Blair, 1999). CRH is the main regulator of the release of adrenocorticotropic hormone (ACTH), also known as corticotrophin, from the anterior lobe of the pituitary gland into the systemic circulation (Carrasco & Van de Kar, 2003; Levens, 1990). AVP has a synergistic role in helping CRH to cause ACTH release, however, it is ineffective in the absence of CRH (Chrousos, 1995). CRH neurons also stimulate ACTH production, as some of them project from the paraventricular nucleus of the hypothalamus onto pro-opiomelanocortin-containing neurons in the hypothalamic arcuate nucleus. They stimulate pro-opiomelanocortin (POMC) release, which is cleaved to form ACTH (Keegan & Hammer, 2002).

ACTH binds to MC2R (melanocortin receptor 2), a 7-transmembrane G-protein coupled receptor (GPCR), causing the α-subunit of the heterotrimeric G_s-protein to associate with adenylate cyclase. This catalyses the conversion of ATP to cAMP, and causes activation of downstream signalling pathways, including protein kinase A (PKA). PKA phosphorylates and activates cholesteryl ester hydrolases and StAR, increasing the amount of cholesterol delivered to the inner mitochondrial membrane. cAMP also induces the transcription of StAR and CYP11A1, and CYP17 to promote cortisol production (Aumo et al, 2010; Rainey et al, 2004).

Cortisol is the principal glucocorticoid produced by the zF of the human adrenal cortex, and has influential effects on metabolism, the cardiovascular system and the immune system. Although at basal levels it has a rather permissive role, allowing the effects of other agents, it is released in response to stress. Glucocorticoids increase blood glucose levels by stimulating gluconeogenesis, inhibiting glucose storage and stimulate lipolysis in adipose tissue releasing free fatty acids. They can also cause proteolysis in some muscle tissues. In the cardiovascular system cortisol increases the transcription

of receptors for angiotensin II, epinephrine and norepinephrine, to regulate blood pressure, contractility and tone of the heart (Sakaue & Hoffman, 1991).

Glucocorticoids are released as a feedback mechanism of the immune system to reduce inflammation, by inhibiting the actions of immune cells (T and B lymphocytes), and the synthesis and release of cytokines (interleukins 1-6, IL-12, IFN-γ, TNF-α, chemokines) and other inflammatory mediators (histamine, bradykinin). In this way cortisol prevents excessive inflammation, and tissue and organ damage. They also form a negative feedback loop inhibiting the secretion of CRH and AVP by the hypothalamus, and POMC cleavage in the pituitary to reduce the production of ACTH and therefore cortisol itself (de Kloet, 1995).

The renin-angiotensin-aldosterone (RAA) system has little control over arterial blood pressure under normal circumstances, but plays a pivotal role when sodium levels fall or haemorrhage occurs, as it has major vasoconstrictor capabilities (Collier et al, 1973; Scornik & Paladini, 1964). Renin is a proteolytic enzyme that cleaves angiotensinogen, synthesised by the liver, into angiotensin I (Miller, 1981). It is released from the juxtaglomerular cells of the kidney into the blood, stimulated by sympathetic nerve inputs, catecholamines, decreased renal perfusion pressure and decreased sodium delivery to the distal tubule (Johnson & Davis, 1973; Tobian et al, 1959). Angiotensin I is hydrolysed by angiotensin I-converting enzyme (ACE), found at the surface of pulmonary and renal endothelium, forming angiotensin II (AngII) (Oparil et al, 1970). This causes vasoconstriction of arteriolar smooth muscle, increases the contraction of the heart (positive inotropic effect) and stimulates the release of catecholamines. It also stimulates aldosterone production by the zG of the adrenal cortex.

Aldosterone production is controlled by plasma potassium levels and ACTH, although AngII is the primary regulator. AngII binds the AT1 cell surface receptor, which is a GPCR coupled to phosphoinositidase C (PI3C) (Bird et al, 1993). PI3C causes hydrolysis of phosphatidylinositol 4,5-bisphosphate (PtdIns(4,5)P_2), generating inositol 1,4,5-trisphosphate (Ins(1,4,5)P_3) and 1,2-diacylglycerol (DAG). Ins(1,4,5)P_3 is an intracellular second messenger that opens calcium channels on intracellular stores, resulting in the release of calcium into the cytoplasm, increasing its concentration (Wojcikiewicz &

Nahorski, 1993). Elevated intracellular calcium levels activate calmodulin (calcium modulated protein) and CaMK (calmodulin dependent protein kinases), which modulate aldosterone production, possibly by phosphorylation of transcription factors regulating CYP11B2 transcription (Pezzi et al, 1997). DAG activates protein kinase C (PKC) resulting in phosphorylation and activation of other second messenger cascades.

Aldosterone is the primary mineralocorticoid produced by the zG of the adrenal cortex, regulating sodium retention, water balance and blood pressure. Sodium is actively reabsorbed in the distal nephron of the kidney via ENaC sodium channels, which are mediated by aldosterone. This coincides with passive water reabsorption, to increase the extracellular and blood fluid volumes, and therefore blood pressure (Miller, 1981). Aldosterone also has effects on the cardiovascular system, and can cause cardiac fibrosis due to activation of an inflammatory cascade (Fuller & Young, 2005; Wehling et al, 1998).

While the stress response is important in certain circumstances, chronic elevated glucocorticoids however can lead to a myriad of health problems. It can be associated with muscle wastage and diabetes due to excess energy mobilisation, hypertension due to increased blood pressure, stomach ulcers, irregular periods/amenorrhea or reduced testosterone levels due to suppressed reproductive function, and increased susceptibility to infectious diseases due to chronic suppression of the immune system. In rare cases, children may also suffer from psychogenic dwarfism; short stature as a result of growth inhibition caused by excessive stress (Sapolsky, 2000).

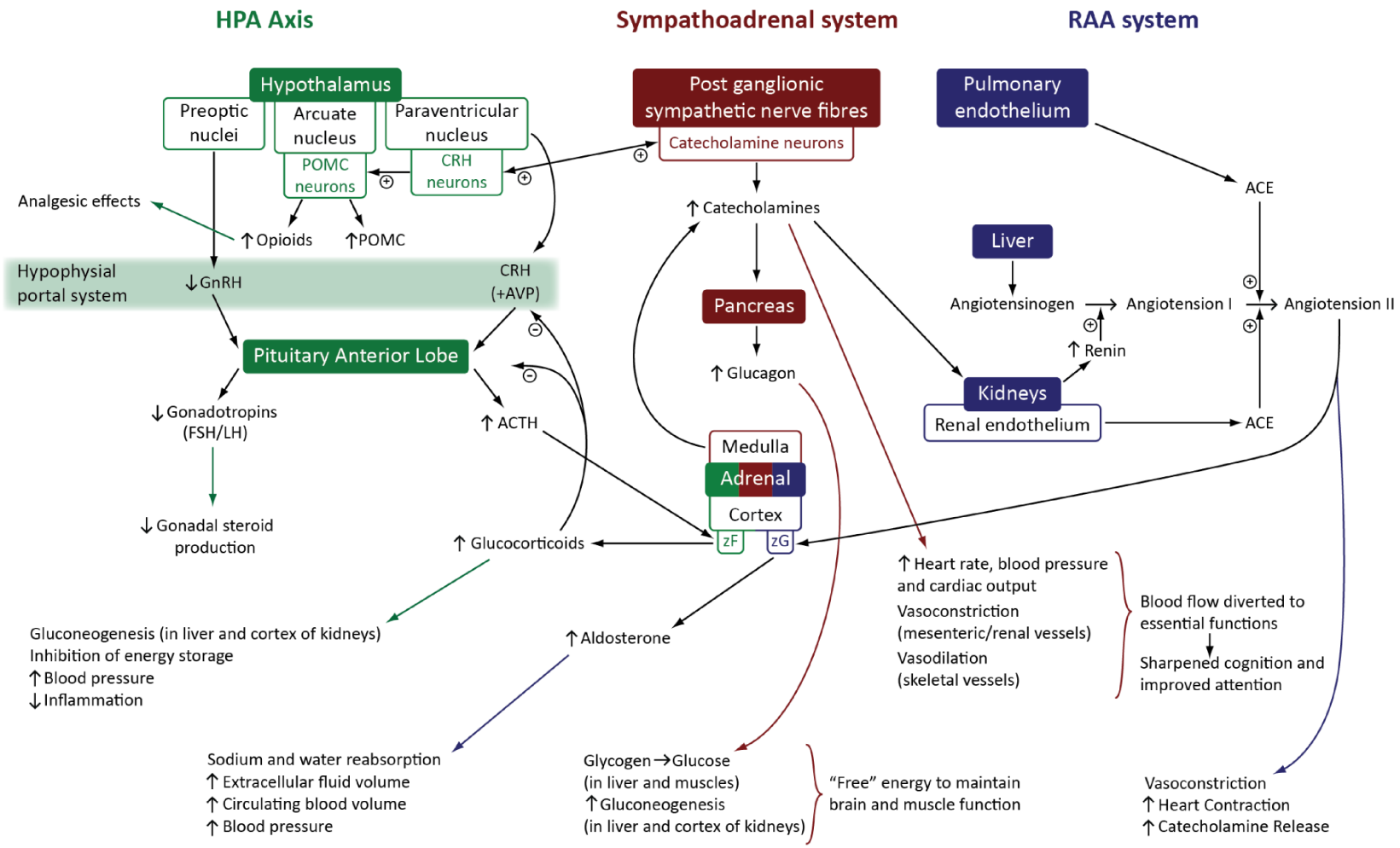

Figure 1.1.3 – The Stress System

Schematic diagram depicting the stress system, showing the interactions between the HPA (hypothalamic-pituitary-adrenal) axis, sympathoadrenal system and RAA (renin-angiotensin-aldosterone) system. POMC; pro-opiomelanocortin, CRH; corticotropin-releasing hormone, AVP; arginine vasopressin, GnRH; gonadotropin-releasing hormone, FSH; follicle-stimulating hormone, LH; leutinising hormone, ACE; angiotensin-converting enzyme, zG; zona glomerulosa, zF; zona fasciculata.

1.1.3 Cortisol, aldosterone and adrenal androgens

As described above; glucocorticoids stimulate gluconeogenesis, inhibit further energy storage and have a permissive role in increasing blood pressure. Cortisol exerts its actions by binding to glucocorticoid receptors (GRs) in the cytoplasm of target cells. These are ligand-activated transcription factors, which bind glucocorticoids at the carboxy terminus (Arlt & Allolio, 2003). GRs are associated with a complex of heat shock proteins including hsp90, which facilitate the binding of cortisol, and then dissociate from the active steroid-receptor complex (Rhen & Cidlowski, 2005; Sinars et al, 2003; Tao & Zheng, 2011). This then translocates to the nucleus and binds to glucocorticoid-response elements (GRE) in the enhancers or repressors of target genes, causing either their up-regulation or down-regulation. The steroid-receptor complex may also interact with other transcription factors (Marik, 2007).

Aldosterone stimulates sodium and water reabsorption in the kidney to increase blood pressure. It exerts its actions by binding to the intracellular mineralocorticoid receptor (MR) at its C-terminal ligand binding domain. It is a ligand-activated transcription factor, and like the glucocorticoid receptor (GR), hsp90 facilitates ligand binding which causes an activating conformational change (Couette et al, 1998). The ligand-receptor complex then translocates to the nucleus to mediate transcription of mineralocorticoid-responsive genes, or stimulate second messenger pathways, although its primary role is as a transcription factor (Fuller & Young, 2005).

Both mineralocorticoids and glucocorticoids, two different classes of steroid hormones, can bind the mineralocorticoid receptor. They bind with an equal affinity (Rupprecht et al, 1993), however circulating levels of cortisol are much greater than those of aldosterone (Rogerson & Fuller, 2000), and so mechanisms are required to allow aldosterone-specific activation of the receptor and downstream signalling. In most tissues expressing mineralocorticoid receptors, glucocorticoids are inactivated by 11β-hydroxysteroid dehydrogenase (11βHSD2), which converts cortisol to cortisone, and corticosterone in rodents to 11-dehydrocorticosterone (Sapolsky et al, 2000). This is referred to as pre-receptor regulation of steroid access. Activation of the ligand-receptor complex by cortisol requires 10 times the concentration needed for activation

by aldosterone, as aldosterone has a higher efficacy. This confers aldosterone specificity upon the receptor, by intrinsic-receptor mechanisms (Lombes et al, 1994).

Adrenal androgens, dehydroepiandrosterone (DHEA), dehydroepiandrosterone sulphate (DHEAS) and androstenedione, also known as C_{19} steroids, are produced by the zR. They are precursor sex hormones released into the blood stream, and taken up by the testis and ovaries to produce testosterone and oestrogen. Their production is regulated by ACTH, however it is unclear exactly how, or what regulatory machinery is involved, as only primates produce adrenal androgens, making them more difficult to study.

1.2 Development of the adrenal glands

1.2.1 Organogenesis and zonation

Although there are some differences between species in the structure and function of the mammalian adrenal gland, the basic principles of cortex development are very similar (Figure 1.2.1). The urogenital ridge is the shared common origin of the adrenals, gonads and kidneys (Hatano et al, 1996; Mesiano & Jaffe, 1997; Morohashi, 1997), and contains the adrenogonadal primordium composed of coelomic epithelium and the surrounding mesenchymal cells. The urogenital ridge is the first tissue to express the transcription factor SF-1 (steroidogenic factor 1) during development, and therefore is the earliest developing steroidogenic tissue, as SF-1 is a marker of steroidogenic capacity (Kim & Hammer, 2007; Mesiano & Jaffe, 1997). SF-1 expression is first seen at embryonic day 9 (E9) in mice, and embryonic week 4 (Ewk4) in humans. It is required for both adrenal and gonadal development, with SF-1 null mice lacking both these tissues (Luo et al, 1994).

The adrenogonadal primordium splits to form the adrenocortical primordium and the gonadal primordium, with the former going on to form the adrenal cortex. Migrating sympathetic neural crest cells move into the ‘adrenal anlage’, forming chromaffin cells of the medulla (Mitani et al, 1999), while the gland is encapsulated by mesenchymal

cells. As the cells proliferate, the cortex grows and expands, and concentric zones of steroidogenically-distinct cells start to form.

The human adrenocortical primordium consists of a large 'foetal' zone, surrounded by a much smaller definitive zone (Mesiano & Jaffe, 1997). The foetal zone is responsible for steroidogenesis during gestation, while the definitive zone takes over after birth. This is reflected by the gradual expansion and zonation of the definitive zone perinatally, and the regression of the foetal zone by 6 months. The foetal zone produces DHEA and DHEAS (Mesiano & Jaffe, 1997), with aldosterone and cortisol being produced when the zG and zF form. In mice, the foetal/X zone is of unknown function and involutes at the onset of puberty in males, and after the first pregnancy in females (Laufer et al, 2012). CYP11B1 expression is detected in the definitive adrenal by E16, marking a functionally active zF, while development of the zG lags behind, with CYP11B2 expression evident at E20, just before birth (King et al, 2009; Mitani et al, 1999).

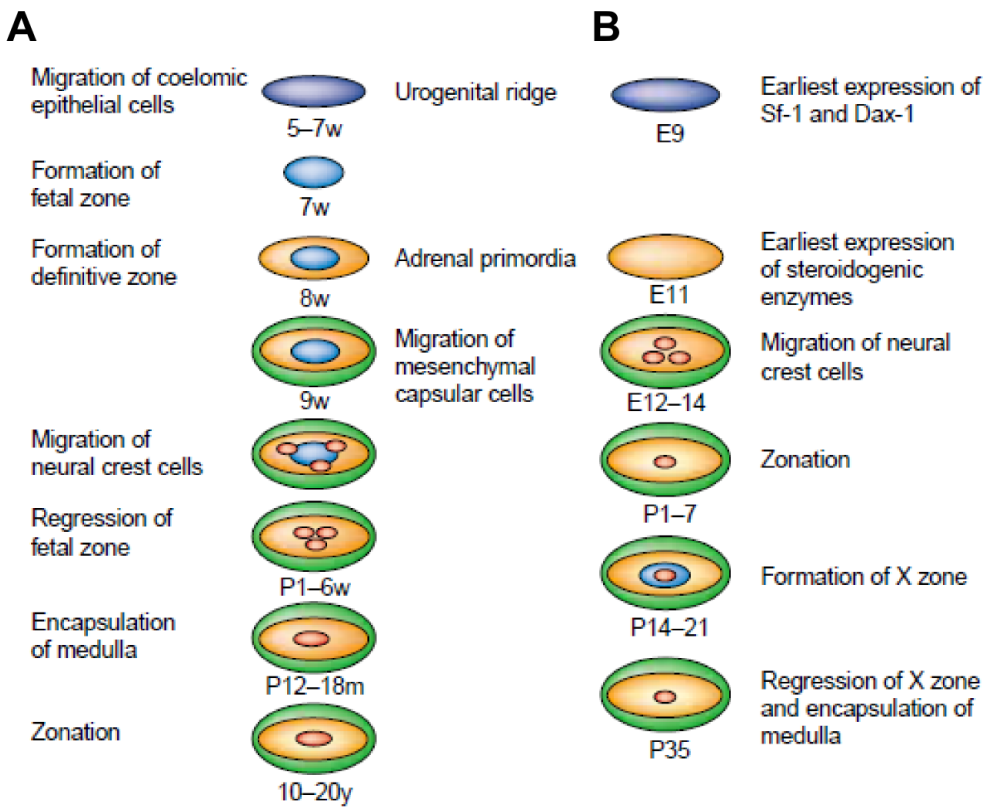

Figure 1.2.1 – Adrenal development (Keegan & Hammer, 2002)
Comparison of human (A) and mouse (B) adrenal development. Sf-1; steroidogenic factor-1, Dax-1; dosage-sensitive sex-reversal adrenal hypoplasia congenita on the X chromosome, gene 1, w; week, E; embryonic day, P; postnatal day, m; month, y; year.

1.2.2 Signalling pathways

Signalling pathways and transcription factors that govern initial formation of the adrenocortical primordium, as well as its differentiation and zonation to form the cortex, are not well characterised. The hedgehog (Hh) signalling pathway has been identified as a key player in adrenal development, and possibly the maintenance of a (sub)capsular mesenchymal stem cell population in adults (King et al, 2009). It is discussed further in section 1.4. Disruption of this pathway may be responsible for some cases of adrenal hypoplasia (King et al, 2008; Laufer et al, 2012).

Other factors of interest include WT1 (Wilms' tumour 1), Cited2 (CREB-binding protein/p300-interacting transactivator, with ED-rich tail, 2) and SF-1. WT1 is a tumour suppressor gene, and transcriptional regulator. It is one of the earliest genes to specify kidney, gonadal and adrenal cell lineages during development (Keegan & Hammer,

2002), with WT1 mutant mice lacking all three (Kreidberg et al, 1993; Moore et al, 1999). The transcriptional co-factor Cited2 interacts with WT1, and together they stimulate SF-1 expression in the adrenogonadal primordium, which is essential for adrenocortical development (Val et al, 2007). WT1 is present in the urogential ridge at E9, but is not expressed in the adrenal glands, while Cited2 expression is first detected at E10. Cited2$^{-/-}$ mice have reduced SF-1 expression, and fail to develop adrenals.

The transcription factor SF-1 is an orphan nuclear receptor, and as previously mentioned, is the earliest marker of steroidogenic capacity, with its absence leading to failure of the adrenal glands and gonads to develop (Luo et al, 1994; Luo et al, 1995; Sadovsky et al, 1995). It is co-activated by WT1, and is required for adrenal cortex formation and differentiation. It stimulates the transcription of many steroidogenic genes, including StAR and CYP11A1, and in adults is expressed throughout the cortex, although it is not present in the capsule (Babu et al, 2002; Luo et al, 1994). A small subset of subcapsular cells that are SF-1-positive, do not express steroidogenic enzymes due to inhibition of SF-1 mediated transcription (Kim & Hammer, 2007). The mechanisms by which SF-1 is inhibited in these cells is still unclear, but may involve varying degrees of SF-1 sumoylation (Lee et al, 2011).

Dax1 (dosage-sensitive sex-reversal adrenal hypoplasia congenita on the X chromosome, gene 1), is also a nuclear hormone receptor implicated in adrenocortical and gonadal development. It co-localises with SF-1 at the urogenital ridge at E9.5 in mice (Ikeda et al, 1996), but its exact function may vary between different mammalian species. Dax1 knockout (KO) mice show decreased CYP11A1 expression in the zF, with otherwise normal adrenal function (Ito et al, 1997; Yu et al, 1998). However, in humans, mutations or deletion of Dax1 are responsible for X-linked adrenal hypoplasia congenita (AHC) (Muscatelli et al, 1994; Zhang et al, 1998). Patients present with primary adrenal insufficiency, characterised by reduced glucocorticoid and mineralocorticoid levels. They also lack clearly defined cortex zonation.

Wnt (wingless-related mouse mammary tumour virus integration site) signalling has roles in proliferation, cell fate specification, stem cell maintenance and differentiation (Logan & Nusse, 2004), and is another pathway implicated in adrenal development. In

the absence of the Wnt ligand, cytoplasmic β-catenin is degraded via ubiquitin-mediated proteolysis, by a complex consisting of Axin, APC (adenomatous polyposis coli) and Gsk3β (glycogen synthase kinase 3β) (Figure 1.2.2). When Wnt binds to the membrane receptor frizzled, the protein dishevelled is recruited, disrupting this complex, and permitting β-catenin accumulation and translocation to the nucleus. There it interacts with Lef/Tcf (lymphoid enhancer-binding factor/T-cell factor) to activate the transcription of canonical Wnt signalling target genes (Kim et al, 2008a; Lienkamp et al, 2012). The protein inversin inhibits dishevelled-stimulated canonical Wnt signalling, and promotes non-canonical PCP (planar cell polarity) signalling (Lienkamp et al, 2012).

β-catenin is expressed in the adrenocortical primordium at E12.5 in mice, overlapping with the expression of SF-1. It then becomes restricted to the subcapsule, with only a subset of these cells maintaining active canonical Wnt signalling in the adult. Mice with conditionally inactivated β-catenin have adrenal aplasia by E18.5, with reduced SF-1 expression in adrenal cells prior to this. This is due to decreased proliferation of adrenocortical precursor cells causing regression of the gland. Partial β-catenin inactivation also shows depletion of adrenocortical cells in the adult by apoptosis (Kim et al, 2008a). β-catenin forms part of a transcriptional protein complex with SF-1 to synergistically activate target genes (Gummow et al, 2003; Mizusaki et al, 2003), possibly those essential for adrenocortical proliferation, or to inhibit apoptosis, and those required to maintain the cortex in the adult.

Wnt4 is expressed in the urogenital ridge at E11.5, also in a pattern corresponding to that of SF-1 at this time. This area of Wnt4 is later distinguished as the cortex, and in particular the zG, with expression correlating to the zG markers CYP11B2 and PREF1 (preadipocyte factor 1). Wnt4 mutant mice have reduced CYP11B2 levels, and therefore aldosterone, as well as reduced PREF1, indicating problems with development of the zG (Heikkila et al, 2002). They also show signs of abnormal kidney development (Vainio & Uusitalo, 2000), and have partial female to male sex reversal (Heikkila et al, 2002) as the urogenital ridge is the shared common origin of the adrenal, gonads and kidneys. Wnt4, is therefore likely to be required for proper formation of the zG. In humans, a Wnt4 loss of function mutation has been identified

in SERKAL (SEx Reversion, Kidneys, Adrenal and Lung dysgenesis) syndrome (Mandel et al, 2008). This is an autosomal recessive disorder resulting in female to male sex reversal, and renal, adrenal and lung dysgenesis.

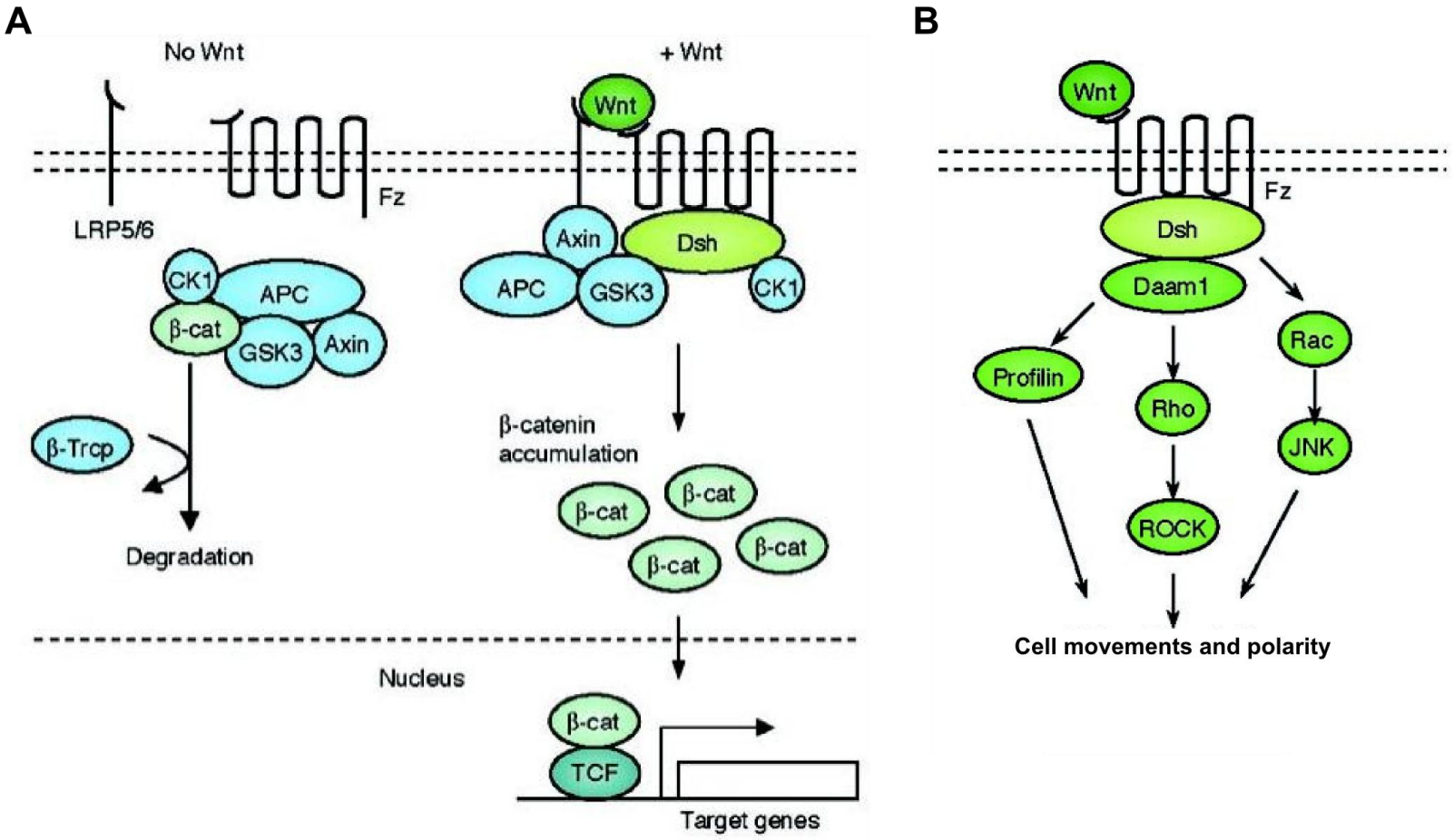

Figure 1.2.2 – The Wnt signalling pathway (Komiya & Habas, 2008; Wang, 2009)

Schematic diagram depicting canonical Wnt (A) and non-canonical Wnt/PCP (B) signalling pathways. Wnt; wingless-related mouse mammary tumour virus integration site, LRP5/6; low-density-lipoprotein-related protein5/6, Fz; frizzled, CK1; casein kinase 1, APC; adenomatosis polyposis coli, β-cat; β-catenin, GSK3; glycogen synthase kinase 3, β-Trcp; β-transducing repeat-containing protein (E3 ubiquitin ligase), Dsh; dishevelled, TCF; T-cell factor, Daam1; dishevelled associated activator of morphogenesis, JNK; Jun N-terminal kinase, ROCK; Rho-associated kinase.

1.2.3 Adrenocortical stem/progenitor cells

It has long been thought that undifferentiated, pluripotent stem cells exist in the adrenal cortex to maintain homeostasis in the adult. For instance, in remodelling experiments, feeding rats a low sodium diet results in expansion of the zG. This allows CYP11B2 activity to increase, and produces a greater secretion of aldosterone to cope with the new demands imposed on the system (Aguilera et al, 1980; LeHoux et al, 1997). Stem/progenitor cells within the cortex must therefore undergo proliferation and differentiation to provide the means to supply the necessary steroidogenic output. Transplantation of primary bovine adrenocortical cells to adrenalectomised SCID mice results in the formation of fully functional, and architecturally normal, adrenocortical tissue (Thomas et al, 2000), also indicating the presence of stem cells within the adrenal cortex.

While many agree on the existence of a stem cell population in the adrenal cortex, the origin of these regenerating cells remains ambiguous. An initial hypothesis; that each zone has its own stem cell population, now seems rather unlikely, as the majority of proliferation takes place in the subcapsular region, and apoptosis mainly occurs at the zR:medullary boundary. It is now thought that the capsule and subcapsular region are a likely source of stem cells, and this hypothesis would support the migration theory, first proposed by Gottschau in 1883 (Gottschau, 1883).

The migration theory proposes that cells migrate centripetally from the outer to the inner adrenocortical layers, ending up at the medullary boundary, where macrophages reside and therefore apoptosis occurs. This would require a stem cell population to reside in the capsule or subcapsular region, and for each cell to be able to differentiate from a zG cell into a zF cell. Although the process of lineage determination is still currently being investigated, enucleation and lineage studies support both the centripetal migration theory and the existence of a stem cell population in the capsule/subcapsular region.

Enucleation studies involve the removal of the inner contents of the adrenal leaving just the capsule and subcapsular cells. The ability of the cortex to regenerate from these cells alone is then examined. Studies using this technique have shown that the

cortex is able to regenerate and form steroidogenically functional tissue (Greep & Deane, 1949; Ingle, 1938; Perrone et al, 1986; Skelton, 1959), indicating that a stem cell population must reside within the capsule and/or subcapsule.

Lineage studies involve labelling a parental cell with a specific marker, which can then be passed on to all of its progeny. This can include dyes such as trypan blue, and genetic markers for example GFP. Genetic recombination is also a frequently used tool for lineage tracing (Kretzschmar & Watt, 2012). A combination of studies, using a variety of different labelling techniques, have revealed the presence of perpendicular columns of cells spanning from the capsule to the medulla (Greep & Deane, 1949; King et al, 2009; Morley et al, 1996; Salmon & Zwemer, 1941; Zajicek et al, 1986), and have shown that both Shh (sonic hedgehog)-expressing cells, and capsular cells are capable of giving rise to all steroidogenic cells types of the cortex. It is therefore possible that several different pools of stem cells may exist within the adrenal cortex (King et al, 2009).

Shh-expressing cells also express SF-1, but they do not express the terminal steroidogenic enzymes CYP11B1 and CYP11B2, and are therefore considered to be steroidogenically inactive. These undifferentiated cells form a layer between the zG and the zF of the rat adrenal cortex, termed the zU, first identified by Mitani et al. in 1994 (Mitani et al, 2003; Mitani et al, 1994). Further analysis of the zU has revealed it is composed of two types of cells. An outer layer, next to the zG that is Shh-positive, SF-1-positive and weakly CYP11A1-positive, and an inner layer bordering the zF, which is Shh-negative, SF-1-positive and has higher CYP11A1 expression equivalent to that of the zG and zF, but is still aberrant of CYP11B1 and CYP11B2 expression (Guasti et al, 2011).

The exact function of the zU is still unknown, however, it has been stipulated that these cells may be progenitor cells for steroidogenic cortical lineages, and/or their expression of Shh could be involved in maintaining a stem cell niche within the capsule/subcapsule, the location of Hh-responsive cells (Laufer et al, 2012). Either way, this population of cells, albeit in different histological locations, is conserved between species. In mice, non-steroidogenic, Shh-expressing cells are found in clusters within

the zG (King et al, 2009), and a similar expression pattern is predicted in the human adrenal cortex (Laufer et al, 2012).

1.2.4 Adrenal dysregulation

Adrenal dysfunction can occur for a number of reasons. It can result from incorrect or incomplete adrenal development, defects in steroidogenesis, disturbances in pituitary-adrenal communication or degenerative immune disorders (Else & Hammer, 2005; Kempna & Fluck, 2008). As a consequence, levels of circulating adrenal steroids may be altered, and the adrenal cortex may appear hypo- or hyper- plastic.

Adrenal hypoplasia congenita (AHC) is an example of adrenal insufficiency. Patients have increased serum ACTH, while cortisol and aldosterone production is severely reduced. This results in symptoms such as dehydration, hyponatremia, hyperkalemia, hypotension, hypoglycaemia and hyperpigmentation. The majority of cases are caused by mutations in the Dax1 gene on the X chromosome, and therefore adrenal development is disrupted. The adrenal cortex appears disorganised, with enlarged vacuolated cells, and persistence of the foetal zone. In males, hypogonadotropic hypogonadism is also common (Else & Hammer, 2005; Scriver, 1995; Zanaria et al, 1994). Several patients, in which no Dax1 mutation is present, have mutations in SF-1, also essential for correct adrenal development (Phelan & McCabe, 2001). Another type of AHC exists in which normal adrenal zonation is apparent, but the gland is undersized. The underlying genetic causes for this have not as yet been identified (Scriver, 1995).

Adrenal hypoplasia has also been described in patients with familial glucocorticoid deficiency (FGD) caused by mutations in the ACTH receptor, MC2R (Clark & Weber, 1998; Lin et al, 2007), or its accessory protein, MRAP (Akin et al, 2010), and in the MC2R knockout mouse, a model of FGD type 1 (Chida et al, 2007). Symptoms of FGD include hypoglycaemia, jaundice and hyperpigmentation due to increased plasma ACTH and reduced cortisol (Chung et al, 2010; Clark et al, 1993; Metherell et al, 2005). ACTH is required to provide trophic support for the adrenal cortex during development and in the adult, and mutations in MC2R or MRAP prevent its downstream signal transduction.

Unlike AHC and FGD, which manifest themselves in early childhood, the onset of Addison's disease usually occurs in adults. While development of the adrenal glands is normal, an autoimmune response against CYP21, and the tissue where it is synthesised, results in their destruction (Nikoshkov et al, 1999). Glucocorticoids and mineralocorticoids can therefore not be produced, causing chronic hypoadrenocorticism with corresponding elevated serum ACTH. Patients present with fatigue, muscle weakness, weight loss, vomiting and hyperpigmentation (Zhou et al, 2009). It is unknown what triggers the autoimmune response.

CYP21 deficiency, when not associated with a degenerative immune disorder, is the most common cause of congenital adrenal hyperplasia. These patients cannot produce adequate levels of cortisol, and inefficient aldosterone production is also common. Adrenal androgens are produced in excess, as this is the only biosynthesis pathway available for the accumulating cortisol precursors. CRH in the hypothalamus and ACTH from the pituitary are over synthesised due to the absence of negative feedback loops. Symptoms include virilised external genitalia in females, accelerated growth, hyperplasia of the adrenal glands and hyponatremic dehydration (Mornet et al, 1989; Scriver, 1995; White & Speiser, 2000).

Adrenal hyperplasia can also be caused by lipid accumulation or tumour formation. Mutations in StAR cause congenital lipoid adrenal hyperplasia. Cholesterol cannot be converted to pregnenolone resulting in the accumulation of cholesterol esters in lipid droplets within the cells of the adrenal cortex. As the lipid droplets increase in size, they cause cellular damage, and further perturb steroidogenesis. Cortisol, aldosterone and androgen levels are reduced, while plasma ACTH is increased. Patients have hyponatremia, hyperkalemia, hypotension, dehydration, hypoglycaemia, hyperpigmentation and males have female external genitalia (Bose et al, 1996).

ACTH overproduction by benign pituitary corticotroph adenomas cause the most frequent type of Cushing's disease. Pituitary derived ACTH is required for adrenal growth and maintenance, but excess ACTH leads to adrenal hyperplasia and chronic glucocorticoid excess. Cushing's patients have increased plasma cortisol which causes

weight gain, hypertension, osteoporosis and adrenal hyperplasia. Overproduction of cortisol is also caused by adrenal tumours (Dworakowska & Grossman, 2011).

Glucocorticoid and mineralocorticoid replacement therapy is the main treatment for adrenal insufficiency. They may also be required after the removal of pituitary or adrenal tumours causing glucocorticoid excess, if normal pituitary or adrenal function is not restored. A better understanding of adrenocortical development and remodelling, and the role primary cilia play, will hopefully lead to improved management of adrenal dysfunction, and pave the way for progression towards gene repair and cell replacement therapies. These would be a welcome alternative to lifelong therapeutic intervention by hormone replacement, which is still associated with reduced quality of life and significantly increased mortality, that can have the side effects of psychological disturbances and does not address secondary issues present occasionally, such as infertility.

Adrenocortical cancer is another form of adrenal dysregulation. The majority of tumours are benign adrenocortical adenomas (ACAs), with malignant adrenocortical carcinomas (ACCs) occurring far less frequently. ACAs tend to be asymptomatic, while ACCs are far more aggressive and have a poor prognosis (Lehmann & Wrzesinski, 2012). Adrenocortical tumours (ACTs) may secrete cortisol, aldosterone or androgens (Low et al, 2012).

The underlying molecular basis of ACTs is not well characterised. SF-1 up-regulation has been reported in ACCs (Almeida et al, 2010), as well as excessive canonical Wnt signalling resulting from β-catenin stabilisation, or loss of the repressor APC (El Wakil & Lalli, 2011; Gaujoux et al, 2011; Simon & Hammer, 2012). IGF2 (insulin-like growth factor 2), required for growth of the adrenal gland during embryogenesis, and expressed in the capsule in the adult (Mesiano et al, 1993), is also overexpressed in ACAs and ACCs (Demeure et al, 2011; Lehmann & Wrzesinski, 2012). Loss of function mutations in the gene encoding p53, which regulates the cell cycle and apoptosis, occur in approximately 50% of all cancers, including ACTs (Lin et al, 1994; Reincke et al, 1994). Although aberrant Hh signalling or Gli expression has been implicated in many

cancers, especially medulloblastomas and BCCs, there have been no reports of up-regulation of Hh pathway constituents in ACCs (Giordano et al, 2009). Further characterisation of adrenocortical stem/progenitor cells will be beneficial for the identification of the underlying molecular mechanisms involved in adrenocortical tumourigenesis, and may reveal new therapeutic targets (Simon & Hammer, 2012).

1.3 Adrenal cell lines

When identifying adrenal model systems, one needs to consider cell growth, response to agonists, and steroidogenic capacity (steroidogenic enzyme expression), which can change over time in culture. Primary cultures may be used, but these require frequent animal sacrifice, as cells have a limited life span ending in senescence (Staels et al, 1993). Also, not all cells isolated will have steroidogenic capacity, and those that do rapidly loose ACTH and cAMP responsiveness (Rainey et al, 2004).

One of the first cell lines used to study adrenal endocrinology is the Y1 cell line, derived from a zF originating tumour from a male LAF_1 mouse. These cells are hypodiploid, containing 39 chromosomes instead of 40 (Yasumura et al, 1966), and have a doubling time of approximately 30-40hrs. The original tumour produced corticosterone and responded to ACTH (Cohen et al, 1957), however, the cell line produces 20αdihydroxyprogesterone, 11β,20α-dihydroxyprogesterone, and 20α-hydroxysteroid dehydrogenase (Pierson, 1967), but is deficient of CYP21, so cannot produce corticosteroids. They can be transfected with genomic plasmids encoding CYP21, to restore its activity, and corticosterone synthesis (Parker et al, 1985). ACTH can stimulate steroid biosynthesis in Y1 cells, but the amount produced varies between clonal isolates, and some are completely resistant to it (Yasumura et al, 1966). They do not respond to AngII stimulation, and as they are murine cells they do not produce cortisol or adrenal androgens. These cells are now mainly used to study the actions and mechanisms of ACTH.

The human adrenal carcinoma cell line NCI-H295 was the first adrenal cell line established that retains its steroidogenic capacity, and expresses all enzymes required

for adrenocortical steroidogenesis (Staels et al, 1993). It was isolated from an adrenocortical carcinoma belonging to a 48 year old black female (Gazdar et al, 1990). H295 cells are aneuploid and hypertriploid, with the modal number of chromosomes being 62, held by approximately 30% of cells (Gazdar et al, 1990). This original line grows slowly in suspension, with a doubling time of approximately 5 days (Rainey et al, 2004). They produce their own cholesterol for steroidogenesis, and like the tumour from which they originated, mainly produce androgens, with low mineralocorticoid and glucocorticoid synthesis, making them analogous to the foetal adrenal, with pluripotent capabilities (Gazdar et al, 1990).

Like adrenocortical cells *in vivo*, they respond to second messenger pathways (Staels et al, 1993). AngII increases intracellular calcium levels via AT1 activation, and this along with PKC signalling preferentially induces CYP11B2 transcription to produce aldosterone (Bird et al, 1993). Potassium also causes increased intracellular calcium levels, and aldosterone release (Pezzi et al, 1997). This response is identical to AngII and potassium stimulation of the zG. Most strains are however, unresponsive to ACTH, probably stemming from low MC2R levels (Mountjoy et al, 1994), but as the cAMP pathway remains intact, it can be activated by forskolin (Fsk). Fsk acts at adenylate cyclase to increase cAMP levels, preferentially inducing CYP17 and CYP11B1 transcription, resulting in cortisol production (Denner et al, 1996). It also activates the PKA pathway. This response is the same as ACTH stimulation of the cAMP pathway via MC2R in the zF. Chronic Fsk treatment shifts the steroidogenic pathway towards androgen production of the zR, with increased DHEA and DHEAS levels (Cobb et al, 1996).

A strain of H295 cells selected for their ability to grow in an adherent monolayer, and their shorter population doubling time of approximately 2 days, is now the adrenal cell line most frequently used. This strain, named H295R, also expresses all enzymes required for steroidogenesis, produces mainly androgens with low levels of cortisol and aldosterone, and is responsive to AngII, potassium and Fsk. By altering steroid production to resemble that of the zG or zF/zR with the addition of AngII or Fsk respectively, these cells can be used to study adrenal development and zonation *in vitro*. Without the addition of AngII or Fsk, H295/R cells are zonally undifferentiated.

More recently, another adrenocortical cell line has been developed that is reported to express all enzymes required for cortisol, aldosterone and DHEA production, and are responsive to Fsk, AngII and potassium. These human adrenocortical carcinoma cells, named HAC15 (Parmar et al, 2008), were derived from an adrenal tumour in an 11 month old female, but are not yet readily available for purchase. They have a similar steroidogenic profile to H295/Rs, but produce slightly more cortisol than aldosterone. Unlike H295/Rs, they also respond well to ACTH treatment and have higher MC2R levels. Chronic AngII or ACTH treatment has not yet been tested, but as the only alternative human adrenocortical cell line available, and the first to respond to ACTH as well as potassium and AngII, they will be an essential part of further studies on the actions and mechanisms of ACTH.

1.4 Shh signalling

The Hedgehog gene was first identified in the 1980s in the fruit fly; *Drosophila melanogaster* (Nusslein-Volhard & Wieschaus, 1980). It is a segment polarity gene, which when mutated results in altered segment organisation and patterning in Drosophila larva (Bumcrot et al, 1995; Nusslein-Volhard & Wieschaus, 1980). Many invertebrate and vertebrate homologues have since been identified all of which have been shown to encode intercellular signalling proteins important for embryonic development (Ingham & McMahon, 2001). Hh proteins are involved in tissue patterning such as the anterior-posterior axis of the limb and the dorso-ventral axis of the neural tube, heart development and inducing asymmetry in the left-right body axis. They are also involved in cell proliferation and differentiation, and in the adult, tissue homeostasis and maintaining stem cell niches (Christensen et al, 2007).

1.4.1 Hh proteins

There are three vertebrate homologues of the Drosophila Hh gene, encoding extracellular signalling proteins of the same name. These are Desert hedgehog (Dhh), mainly involved in germ cell development (Bitgood et al, 1996), Indian hedgehog (Ihh),

for bone development (Vortkamp et al, 1996), and Sonic hedgehog (Shh), also known as vhh-1 or Hhg-1 (Bumcrot et al, 1995). Shh is the best characterised and plays the most extensive role in development.

All three Hh proteins are produced at the endoplasmic reticulum as approximately 45kDa full length precursor proteins. They are then processed post-translationally to give rise to a 19-20kDa amino terminal fragment (Hh-N), and a 25-27kDa carboxy terminal fragment (Hh-C). Hh-N is further modified by the addition of cholesterol and a palmitoyl moiety (Buglino & Resh, 2008; Chamoun et al, 2001; Etheridge et al, 2010), and is responsible for transducing the Hh signal. The Hh-C fragment is thought to be required for the autocatalytic internal cleavage of peptide bonds resulting in the two proteins (Porter et al, 1996). Secretion of Hh-N from the cell involves the 12-pass transmembrane protein Dispatched1, which facilitates the formation of Hh-N multimers, wherein all hydrophobic lipid modifications are concealed, making a soluble and freely diffusible structure (Zeng et al, 2001).

1.4.2 Signalling components

Once released from the cell, Hh binds to a complex of proteins on a Hh-receiving cell. This complex includes the Hh-binding protein Patched-1 (Ptch1), which has a high affinity for all Hh ligands (Stone et al, 1996). It is a 12-pass transmembrane protein, and in the absence of Hh inhibits the actions of the downstream signalling component Smoothened (Smo). The mechanism by which Ptch1 exerts this effect is not well characterised, but it does not bind directly to Smo (Taipale et al, 2002), and current hypotheses involve Smo regulation by an as yet unidentified small molecule, possibly an oxysterol, which are natural intracellular Smo agonists (Corcoran & Scott, 2006; Dwyer et al, 2007; Rohatgi & Scott, 2007). Ptch1 is related to the resistance, nodulation, cell division (RND) family of bacterial proton-driven transmembrane molecular transporters. By containing a proton-pump (Etheridge et al, 2010), Ptch1 may change the concentration or localisation of a small-molecule that regulates Smo conformation and localisation.

Upon binding of Hh to Ptch1, inhibition of Smo in relieved (Figure 1.4.1). Smo is the Hh pathway signal transducer, and a member of the GPCR superfamily, with seven structurally similar transmembrane domains. Activation of Smo involves changes in its conformation in the extracellular and cytosolic domains, conferring different degrees of activity (Chen et al, 2002b; Wilson et al, 2009). In an active conformation, Smo prevents the processing of the Gli transcription factors, either by directly interacting with them, or via interactions with the complex of proteins involved in their processing (Yue et al, 2008).

There are three Gli genes in mammals; Gli1, Gli2 and Gli3, homologues of the single *Drosophila* gene *Cubitus interruptus* (Ci). They encode a family of zinc finger transcription factors. In the absence of Hh and activated Smo, full length Gli3 and Gli2 are proteolytically processed resulting in the removal of the carboxyl-terminal activation domain (Pan & Wang, 2007). In this form (GliRs), these transcription factors act to repress transcription, although the majority of Gli2R is degraded by the proteasome (Pan et al, 2006). Disruption of this processing by Smo, allows full length Gli3 and Gli2 to translocate to the nucleus and act as transcriptional activators (GliAs). Gli1 is not expressed in the absence of Hh, but is up-regulated by the pathway, so can be used as a marker for active Hh signalling (Vokes et al, 2007). It only acts as a transcriptional activator, further augmenting Hh pathway activity. The ratio between GliRs and GliAs varies as the concentration of Hh ligand changes, allowing different target genes to be expressed or de-repressed. There may also be different GliA and GliR binding sites within the promoters of target genes, or these sites may have different affinities for each Gli transcription factor (Vokes et al, 2007).

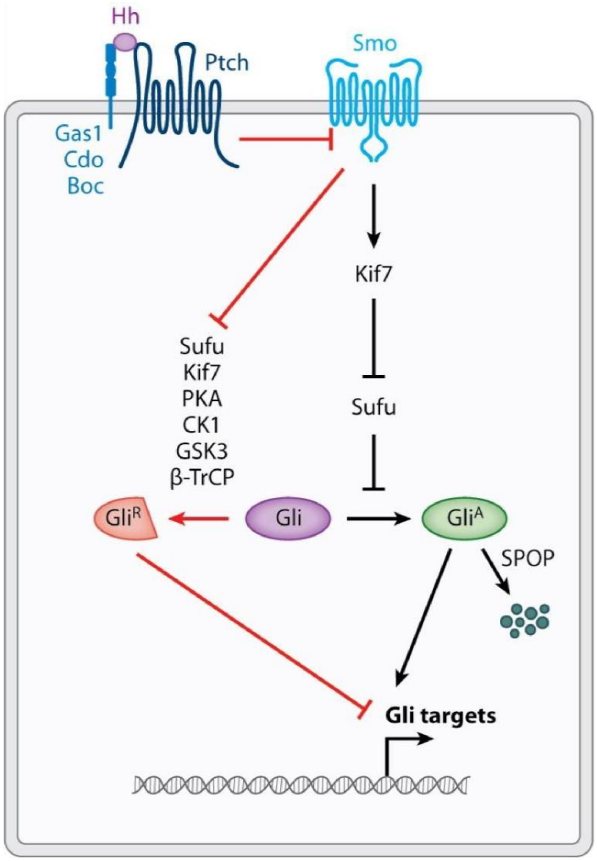

Figure 1.4.1 – Schematic diagram of the mammalian Hh pathway (Hui & Angers, 2011)
Hh; hedgehog, Ptch; patched, Smo; smoothened, Gas1; growth arrest-specific protein 1, Cdo; CAM-related/down-regulated by oncogenes, Boc; brother of Cdo, Kif7; kinesin family member 7, SuFu; suppressor of fused, PKA; protein kinase A, CK1; casein kinase 1, GSK3; glycogen synthase kinase 3, β-TrCP; β-transducing repeat-containing protein, Gli^R; Gli repressor, Gli; glioma-associated, krupple family member, Gli^A; Gli activator, SPOP; speckle-type PDZ protein.

It is now generally accepted that correct Hh signalling is highly dependent on the structural cellular component, the primary cilium (see section 1.5). Ptch1 is located within the ciliary membrane, but when bound to Hh, the Hh-Ptch1 complex is internalised (Figure 1.4.2). This then moves out of the cilium, as Smo moves in (Rohatgi et al, 2007). Gli transcription factors, and components of the protein complex required for their proteolytic processing, have also been found localised at the tip of the cilium (Haycraft et al, 2005; Satir & Christensen, 2007).

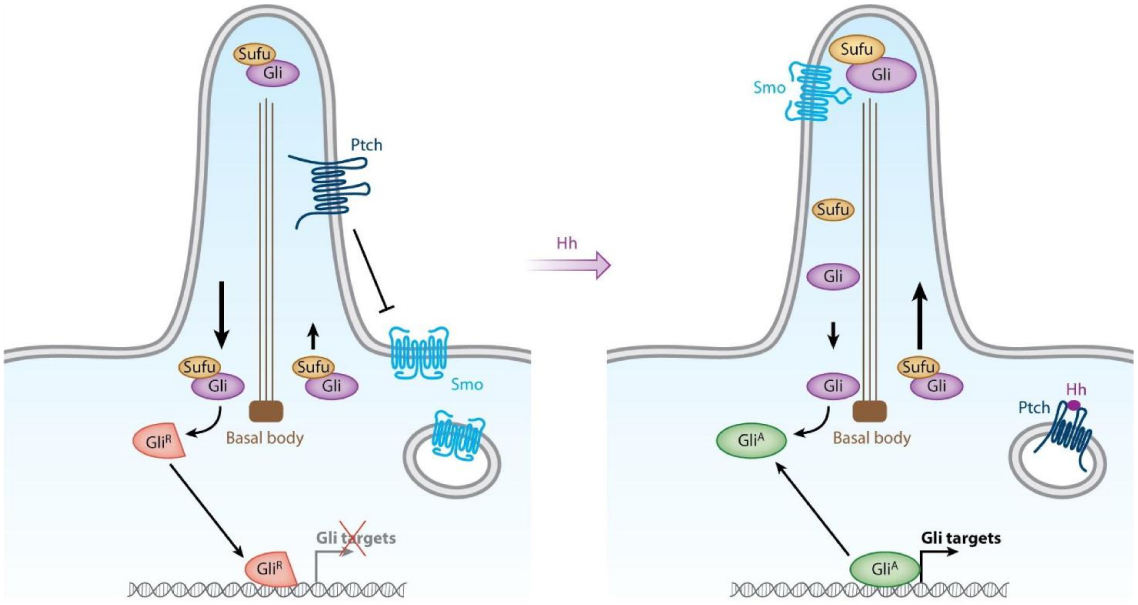

Figure 1.4.2 – Primary cilia and Hh signalling (Hui & Angers, 2011)
Schematic diagram showing the involvement of primary cilia in Hh signal transduction. SuFu; suppressor of fused, Gli; glioma-associated, krupple family member, Ptch; patched, Smo; smoothened, Gli^R; Gli repressor, Hh; hedgehog, Gli^A; Gli activator.

1.4.3 Agonists and Antagonists

The majority of Hh pathway agonists and antagonists exert their actions via Smo, binding to its heptahelical bundle and causing changes in its conformation. Commonly used agonists include purmorphamine and SAG (smoothened agonist) which allow Smo ciliary translocation (Wang et al, 2009). Cyclopamine is the main antagonist, derived from the *Veratrum Californicum* genus of plants, and was the first small molecule shown to selectively inhibit Hh signalling in vertebrates. It also causes translocation of Smo to the cilium, but in an inactive conformation (Wang et al, 2009).

1.4.4 Hh signalling in the adrenal

Shh is first present in the adrenocortical primordium at E12.5 in mice (King et al, 2009). It is expressed along with SF-1, but not CYP11B1 or CYP11B2, at the periphery of the adrenal cortex (Bitgood & McMahon, 1995; Ching & Vilain, 2009; Huang et al, 2010; King et al, 2009). At E12.5-14.5, Gli1 and Ptch1 are expressed in the mesenchyme surrounding the SF-1-positive cells, and at later time points, in the capsule and a few subcapsular cells that are non-steroidogenic (King et al, 2009).

Conditional Shh-inactivation results in reduced adrenal mass and adrenal hypoplasia with thinning of the capsule compared to the wild-type mice (Ching & Vilain, 2009; Huang et al, 2010; King et al, 2009). Bose et al. also report that truncated Gli3 mutant mice, in which Gli3 cannot become a transcriptional activator, have adrenal agenesis, first detectable at E15.5 (Bose et al, 2002). In humans, patients with holoprosencephaly frequently present with adrenal hypoplasia and insufficiency (Begleiter & Harris, 1980), and of the seven genes implicated in causing it, three are from the Hh pathway; Shh, Ptch and Gli2 (Dubourg et al, 2007).

Shh signalling is clearly required for normal development of the adrenal cortex, however its exact function in this process is still to be determined. King et al. have proposed a novel two-lineage model of adrenocortical development involving Hh (King et al, 2009). In this model, a primary adrenal lineage is derived from SF-1-positive cells of the adrenogonadal primordium, in a Shh-independent manner. As the adrenal anlage segregates, these cells then start to express Shh, which induces Gli1 expression in the surrounding mesenchymal cells. The mesenchymal cells move in and encapsulate the gland, possibly in part due to the chemoattractive properties of Shh. The majority go on to form the capsule; however, a few cells end up residing in the subcapsular region. It is proposed that some Gli1-positive, SF-1-negative cells, possibly those in the subcapsule, form a secondary adrenal cell lineage, dependent upon Hh-signalling.

Evidence for this model stems from the formation of the adrenal gland in conditional Shh null mice, and therefore a Hh-independent lineage must exist. However, the gland that forms in these mice is significantly smaller in size, and has a thinner capsule, representative of failure of expansion and maintenance of the gland in the absence of Hh signalling. Lineage studies performed by the group also show that both Shh-positive cells and Gli1-positive cells are capable of giving rise to steroidogenic adrenocortical cells, suggesting either or both may be the location of a stem/progenitor cell population, and a secondary adrenal lineage could arise from the Gli1-positive capsular cells.

Huang et al. also show that the adrenal cortex can form with proper zonation and the ability to produce steroids in the absence of Shh (Huang et al, 2010), consistent with the idea of a Hh-independent primary cell lineage. They too report that the gland is smaller, with a thinner capsule and cortex than the wild-type mice, which is due to reduced proliferation in the capsule. Zonation and differentiation of a primary cell lineage appear to be Hh-independent processes, while expansion of the capsule and cortex by stem/progenitor cells, both during development and in the adult rely on Hh signalling.

1.5 Primary Cilia

Cilia are organelles which evolved in eukaryotes as separate cytoplasmic compartments. There are three different types; motile, nodal and primary. Motile cilia are usually present in large numbers, and beat in unison to cause fluid flow. They have 9 pairs of microtubules around the outside of the ciliary axoneme, connected by radial spokes to a central pair of microtubules. These move relative to each other, causing the cilium to bend and therefore move (Tobin & Beales, 2007). Nodal cilia can also beat, but lack the central pair of microtubules. They are present on cells of the embryonic node during development, and cause preferential morphogen gradients helping to establish left-right body axis asymmetry. Exactly how they are able to beat is still unclear.

Primary cilia (Figure 1.5.1) have only recently become of interest in the last 10 years, and were previously considered vestigial. As the name suggests, only one projects from each cell, but they are present on nearly all cells during interphase (Santos & Reiter, 2008). They have a 9+0 microtubule arrangement, so they do not have the central pair of microtubules, and are therefore immotile. They extend from the cell surface with an axoneme diameter of approximately 0.25µm, but they vary in length depending on cell type and function. Their membrane is continuous with that of the cell membrane, but they are separated from the main cytoplasm by the transition zone, where the basal body resides. The basal body forms from the mother centriole of the cell (Jurczyk et al, 2004), which is required to migrate to the membrane where the

cilium will assemble (Kim et al, 2008b). It is here that proteins are sorted and screened for those containing ciliary localisation motifs. All proteins must pass through the transition zone to enter or leave the cilium, as it is devoid of ribosomes so no protein synthesis occurs within (Singla and Reiter 2006).

The main function of primary cilia is to act as chemo- and mechano-sensors (Satir & Christensen, 2007), to transfer information from the extracellular environment to the inside of the cell. This signal transduction usually leads to a change in transcription rates, and can therefore control a cellular process to suit the needs of the cell. The cilium is thought to be an ideal candidate for passing sensory information to the cell, as it acts to concentrate signalling modules resulting in efficient and rapid signal transduction (Marshall & Nonaka, 2006). It may also order and allow a specific sequence of protein interactions or modifications to occur (Caspary et al, 2007).

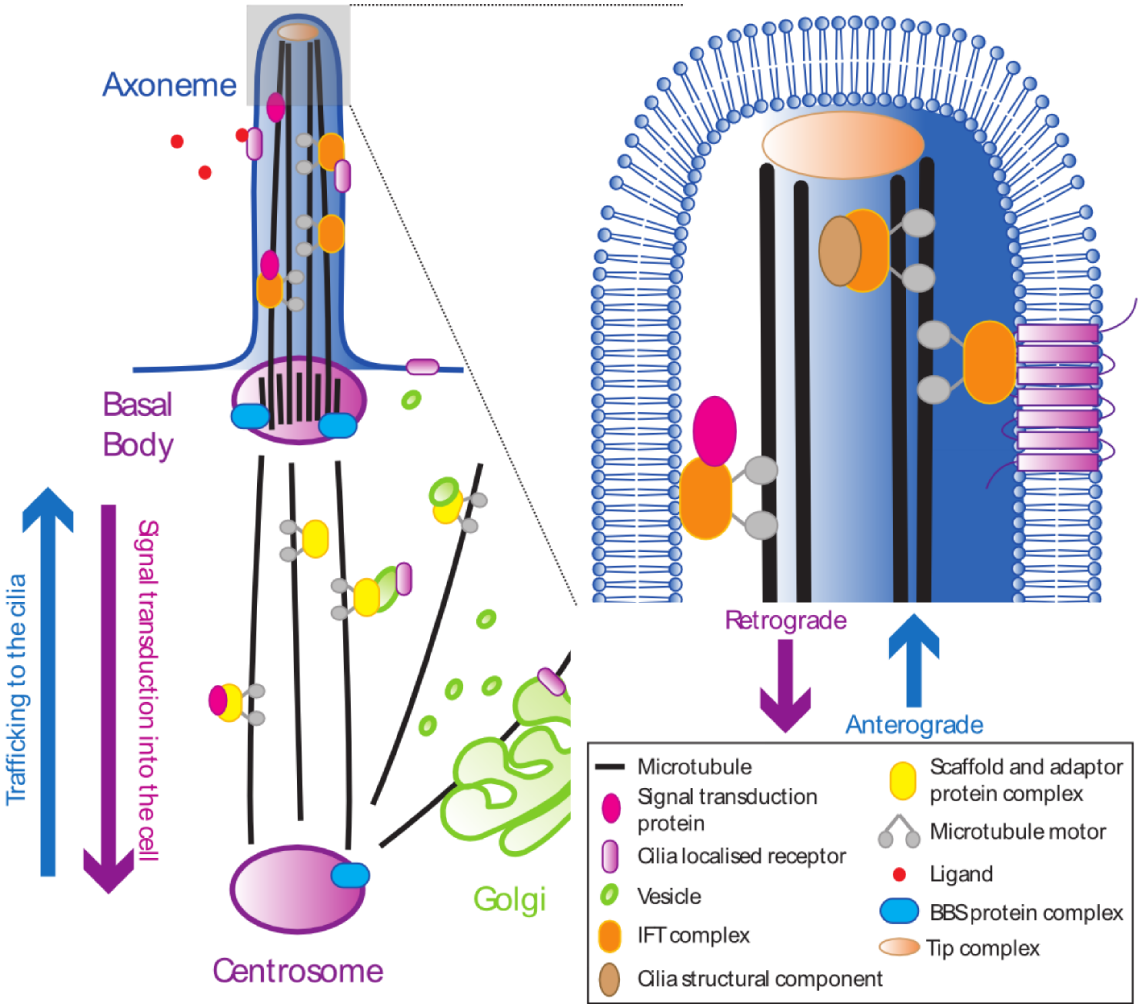

Figure 1.5.1 – Schematic representation of a primary cilium (Sen Gupta et al, 2009)

1.5.1 IFT

The intraflagellar transport (IFT) system is responsible for axoneme assembly and maintenance. It is an ancient process that evolved along with the establishment of cilia in early eukaryotic development (Christensen et al. 2007), and so is highly conserved between many organisms. It is a bidirectional system, consisting of two motors, plus a number of IFT protein particles.

The IFT particles are composed of approximately 17 proteins arranged into two complexes; A and B. Proteins identified in complex A so far include; IFT43, IFT122A, IFT122B, IFT139, IFT140 and IFT144, while IFT20, IFT27, IFT46, IFT52, IFT57, IFT72, IFT74, IFT80, IFT81, IFT88 and IFT172 have been found in complex B (Tobin & Beales, 2009). These complexes are bridged together by accessory proteins, and contain protein-protein interaction motifs like TPRs (tetratricopeptide repeats). These are likely to facilitate the particle's interaction with axonemal and signalling pathway components, to transport them within the cilium.

Proteins that are intended to enter the cilium are transported in vesicles from the golgi to the transition zone, where they are loaded onto IFT protein particles attached to microtubule motor protein complexes. As growth of the cilium occurs from the distal tip (Sen Gupta et al, 2009), the motors move the IFT protein particles and cargo along the microtubules of the cilium in an anterograde direction, to deposit components of ciliary assembly and signalling pathways. They transport material out of the cilium, by moving the particles and cargo in a retrograde direction. Anterograde transport is powered by a kinesin-2 microtubule motor protein, while a cytoplasmic dynein-dynactin motor complex powers retrograde transport.

To prevent accumulation of IFT particles and cargo in the cilium, retrograde transport is slightly faster than anterograde transport, 1.1μm/s and 0.7μm/s respectively (Blacque et al, 2004; Tobin & Beales, 2009). However, it is still unclear how the IFT system switches between the anterograde and retrograde transport motors (Marshall and Nonaka 2006). Disrupting the IFT system can lead to complete loss of cilia, or their stunted growth (Pazour et al, 2000), with obvious repercussions on the signalling pathways that utilise them.

1.5.2 Signalling pathways

Signalling pathways known to rely, at least in part, on primary cilia include; Hh signalling (Haycraft et al, 2005; Roy, 2012), PDGFRα growth factor signalling (Schneider et al, 2010; Schneider et al, 2005), epidermal growth factor signalling (Ma et al, 2005), 5-HT6 serotonin signalling (Brailov et al, 2000), Wnt signalling and polycystin signalling. It is likely though that there are a great many more that have not yet been identified.

Many components of the Hh pathway are enriched in the primary cilium, for example; Gli1, Gli2A and Gli3A (Haycraft et al, 2005; Satir & Christensen, 2007). Smo localises to the cilium in response to Shh stimulation (Corbit et al, 2005), and its translocation, which requires the IFT system (May et al, 2005), is essential, although not sufficient alone, for downstream Hh signalling. Ptch1 has now also been shown to localise to primary cilia in mouse embryonic fibroblasts (MEFs), NIH3T3s (a mouse fibroblast cell line) and mouse embryonic mesoderm cells, but is internalised when bound to Hh, and the complex moves out of cilium (Rohatgi et al, 2007). In mice, Tg737 is the gene encoding IFT88. Cilia are absent in $Tg737^{\Delta 2\text{-}3\beta\text{-}gal}$ mutant mice (complete loss of function), and there is no Gli1 or Ptch1 expression. They have high levels of full length Gli3 which would normally be proteolytically processed to its repressor form in the absence of Hh pathway stimulation. Also, primary cultures derived from the limb buds of these mice lack responsiveness to Shh (Haycraft et al, 2005). Cilia are therefore required for up-regulation of Hh target genes in response to pathway agonists, and are also involved in Gli processing and activity (May et al, 2005). The current view is that primary cilia are essential for normal Hh signal transduction in all systems studied (Roy, 2012).

The platelet derived growth factor (PDGF) pathway is involved in tissue homeostasis, inflammation response and wound healing, and cell growth, proliferation, migration, survival and apoptosis. Dimeric PDGF glycoproteins bind and activate PDGF receptor tyrosine kinase homodimers such as PDGFRαα. PDGFRα and downstream signalling components have been shown to localise to the cilium in mouse fibroblast cells (Schneider et al, 2005). $Tg737^{orpk}$ mutant mice (hypomorphic allele), which have severely malformed cilia, have greatly reduced levels of PDGFRα, and reduced phosphorylation of downstream signalling components, such as Mek1/2 and Erk1/2.

(Schneider et al, 2005). IFT proteins are therefore required for PDGFRα up-regulation and signalling (Schneider et al, 2010).

Canonical Wnt signalling regulates cell fate and patterning during development, while non-canonical PCP signalling is required for organogenesis, for example closure of the neural tube. Several pathway components have been found localised to the cilium, including inversin, β-catenin & APC (Corbit et al, 2005; Satir & Christensen, 2007; Simons et al, 2005). Studies have shown that the cilium is required for Wnt signalling in renal cells, regulating canonical and non-canonical pathway activation to prevent excessive proliferation and allow correct tissue patterning during development (Eggenschwiler & Anderson, 2007; Lienkamp et al, 2012). It is however, not essential in all tissues, and therefore characteristics of disrupted Wnt signalling are not always present in ciliopathic disorders.

Correct polycystin signalling in the kidney works in conjunction with Wnt signalling to regulate cell growth and proliferation. Bending of the cilium as a result of fluid flow causes calcium uptake at PC2, a calcium selective ion channel. This stimulates downstream signalling events which regulate cell proliferation. Incorrect localisation of polycystin and Wnt pathway components, or stunted cilia which cannot bend, may lead to polycystic kidney disease (PKD). Kif3B, a subunit of the kinesin 2 motor, and IFT20 have been linked to ciliary localisation of PC2 (Singla & Reiter, 2006; Wu et al, 2006).

1.6 Nonmotile Ciliopathies

Nonmotile ciliopathies are a class of disorders in which disturbed primary ciliogenesis is accountable for the disease phenotypes. An extensive list has been compiled, so far including; Bardet-Biedl Syndrome (BBS), Nephronophthisis (NPHP), Senior-Loken Syndrome (SNLS), Alstrom Syndrome (ALMS), Meckel Syndrome (MKS), Joubert Syndrome (JBTS), Oral-Facial-Digital Type 1 (OFD 1), Jeune Asphyxiating Thoracic Dystrophy (JATD), Ellis Van Creveld (EVC), Leber Congenital Amaurosis (LCA) and both dominant and recessive Polycystic Kidney Diseases (PKD) (Tobin & Beales, 2009).

However, mixed phenotypes within, and overlapping characteristics between ciliopathies make diagnosis of separate syndromes ever more challenging.

Studying ciliopathies has helped to reveal new insights into cell biology and human genetics, and may also help identify the mechanisms of common medical conditions. Obesity, for example, is a feature of many ciliopathies, but is also an ever increasing health concern in the general population. Understanding the underlying mechanisms that contribute to obesity in patients with ciliopathies may help in the development of patient-wide treatments.

1.6.1 Bardet-Biedl Syndrome

Bardet-Biedl Syndrome (BBS; OMIM 209900) has become the most prominently studied ciliopathy due to its lack of early lethality, while maintaining clear phenotypic affects. It also involves many organ systems, and was the first disease to be associated with primary cilia defects.

It is an autosomal recessive disorder characterised by rod-cone dystrophy, polydactyly, obesity, cognitive impairment, hypogonadism and renal anomalies (Beales et al, 1999), phenotypes that are similar to those observed from disrupted Hh signalling. Neurological problems and developmental delay, polyuria/polydipsia, ataxia and poor coordination, mild spasticity, diabetes mellitus, dental anomalies, hepatic fibrosis and hypertension may also be present (Beales et al, 1999). Thus far, 15 genes have been identified which are mutated in BBS patient cohorts. These are BBS1-12, MKS1, MKS3 (Meckel-Gruber syndrome) and CEP290, however the precise function of each of the proteins encoded by these genes is still being elucidated. Nachury et al. in 2007 described a 438kDa BBSome complex containing seven BBS proteins; 1,2,4,5,7,8,9 (Nachury et al, 2007). These are located in two pools; one at the centriolar satellites, and another within the cilium. Proteins within the BBSomes are required for correct targeting of post-golgi vesicles containing ciliary and signalling components. CEP290 may be involved in BBSome formation (Kim et al, 2008b).

BBS6, BBS10 and BBS12 resemble group II chaperonins, involved in the correct folding of proteins, such as those required for IFT/ciliogenesis (Tobin & Beales, 2007), while MKS1 & MKS3 are required for migration of the mother centriole to the apical

membrane (Tobin & Beales, 2009). BBS3 is an ARL (ADP-ribosylation factor-like) protein, which regulate microtubule dynamics and vesicle trafficking (Sen Gupta et al, 2009), and BBS11 is an E3 ubiquitin ligase.

BBS knockout mice have reduced ciliogenesis and/or cilium maintenance, and tend to be obese, have problems with olfaction and vision, and the males may be infertile due to aflagellate spermatozoa (Nachury et al, 2007; Sen Gupta et al, 2009). If BBS genes are knocked down in cultured cells, the Hh signalling pathway cannot be stimulated with administration of exogenous Shh ligand (Tobin et al, 2008; Tobin & Beales, 2009).

1.7 Zebrafish

Zebrafish (*Danio rerio*) are members of the teleost class of ray-finned fish, which originate from East India and Burma (McGonnell & Fowkes, 2006). They are a tropical freshwater fish, and a novel model organism for the study of endocrine development and disease (Hsu et al, 2006). Their popularity for study is growing due to a number of factors. Firstly they are vertebrates, so share many similarities with mammals, including having the capacity to form primary cilia, and secondly the sequencing of their genome is nearing completion, allowing models of genetic human diseases to be created. They have a short generation time; their body plan is established by 24hpf (hours post fertilisation), and most organs are visible by 5dpf (days post fertilisation). Sexual maturity is reached at about 3 months, and females can lay about 200 synchronously developing eggs weekly. External fertilisation and transparency of the embryos make them easily accessible for developmental studies and the use of molecular markers. While many mutant lines are available, and they are a useful tool for reverse genetics, they also have the advantage of being able to be used to carry out large scale forward genetics and drugs screens (Löhr & Hammerschmidt, 2011). Compared to their murine counterparts, they are smaller, cheaper and easier to maintain.

Most major aspects of the endocrine system and glands are conserved between teleosts and mammals, justifying their use as a model for future endocrine research (Liu, 2007; Löhr & Hammerschmidt, 2011; McGonnell & Fowkes, 2006). While the

tissue organisation may be different, the developmental processes of organogenesis and mechanisms controlling steroidogenesis and endocrine function are similar (Hsu et al, 2009; McGonnell & Fowkes, 2006). The interrenal is the zebrafish counterpart of the mammalian adrenal cortex, and sits at the level of the 3rd somite, with more tissue on the right side than the left (Chai et al, 2003; Hsu et al, 2003). Unlike the layered structural appearance of the adrenal gland, interrenal cells are interspersed with the medullary chromaffin cells, within the cephalic region of the teleost kidney (Grassi Milano et al, 1997; Nandi, 1962). However, as in higher vertebrates, the interrenal cells and developing pronephros are derived from intermediate mesoderm, and the medullary cells arise from the neural crest (An et al, 2002; Hsu et al, 2003; Reid et al, 1995). These three cell types develop in parallel, but are governed by separate signalling events (Hsu et al, 2003). Interrenal cells do not contain lipid droplets, but have other typical ultrastructural characteristics of steroidogenic cells, for example they possess many mitochondria with tubulovesicular cristae (Hsu et al, 2003).

1.7.1 Corticosteroids

Cortisol is the main corticosteroid produced by zebrafish interrenal cells. They do not produce aldosterone due to the absence of aldosterone synthase (CYP11B2) (Bridgham et al, 2006). In the primate adrenal cortex, the zona reticularis produces precursor sex hormones (C_{19} steroids). Unlike in rodents, zebrafish interrenals do possess the CYP17 gene, but it does not have 17,20 lyase activity in these cells, and so no C_{19} steroids are produced. Instead, the dual 17α-hydroxylase and 17,20 lyase activities of CYP17 are reserved for the gonadal cells (Zhou et al, 2007). Zebrafish chromaffin cells produce catecholamines in response to stress (Chai et al, 2003).

In teleosts, POMC in the pituitary is cleaved to form ACTH, which acts at MC2R to stimulate cortisol production, a system which is conserved between species (To et al, 2007). As in POMC null mice, in which adrenal hypoplasia occurs perinatally (Yaswen et al, 1999), MC2R mutant zebrafish only start to show signs of reduced steroidogenesis, and decreased interrenal tissue size/mass at the larval stage, at approximately 5dpf (To et al, 2007). Initial adrenal/interrenal development is therefore pituitary-independent.

Due to the absence of aldosterone, cortisol in zebrafish has both energy metabolism and electrolyte homeostasis functions (Chester-Jones et al, 1987; Wendelaar Bonga, 1997). It exerts its action by binding to either the mineralocorticoid or glucocorticoid receptors (MR and GR respectively). 11-deoxycorticosterone (DOC), the closest hormone resembling aldosterone that fish can synthesise, also binds and can activate the MR (Gilmour, 2005). However, recent experiments by McCormick et al. show that it does not appear to be responsible for salt water adaptation/osmoregulatory functions (McCormick et al, 2008), and rather cortisol does this.

The mechanisms by which cortisol regulates hydromineral balance are not clearly understood, and vary between seawater and freshwater fish. In freshwater fish, such as the zebrafish, water is gained and ions are lost passively, due to the plasma osmotic concentration being higher than that of its surroundings (approximately 1/3rd osmotic concentration of seawater). To maintain this concentration, they produce large quantities of dilute urine, and actively take up sodium and chloride ions at the gills and in the kidneys. In these fish it is thought that cortisol acts via the MR to promote ion uptake at the gills. The opposite is the case in seawater fish, so they must drink water and actively pump out ions at the gills and in the kidneys. It is thought that cortisol acts via the GR in these fish to promote salt secretion (McCormick, 2001; McCormick et al, 2008).

1.7.2 Signalling pathways and transcription factors

Ff1b and ff1d are the zebrafish co-orthologs of mammalian SF-1, a marker of steroidogenic capacity (Chai & Chan, 2000; Kuo et al, 2005; von Hofsten et al, 2005). Ff1b is the earliest molecular marker specifying interrenal cell lineages (Chai et al, 2003), while ff1d specifies gonadal cells (von Hofsten et al, 2005). At 20-22hpf, ff1b is first detected in scattered bilateral cells within the pronephric field (Hsu et al, 2003; To et al, 2007). These proliferating non-steroidogenic cells then migrate medially, and coalesce so that by 24hpf two groups of cells are clearly visible either side of the notochord (Figure 1.7.1). It is at this point that expression of CYP11A1 and StAR are detected within a sub-population of the ff1b-positive cells (Chai et al, 2003; Hsu et al, 2003; To et al, 2007). Fusion of the bilateral cell clusters occurs between 24 and 28hpf

(Hsu et al, 2003), and 3βHSD enzymatic activity begins between 28 and 29hpf (Chai et al, 2003; To et al, 2007).

The use of morpholinos (MO) targeted to ff1b have revealed it is absolutely required for initiation of interrenal primordial differentiation and steroidogenesis (Liu, 2007). Zebrafish embryos injected with MO-ff1b lack interrenal tissue, and therefore CYP11A1 and 3βHSD expression is lost, along with 3βHSD enzymatic activity (Chai et al, 2003). This is analogous to the phenotype described in SF-1 knockout mice (Luo et al, 1994; Luo et al, 1995; Sadovsky et al, 1995). If left to develop to larval stages, they develop fluid accumulation most pronounced in the abdomen, a clear sign of impaired osmoregulation, and a consequence of compromised interrenal steroidogenesis and diminished cortisol production (Chai et al, 2003).

WT1, as in mammals, is essential for interrenal and kidney development in teleosts. It is expressed in the pronephric primordium at approximately 20hpf, from which interrenal cells arise, but is not present in the interrenal cells themselves (Chai et al, 2003; Hsu et al, 2003). WT1 knockdown results in a smaller interrenal primordium with reduced ff1b, showing that WT1 is a determining factor for ff1b expression (Hsu et al, 2003). In mice, WT1 is required for SF-1 activation (Val et al, 2007).

Dax1 expression has also been seen in interrenal cells at 31hpf (Zhao et al, 2006). Zebrafish embryos injected with MO-Dax1 have reduced levels of CYP11A1 and StAR, but there is no change in ff1b expression, or the structural organisation of the interrenal tissue. If allowed to develop to larval stages, these fish have disturbed osmoregulation, indicating interrenal function is impaired. It is therefore hypothesised that zebrafish Dax1, although not required for structural development, may be required for the correct acquisition of some aspects of steroidogenic capacity (Ekker, 2000). Dax1 mutations in humans are responsible for X-linked congenital adrenal hypoplasia (Muscatelli et al, 1994; Zhang et al, 1998).

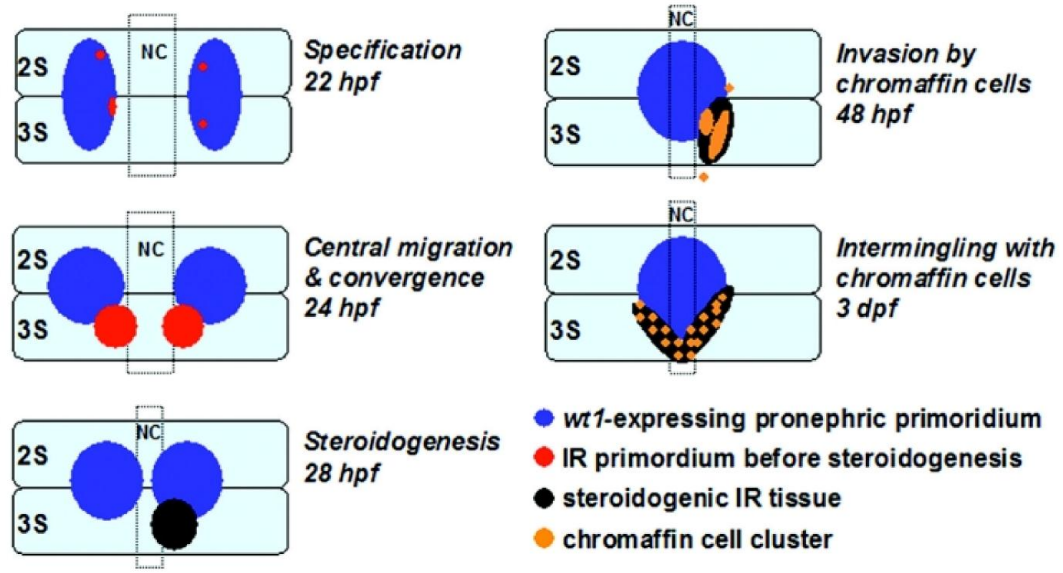

Figure 1.7.1 – Schematic diagram depicting interrenal development in the zebrafish (Liu, 2007)
Dorsal view of the zebrafish embryo at different developmental stages from initial specification of cells, to assembly of the interrenal organ. NC; notochord, 2S; second somite, 3S; third somite, IR; interrenal.

1.7.3 Hh signalling and primary cilia

Experiments by Bergeron et al. indicate that Hh signalling is required, at least in part, for correct interrenal development (Bergeron et al, 2008). Microarray and *in situ* hybridisation analysis showed that both ff1b and WT1 expression was reduced in mutant fish with inactive Hh signalling. Conversely, these transcription factors were increased in fish embryos injected with Shh mRNA. As previously mentioned, WT1 knockdown also results in reduced ff1b expression, so perhaps this is only a secondary characteristic in these experiments. However, disruption of WT1 will have significant implications for both kidney and interrenal development.

The requirement of cilia for Hh and Wnt signalling in non-mammalian vertebrates remains a controversial topic. It was suggested by Lunt et al. that Hh signalling in zebrafish does not require primary cilia (Lunt et al, 2009). However, another report by Huang and Schier attempts to clarify the situation (Huang & Schier, 2009). They suggest that upstream Hh pathway components share functional roles with their mammalian homologues, and are dependent upon cilia. However, the regulation and roles of the Gli transcriptional mediators has diverged. Gli1 is not fully dependent on

Hh signalling (Karlstrom et al, 2003; Ninkovic et al, 2008), and therefore is expressed even in the absence of cilia. Using a germline replacement technique (Ciruna et al, 2002), they generate the MZovl (maternal zygotic oval) mutant. Oval is the gene that codes for IFT88/Polaris, and these mutants lack all cilia. The resultant phenotype is reduced Hh signalling, but in an expanded area, as shown by Ptch1 and Gli1 *in situ* hybridisation. Maximal Hh pathway activation is reduced, but low level signalling does not require cilia. Wnt signalling was not affected in these mutants, and therefore does not rely on cilia for its function. They conclude that there is a conserved requirement of cilia for 'normal' Hh signalling across the entire vertebrate lineage.

1.8 Aims of the project

The key aim of this project is to use cell based and animal models to investigate the role of primary cilia and hedgehog signalling in adrenal function. The human adrenal carcinoma cell line H295R will be used for *in vitro* experiments aimed at advancing our understanding of the role of Sonic Hedgehog signalling in adrenal differentiation, and expanding on preliminary studies indicating that signalling through primary cilia may be involved in this process. The use of mouse and zebrafish models of ciliopathies will also be used to indicate the likely outcomes of cilia defects on adrenal function *in vivo*.

CHAPTER 2: MATERIALS AND METHODS

All chemicals were obtained from Sigma Aldrich unless otherwise stated.

2.1 Cell culture

The human adrenocortical carcinoma cell line H295R (CRL-2128) was obtained from Ian Mason, University of Edinburgh and grown at 37°C with 5% CO_2 in 50% DMEM (Dulbecco's Modified Eagles Medium), 50% Nutrient Mixture F12 Ham, supplemented with 2% Ultroser G (BioSepra), 1% ITS (containing 1mg/ml insulin, 0.55mg/ml transferrin and 0.5μg/ml sodium selenite) and 1% Pen/Strep (5000U/ml penicillin and 5mg/ml streptomycin) (Cobb et al, 1996). The mouse fibroblast cell line Shh Light II (CRL-2795) was obtained from Phil Beachy, The Johns Hopkins University School of Medicine, USA. These cells were grown at 37°C with 10% CO_2 in DMEM containing 4mM L-glutamine, 4.5g/L glucose and 3.7g/L sodium bicarbonate, supplemented with 10% FBS (heat-inactivated foetal bovine serum; Invitrogen), 0.4mg/ml G-418 and 0.15mg/ml Zeocin (Invitrogen) (ATCC product information sheet for CRL-2795).

2.1.1 Trypsinisation

Media was removed from the culture flask or dish and cells washed with DPBS (Dulbecco's Phosphate Buffered Saline). Trypsin-EDTA (0.5g/l trypsin, 0.2g/l Ethylenediaminetetraacetic acid; Invitrogen) was used to detach the cells for 2-5 minutes, and then inactivated by adding media containing 10% FBS. The cell suspension was centrifuged at 160 x g (times gravity) for 5 minutes and the supernatant was removed. The cell pellet was then re-suspended in fresh media and cells were re-plated as required.

2.1.2 Freezing down cells

Cells were grown until confluent, then trypsinised and transferred to a 15ml falcon tube. They were centrifuged at 160 x g for 5 minutes and the media removed. The cell pellet was then re-suspended in a freezing solution containing 90% FBS and 10% DMSO

(Dimethyl Sulfoxide), and cooled at a maximum of 1°C/min to -80°C in 1ml cryotubes. The tubes were transferred to a liquid nitrogen tank for long term storage.

2.1.3 Counting cells – Haemocytometer

After trypsinising, a 50µl sample of cells was removed and injected into the channel of a slide displaying two haemocytometer grids (Figure 2.1.1). Cells were counted in four corners of one of the grids on the slide using the Leica DMIL light microscope with 10x objective. Each corner has an area of 1mm^2 and a depth of 0.1mm, making the volume 100nl. If more than 500 cells were counted, the cell stock was diluted and another sample taken. If there were fewer than 200 cells, all four corners of both grids were counted. The following calculations were then made;

$$\frac{number\ of\ cells\ counted}{number\ of\ corners\ counted} = number\ of\ cells/100nl$$

$$number\ of\ cells/100nl \times 10^4 = number\ of\ cells/ml$$

$$number\ of\ cells/ml \times millilitres\ of\ media\ in\ which\ the\ cells\ were\ diluted = total\ number\ of\ cells$$

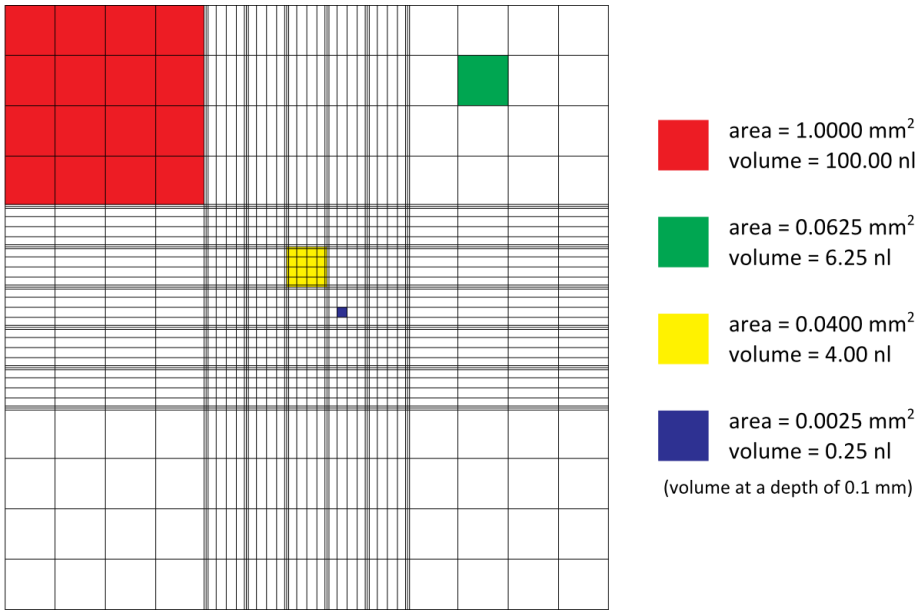

Figure 2.1.1 – Haemocytometer Grid, adapted with permission from (Wheeler, 2010)

2.2 Differentiation

H295R cells were seeded into 6- or 12-well plates and grown until 60-70% confluent. They were then differentiated over a 72-96 hour period, with fresh media containing 10µM Angiotensin II (AngII) or Forskolin (Fsk) added at 0, 24, 48 and 72 hour time points. At the end of the differentiation period, cells were harvested to make RNA, an ELISA assay performed, or if grown on cover slips assayed for 3βHSD content. Some cells were also treated with 0.35µg/ml ShhN (R&D systems) at the same time as AngII or Fsk treatments. Cells transfected with siRNA were differentiated for 40hrs, with 10µM AngII or Fsk given at 0 and 24 hours.

AngII increases intracellular calcium levels, stimulating PKC signalling that preferentially induces CYP11B2 expression, and therefore aldosterone production (Bird et al, 1993; Cobb et al, 1996). Fsk activates adenylate cyclase to increase cAMP levels, thus activating PKA, and preferentially inducing CYP11B1 expression and cortisol production (Denner et al, 1996; Oskarsson et al, 2006).

2.3 RNA Extraction

Cells grown in 6- or 12-well plates were washed with cold PBS (Phosphate Buffered Saline containing 0.01M phosphate buffer, 0.0027M potassium chloride and 0.137M sodium chloride, pH7.4), and lysed directly in the wells by adding 350µl buffer RLT from the Qiagen RNeasy mini kit, containing β-mercaptoethanol. Lysis was aided by using a cell scraper, and then the contents of the wells were transferred to 1.5ml microfuge tubes. RNA was extracted from all samples as described in the Qiagen RNeasy mini kit. The RNA concentration was determined by measuring the optical density of the samples at 260nm using the Nanodrop ND-1000 spectrophotometer.

2.3.1 DNase treatment

2µg RNA, 5µl 10x DNase Turbo buffer (Ambion), 0.5µl RNase inhibitor (40u/µl; Promega) and 1µl Deoxyribonuclease I (≥ 10,000u/mg) were placed in a 1.5ml microfuge tube, and RNase free water (Qiagen) added to a final volume of 50µl.

Samples were then briefly vortexed and centrifuged, and incubated at 37°C for 15 minutes. DNase treatment cleaves and fragments any genomic DNA contamination within the samples. The RNase inhibitor prevents RNases degrading the RNA during the treatment.

2.3.2 Phenol extraction

An amount of phenol (pH4.7) equal to the volume of each sample was added to the microfuge tubes. They were then vortexed for 30 seconds, and centrifuged for 1 minute at >10,000 x g. The upper aqueous layer was removed into a new 1.5ml microfuge tube, and the organic and inter- phases discarded. Phenol is an organic solvent acid used to denature and remove protein contaminants from the RNA. With a pH of 4.7 is will also denature contaminating genomic DNA, so only RNA is partitioned into the aqueous phase.

2.3.3 RNA precipitation

To precipitate RNA from the residual phenol, 3M sodium acetate buffer - pH5.3 (BDH Chemicals) was added at an amount equal to 1/10th of the volume of RNA, along with 2µl glycogen (5mg/ml; Ambion) and 125µl ethanol (2 ½ times the volume of RNA). The samples were then incubated at -20°C for 1 hour or -80°C for 20-30 minutes. After leaving for the allotted time the samples were centrifuged for 10 minutes at 4°C and >10,000 x g to pellet the precipitate. The supernatant was then aspirated and the pellet washed with 70% ethanol to dissolve the sodium acetate. Samples were centrifuged again at 4°C and >10,000 x g for 5 minutes, and the ethanol aspirated.

2.4 First strand cDNA synthesis

To each 2µg pellet of RNA, 12.5µl RNase free water and 0.25µl random primers (500µg/ml; Promega) were added. They were vortexed to dissolve the RNA, and centrifuged briefly before being heated to 80°C for 10 minutes to denature the hydrogen bonds within the single stands of RNA. Samples were then cooled on ice for

1-2 minutes to allow the random primers to anneal within the secondary structure of the RNA, and given a quick centrifuge to ensure pooling of any condensation.

At this point, 1µl was removed from each sample and placed in separate PCR tubes for use as negative reverse transcription (RT) controls. A master mix containing 4µl 5x MMLV RT-buffer (Promega), 2µl DTT (Dithiothreitol 0.1M), 1µl dNTPs (deoxynucleoside triphosphates 10mM A+C+G+T; Promega), 0.5µl RNase inhibitor (40u/µl) and 1µl MMLV RT-enzyme (200u/µl; Promega) per sample was created, and 8.5µl added to each tube (total volume now 20µl). Samples were then vortexed and briefly centrifuged, prior to being incubated at 37°C for 1 hour to allow reverse transcription to occur. After incubation 20µl of distilled water was used to dilute each sample 1 in 2. cDNA was stored at -20°C.

2.5 Polymerase chain reaction

Each 10µl reaction contained 1µl cDNA, 0.5µl dNTPs (10mM A+C+G+T), 1µl primers (10µM Forward+Reverse), 2µl 10x PCR buffer, 15.25µl H_2O and 0.25µl Taq (*Thermus aquaticus*) DNA polymerase (5u/µl).

Standard Program:

Cycles	Temperature	Time	
1	94°C	5 minutes	
35	94°C	30 seconds	**Strand separation** - denaturation of hydrogen bonds within the double stranded cDNA
	58°C	30 seconds	**Annealing** - allows the primers to bind to a section of the single stands of DNA for which they have been specifically designed. This temperature may vary slightly depending on the T_m (melting temperature) of the primers
	72°C	30 seconds	**Extension** - Taq DNA polymerase binds to the primers and uses dNTPs as building blocks to enzymatically synthesise a complementary strand of DNA. The newly formed cDNA contains one strand of parental DNA, and one newly synthesised strand. This process is repeated 25-35 times to amplify the piece of DNA between the forward and reverse primer sequences
1	72°C	7 minutes	Further elongation
1	4°C	∞	Preservation

2.5.1 Gel electrophoresis

After cDNA amplification, samples were combined with 5µl of loading dye containing bromophenol blue (Fermentas) and loaded onto a 1-2% agarose gel containing 0.5µg/ml ethidium bromide, within an electrophoresis chamber filled with TAE buffer (Tris-acetate-ethylenediamenetetraacetic acid buffer; National Diagnostics). The loading dye adds weight to the cDNA to contain it within the wells of the gel. The percentage gel depends on the size of cDNA that has been amplified, as higher molecular weights are separated more easily on lower percentage gels. An electrical current was passed through the tank, and the cDNA visualised in the gel using a UVP UV transilluminator.

2.5.2 Primers, probes and siRNA sequences

Table 2.5.1 – Sequences

Description	T_m (˚C)	Annealing Temperature (˚C)	Sequence 5' – 3'	Product Length (bps)
18S Forward + Reverse		60	Eurogentec RT-CKFT-18S	121
GAPDH Forward	62.5	58-60	TGCACCACCAACTGCTTAG	177
GAPDH Reverse	63.0		GGATGCAGGGATGATGTTC	
Reverse complement			GAACATCATCCCTGCATCC	
PPIA Forward	60.0	58-60	TTCATCTGCACTGCCAAGAC	158
PPIA Reverse	60.0		TCGAGTTGTCCACAGTCAGC	
Reverse complement			GCTGACTGTGGACAACTCGA	
Shh Forward	64.9	58-60	ACATCACCACGTCTGACCG	218
Shh Reverse	65.1		GCTCAGGTCCTTCACCAGC	
Reverse complement			GCTGGTGAAGGACCTGAGC	
Ptch1 Forward	63.8	58-60	TGATGTTTTTCTTCTGGCCC	209
Ptch1 Reverse	64.0		ACACCACTACTACCGCTGCC	
Reverse complement			GGCAGCGGTAGTAGTGGTGT	
Ptch2 Forward	63.6	58-60	AAAATGGAATGATTGAGCGG	217
Ptch2 Reverse	64.0		GCCTTGTCTAGCAGCTCCC	
Reverse complement			GGGAGCTGCTAGACAAGGC	
Smo Forward	63.8	58-60	CAAAGCGGATCAAGAAGAGC	240
Smo Reverse	63.7		TGACAGAAATATCCTGGGGC	
Reverse complement			GCCCCAGGATATTTCTGTCA	
Gli1 Forward	63.7	58-60	CTACAGTGGAGCCCAAGAGG	209
Gli1 Reverse	64.2		GGAGAGGTCTTCAGTGCTGC	
Reverse complement			GCAGCACTGAAGACCTCTCC	
Gli2 Forward	63.6	58-60	CAAGGAAGATCTGGACAGGG	205
Gli2 Reverse	64.0		CTTGAAGGGCTTCTGCTCC	
Reverse complement			GGAGCAGAAGCCCTTCAAG	
Gli3 Forward	63.7	58-60	TATGCAGCCACAGAATGTCC	216
Gli3 Reverse	64.2		AAGGCAGGGAAAAGATGAGG	
Reverse complement			CCTCATCTTTTCCCTGCCTT	
FoxD1 Forward	59.8	58-60	TATCGCGCTCATCACTATGG	217
FoxD1 Reverse	60.9		GTCCAGCGTCCAGTAGTTGC	

Reverse Complement			GCAACTACTGGACGCTGGAC	
NR4A1 Forward	66.4	58-60	ATACACCCGTGACCTCAACCA	151
NR4A1 Reverse	67.3		TTCTGCACTGTGCGCTTGAA	
Reverse complement			TTCAAGCGCACAGTGCAGAA	
(Bassett et al, 2004a; Bassett et al, 2004b)				
IFT88 Forward	63.9	58-60	GAGAGGCTCTGCATTTGACC	197
IFT88 Reverse	64.1		TTCTTCCTGCATCTTTTGCC	
Reverse complement			GGCAAAAGATGCAGGAAGAA	
BBS4 Forward	60.0	60	ACTTTGATGTTGCCCTCACC	143
BBS4 Reverse	59.9		GTAGTTGGCTCGTTTCAGGC	
Reverse complement			GCCTGAAACGAGCCAACTAC	
BBS6 Forward	60.2	60	CCTCAGGTAGGCTGAAGCAG	126
BBS6 Reverse	59.8		TGGAGGCTGTCAGGATCTTT	
Reverse complement			AAAGATCCTGACAGCCTCCA	
AT1 Forward	77.8	58-60	GGCCCTCGGCGGGACGTG	Variable depending on splicing
AT1 Reverse	59.9		ACTGTATAAAGTAGGAATCAT	
Reverse complement			ATGATTCCTACTTTATACAGT	
(Warnecke et al, 1999)				
18S Forward + Reverse (Taqman)		60	Eurogentec RT-CKFT-18S	121
18S Taqman probe			Eurogentec RT-CKFT-18S FAM-TAMRA	
CYP11B1/B2 Forward (Taqman)	66.5	60	GGCAGAGGCAGAGATGCTG	CYP11B1 72 CYP11B2 71
CYP11B1 Reverse (Taqman)	66.3		TCTTGGGTTAGTGTCTCCACCTG	
Reverse complement			CAGGTGGAGACACTAACCCAAGA	
CYP11B2 Reverse (Taqman)	65.5		CTTGAGTTAGTGTCTCCACCAGGA	
Reverse complement			TCCTGGTGGAGACACTAACTCAAG	
CYP11B1 Taqman probe	75.3		TGCTGCACCATGTGCTGAAACACCT FAM-TAMRA	
CYP11B2 Taqman probe	72.0		CTGCACCACGTGCTGAAGCACT FAM-TAMRA	
(Fallo et al, 2002)				

Negative control siRNA	Applied Biosystems AM4611
siIFT88 Sense	GGCAGUUACUAGACCUAUAtt
Target sequence	GGCAGTTACTAGACCTATAGC
siIFT88 Antisense	UAUAGGUCUAGUAACUGCCgt
Target sequence	GCTATAGGTCTAGTAACTGCC
siBBS4 Sense	CUCAAUUUCCUGUAUCUACtt
Target sequence	CTCAATTTCCTGTATCTAC
siBBS4 Antisense	GUAGAUACAGGAAAUUGAGtt
Target sequence	GTAGATACAGGAAATTGAG
siBBS6 Sense	GAGUGAACCACUGACAACUtt
Target sequence	GAGTGAACCACTGACAACT
siBBS6 Antisense	AGUUGUCAGUGGUUCACUCtt
Target sequence	AGTTGTCAGTGGTTCACTC

2.5.3 Gel purification

After cutting out a band of cDNA from the agarose gel, a volume of 6M NaI (sodium iodide) three times that of the gel was added, and heated to 55°C for 5 minutes to dissolve the agarose. 10µl of glass milk (silica in suspension in 3M NaI) was then used to absorb the nucleic acid for 5 minutes at room temperature, and a pellet of cDNA collected by centrifugation for 15 seconds at >10,000 x g. The supernatant was aspirated, and the pellet washed twice with New Wash containing 50mM NaCl (sodium chloride), 10mM TrisHCl pH7.5 (Tris Base; Fisher BioReagents, HCl; BDH chemicals), 50% ethanol and 7.5mM EDTA to remove impurities. The pellet was then re-suspended in 10µl distilled H_2O, heated to 55°C for 2 minutes, and centrifuged for 1 minute at >10,000 x g, to elute the cDNA from the silica (Brown, 1997). The supernatant was transferred to a new tube, and either sent for sequencing, or made up to 50µl with distilled H_2O for use in real-time qPCR standard curves.

2.6 Real-time qPCR

A DNA template is replicated, as in end-point PCR, but then quantified in real time by the detection of fluorescence. The amount of fluorescence recorded is proportional to the amount of DNA amplified, so DNA copy numbers, and therefore mRNA levels can be determined. The Ct value is the threshold cycle value, and the point at which amplification is first detectable above background fluorescence. A lower Ct indicates a greater amount of amplification target in the starting DNA. The Ct is measured during the exponential phase of replication, before a plateaux is reached, and is best recorded just as the fluorescent threshold has been met. A standard curve of known DNA concentrations for each gene of interest (GOI) is used to calculate the DNA copy numbers from the Ct values. The quantity of a reference RNA, such as GAPDH or 18S ribosomal RNA (Ginzinger, 2002), is also determined to account for differences in the amount of cDNA loaded. A sample containing H_2O instead of cDNA, termed the no template control (NTC), is measured to distinguish between actual gene expression and background. The Ct of the NTC must either be undetectable, or much higher than that of the GOI.

The following criteria were used for results inclusion;

$$standard\ curve\ gradient = -3.3\ (\pm 0.3)$$
$$efficiency = 100\%\ (\pm 10\%)$$
$$R^2 = 0.97 - 1.00$$

2.6.1 $SYBR_{GREEN}$ I

$SYBR_{GREEN}$ is a DNA-binding dye that will fluoresce with light excitation when bound to double stranded DNA. This method of generating a fluorescent signal is cheap and easy to use, as the same dye can be used for all genes. However, this does mean it lacks in specificity, so the quantity of only one gene per well can be measured. Amplification in the NTC is also often seen, as it cannot distinguish between real template and artefact bands, such as those created by primer-dimers.

Each 10µl reaction contained 2µl cDNA template, 5µl 2x $SYBR_{GREEN}$ I master mix (KapaBiosystems), 0.2µl low ROX (KapaBiosystems), 0.5µl primers (10µM Forward+Reverse) and 2.3µl sterile H_2O. The 2x $SYBR_{GREEN}$ I master mix contains the $SYBR_{GREEN}$ I fluorescent dye, $MgCl_2$, dNTPs, stabilisers and DNA polymerase. ROX is used as a reference dye for evaporation during cycling. See Table 2.5.1 for list of primers.

Using the Stratagene MX4000 real-time thermocycler a quantitative cycle program was selected, with results displayed as DNA copy numbers. Comparisons of the data can be made once the GOI values have been divided by the values obtained for the reference gene.

Quantitative fast cycle program:

Cycles	Temperature	Time	
1	95°C	3 minutes	
35	95°C	3 seconds	Strand separation
	60°C	30 seconds	Annealing and extension
	72°C	1 second	
1	95°C	1 minute	
1	60°C	30 seconds	Dissociation melt
1	95°C	30 seconds	

The dissociation melt separates double stranded DNA back to its single stranded form. As different genes have different melting temperatures, the quality of the amplification product can be assessed. All wells amplified with the same primers should contain the same cDNA, with only one peak detected. Primer-dimers, or amplification of more than one DNA template may result in a second smaller peak.

2.6.2 Taqman

The Taqman method for generating a fluorescent signal requires specifically designed dual-labelled oligonucleotide probes, with a 5' fluorophore such as FAM (6-carboxyfluorescein), in close proximity to a 3' quencher such as TAMRA (tetramethylrhodamine). This probe will bind a region in the 3'-5' strand of the cDNA targeted for amplification, without emitting a fluorescent signal due to FRET (fluorescence resonance energy transfer) by the quencher. As this strand is amplified by extension of the primers, the probe is degraded by the exonuclease activity of Taq polymerase, allowing the fluorophore to move away from the quencher, and a fluorescent signal to be detected.

By specifically designing probes that anneal to the region of DNA for amplification, fluorescence is directly correlated to the amount of real template, without the detection of artefact bands. This means there should be no amplification in the NTC, and there is little need to perform a dissociation melt. Multiple probes, and corresponding primers, can also be added to the same well to record the expression of several genes, provided they utilise different fluorophores and quenchers. However, with increased specificity comes an increase in cost, as new probes must be created for every gene template.

Each 10µl reaction contained 2µl cDNA template, 5µl 2x Taqman Universal PCR master mix (Applied Biosystems), 0.5µl primers (10µM Forward+Reverse), 0.2µl Taqman probe (10µM) and 2.3µl sterile H_2O. The Taqman master mix contains AmpliTaq Gold DNA polymerase, dNTPs, a passive reference dye, buffer components and AmpErase UNG to prevent reamplification of carryover PCR products. See Table 2.5.1 for a list of primers and probes.

Plates were run by the Queen Mary Genome Centre, using the ABI 7900HT Fast Real-time PCR instrument, and a quantitative cycle program.

Quantitative cycle program:

Cycles	Temperature	Time	
1	50°C	2 minutes	UNG activation
1	95°C	10 minutes	Strand separation, AmpliTaq Gold DNA polymerase activation and UNG inactivation
40	95°C	15 seconds	Strand separation, annealing and extension
	60°C	1 minute	
1	4°C	∞	Preservation

2.7 Transfections

Lipofectamine 2000 (Invitrogen) was diluted with optimem I (Gibco), and left to stand at room temperature for 5 minutes. The DNA or RNAi was also diluted with optimem I then combined with the lipofectamine, vortexed, and left at room temperature for 20 minutes. Cells were then given fresh media and 100µl of the lipofectamine/DNA or lipofectamine/RNAi mix. After 8-24 hours the media was changed again. Table 2.7.1 shows the quantities used for transfection.

Table 2.7.1 – Quantities used for transfection, adapted from Invitrogen Lipofectamine 2000 data sheet

Cell type	Culture vessel	Surface area per well	Shared reagents		DNA transfection		RNAi transfection	
			Volume of plating medium	Volume of dilution medium	DNA	Lipofectamine 2000	RNA	Lipofectamine 2000
H295R	6-well	$10cm^2$	1ml	2 x 50µl	6µg	10µl	100nM	7µl
H295R	12-well	$4cm^2$	500µl	2 x 50µl	3µg	5µl	100nM	4µl

2.7.1 siRNA transfections

H295R cells were seeded into 12-well plates and grown until 40-60% confluent. They were then transfected with 100nM siRNA, or a negative control (small interfering RNA; Applied Biosystems), using 4µl Lipofectamine 2000. After a minimum of 8 hours the media was changed, and some cells differentiated with the addition of 10µM

angiotensin II or forskolin at 8 and 32 hours after transfection (0 and 24 hours into the differentiation period, see section 2.2). Cells transfected with siRNA were grown for a maximum of 48 hours before being harvested to make RNA or for protein analysis, or if grown on cover slips processed for immunofluorescence.

2.7.2 Dual-Luciferase reporter transfections

H295R cells were seeded into 6- or 12-well plates and grown until approximately 70% confluent. They were then co-transfected with a firefly luciferase "experimental" reporter, and the pRL-CMV *Renilla* luciferase "control" reporter (Promega). After 48 hours cells were harvested and a dual-luciferase reporter assay conducted. The "control" reporter is used to measure baseline luciferase activity inside the cells that should not vary with expression of the transcription factor of interest. The "experimental" reporter contains a promoter with binding sites for the transcription factor of interest, upstream of the firefly luciferase gene (Promega Technical Manual TM040).

2.8 Dual-Luciferase reporter assay

Cells co-transfected with a firefly luciferase "experimental" reporter, and the pRL-CMV *Renilla* luciferase "control" reporter (Promega) were washed twice in ice cold PBS. They were lysed by the addition of 120µl 1x passive lysis buffer (Promega) and the use of a cell scraper. Cell lysates were collected in 1.5ml microfuge tubes and incubated on ice for 20 minutes. After pelleting the cell debris by centrifuging for 1 minute at >10,000 x g, the supernatant was removed and 30µl transferred to a white walled 96-well plate (Greiner Bio-One). The Promega Dual-Luciferase Reporter Assay System Kit, and BMG Labtech Omega luminometer were used to measure luciferase activities. Briefly, 80µl of Luciferase Assay Reagent II (LARII) was injected into the well containing the lysate. The firefly luciferase produced by the "experimental" reporter gene catalyses the conversion of beetle luciferin within LARII to oxyluciferin releasing a luminescent signal. 80µl of Stop & Glo Reagent was then injected into the well,

quenching the firefly luminescence reaction, and simultaneously activating the *Renilla* luciferase reaction, by providing the substrate coelenterazine. Coelenterazine is converted by the *Renilla* luciferase produced by the "control" reporter into coelenteramide and releases a luminescent signal. Both luminescent signals were measured, and the final luciferase values calculated by dividing the firefly luciferase readings by the *Renilla* luciferase values (Promega Technical Manual TM040).

2.9 Shh Light II luciferase reporter assay

Shh Light II cells were seeded into 12-well plates. After reaching confluence they were grown for a further 24 hours to achieve full contact inhibition of growth. They were then treated with 8µl/ml DMSO, 2µM Purmorphamine (Calbiochem), 0.35µg/ml ShhN (R&D Systems), 200nM SAG (Enzo Life Sciences), 2µM Cyclopamine (LC Laboratories), 2µM Tomatidine, 20nM Vismodegib (LC Laboratories), 2µM Sant1 (Tocris Bioscience), 10µM Forskolin, or 80µg/ml Cycloheximide (Calbiochem) in DMEM supplemented with 0.5% FBS and 5mM HEPES buffer (pH 7.4). After 48 hours the cells were washed with ice cold PBS, and lysed using 120µl of 1x passive lysis buffer (Promega) and a cell scraper. The contents of the wells was then transferred to 1.5ml microfuge tubes and incubated on ice for 20 minutes. The tubes were centrifuged for 1 minute at >10,000 x g to pellet the cell debris, and 30µl of the supernatant loaded into a white walled 96-well plate. (Greiner Bio-One). As in the dual-luciferase reporter assay system, the Promega kit and BMG Labtech Omega luminometer were used to measure luciferase activities. Shh Light II cells are stably transfected with the GLI-responsive firefly luciferase "experimental" reporter (Sasaki et al, 1997), and pRL-TK constitutive *Renilla* luciferase "control" reporter (Promega) (ATCC product information sheet for CRL-2795).

2.10 Enzyme-Linked Immunosorbent Assay (ELISA)

2.10.1 Aldosterone and Cortisol

H295R cells were seeded into 12-well plates and differentiated for 96 hours with AngII or Fsk (see section 2.2). The media was then removed and centrifuged for 15 seconds at >10,000 x g to pellet any debris, and 25µl of supernatant was added to each well of a Demeditec ELISA microtiter plate. Plates were pre-coated with either an anti-aldosterone or an anti-cortisol antibody. A standard curve containing known quantities of aldosterone or cortisol was also plated. 150µl of enzyme conjugate containing horseradish peroxidase was then added to each well and mixed for 10 seconds before being incubated at room temperature. After 60-90 minutes the contents of the wells were removed, and the wells washed five times with wash solution. 200µl of substrate solution containing tetramethylbenzidine was added to each well and incubated for 15-20 minutes at room temperature. The enzyme reaction was stopped by adding 100µl of stop solution, and the absorbance measured at 450nm using the Perkin Elmer Wallac Victor2 1420 Microplate reader. Aldosterone and cortisol concentrations were determined from the absorbance values generated by the standard curve.

2.10.2 Corticosterone

25µl of mouse serum was added to each well of an Abnova ELISA microplate, pre-coated with an anti-corticosterone antibody. A standard curve containing known quantities of corticosterone was also plated. 25µl of biotinylated corticosterone was then added to each well and incubated at room temperature for 2 hours. The contents of the wells were removed, and the wells washed five times with wash buffer. 50µl of streptavidin-peroxidase conjugate was then added to each well. After 30 minutes incubation at room temperature, as before, the wells were washed five times with wash buffer. 50µl of chromogen substrate containing tetramethylbenzidine was then added to the wells and incubated for 20 minutes at room temperature. The enzyme reaction was stopped by adding 50µl of stop solution, and the absorbance measured at 450nm using the Perkin Elmer Wallac Victor2 1420 Microplate reader. The

concentration of corticosterone was determined from the absorbance values generated by the standard curve.

2.11 Cytotoxicity assays

2.11.1 Lactate dehydrogenase (LDH)

H295R cells were seeded into 96-well plates at a concentration of approximately $4x10^4$ cells per well, and left to attach overnight. They were then treated for 72 hours with 8µl/ml DMSO, 2µM Purmorphamine (Calbiochem), 0.35µg/ml ShhN (R&D Systems), 200nM SAG (Enzo Life Sciences), 2µM Cyclopamine (LC Laboratories), 2µM Tomatidine, 20nM Vismodegib (LC Laboratories), 2µM Sant1 (Tocris Bioscience), 10µM Forskolin, or 80µg/ml Cycloheximide (Calbiochem). The Promega CytoTox 96 Non-Radioactive Cytotoxicity Assay Kit was used to measure LDH levels. To record an average maximum LDH level, 10µl of lysis solution was added to six untreated wells of the 96-well plate containing cells to be analysed, and incubated at 37°C with 5% CO_2 for 45 minutes. The media was then removed from all wells, centrifuged for 15 seconds at 4°C and >10,000 x g to pellet any debris, and 50µl of supernatant added to each well of a new 96-well plate. 50µl of fresh media was also added to three of the wells to obtain an average background reading. 50µl of substrate mix was added to each sample, the plate gently mixed, and left for 30 minutes at room temperature protected from light. After 30 minutes 50µl of stop solution was added to each sample, the plate gently mixed, and the absorbance measured at 490nm using the Perkin Elmer Wallac Victor2 1420 Microplate reader. The average background absorbance value was subtracted from each of the other absorbencies recorded, and the maximum LDH values adjusted for the dilution created by adding the lysis solution. The percentages of cytotoxic cells were then calculated using the following equation;

$$\frac{experimental\ LDH\ release\ (OD_{490})}{maximum\ LDH\ release\ (OD_{490})} = \%\ cytotoxicity$$

2.11.2 Fluorescence-activated cell sorting (FACS)

H295R cells were seeded into T-25 flasks at a concentration of approximately $0.7x10^6$ cells per flask, and left to attach overnight. As above, they were treated with 8µl/ml DMSO, 2µM Purmorphamine (Calbiochem), 0.35µg/ml ShhN (R&D Systems), 200nM SAG (Enzo Life Sciences), 2µM Cyclopamine (LC Laboratories), 2µM Tomatidine, 20nM Vismodegib (LC Laboratories), 2µM Sant1 (Tocris Bioscience), 10µM Forskolin, or 80µg/ml Cycloheximide (Calbiochem). After 72 hours, the media was removed and collected in 50ml falcon tubes, along with any PBS used to wash the cells. The cells were then trypsinised and added to the previously collected media. The tubes were centrifuged for 5 minutes at 160 x g, and the cell pellet washed with PBS. The cells were fixed in 70% ethanol at 4°C overnight. After fixation, the ethanol was removed by centrifuging the cells for 5 minutes at 690 x g, and washing them with PBS. The cell pellet was then re-suspended at a concentration of 1-2 x 10^6 cells per ml in a PI/RNase mixture containing 50µg/ml propidium iodide, 100µg/ml RNase A and 3.8mM sodium citrate in sterile PBS, and incubated overnight at 4°C, protected from light. The samples were transferred to FACS tubes and analysed by flow cytometry, using the LSRII flow cytometer with FACSDiva software (v 5.1.03; BD Biosciences). 50,000 events were recorded per sample, with gating on pulse width and area to exclude clumps and doublets. Propidium iodide excitation occurs at 488nm, with emission collected in the 610-620 channel.

2.12 Protein Analysis

2.12.1 Western Blot

Cells were washed with cold PBS, and lysed by the addition of 120µl SDS PAGE (Sodium Dodecyl Sulfate PolyAcrylamide Gel Electrophoresis) buffer containing 4% SDS, 20% glycerol, 10% 2-mercaptoethanol, 0.004% bromophenol blue, 0.125 M Tris HCl – pH6.8 and protease inhibitors, followed by scraping. The lysates were transferred to 1.5ml microfuge tubes and heated to 95°C for 2-5 minutes. They were then centrifuged briefly, and 15µl of each sample was loaded on an Invitrogen NuPAGE Bis-Tris gel. The

gel was run at 150V for approximately 1 hour 15 minutes using MOPS running buffer containing SDS (Invitrogen).

Semi-dry transfer was carried out at 15V for 45 minutes using a nitrocellulose transfer membrane (Whatman), and transfer buffer containing 25mM Tris base, 192mM glycine and 20% methanol. The membrane was blocked with 5% milk powder for 1 hour, then incubated overnight with primary antibodies for β-tubulin and IFT88 or BBS4 (Table 2.12.1) . After washing in PBS-tween 0.1%, the secondary antibodies were added for 45 minutes.

The membrane was scanned using the Licor Odyssey infrared scanner. This system involves direct scanning of the membrane by two independent lasers, allowing detection of the infrared fluorescence emitted by two different secondary antibodies. The two colour detection system uses a 700nm and an 800nm channel, pseudo-coloured with red and green respectively. Images of the blots were quantified using the Licor Odyssey imaging systems software.

Table 2.12.1 – Antibodies used for western blotting

Ab	Antigen/Fluorophore	Species	Company	Dilution
1°	β-tubulin	Mouse monoclonal	Sigma Aldrich T8328	1 in 5000
2°	IRDye 680CW	Donkey anti-mouse	Licor 926-32222	1 in 10,000
1°	IFT88	Rabbit polyclonal	ProteinTech Group 13967-1-AP	1 in 1500
2°	IRDye 800CW	Donkey anti-rabbit	Licor 926-32214	1 in 10,000
1°	BBS4	Rabbit polyclonal	Phil Beales, UCL London	1 in 1000
2°	IRDye 800CW	Donkey anti-rabbit	Licor 926-32214	1 in 10,000

2.13 Cytology

2.13.1 Fixation

Cells grown on cover slips were washed twice with ice cold PBS, and fixed for 15 minutes in 4% PFA (paraformaldehyde; BDH Chemicals) on ice. PFA holds the cells

architecture in place by creating chemical cross-links that join proteins via their amino side chains.

2.13.2 Immunofluorescence

After fixation, cells were blocked for 1 hour with 10% normal donkey or goat serum in PBS-triton-Na azide containing 0.1% triton X-100 and 0.2% sodium azide (Fluka BioChemika), then incubated overnight at room temperature with primary antibodies (Table 2.13.1). Residual unbound primary antibodies were removed by washing the cells three times in PBS with 0.1% triton X-100 (PBS-triton) for 10 minutes each. Incubation with secondary antibodies was carried out for 3 hours at room temperature, before repeating the washes in PBS-triton to remove any unbound secondary antibodies. One drop of DAPI (4',6-diamidino-2-phenylindole, 1 in 5000) was then added to each cover slip for 1 minute before being washed away. Cover slips were transferred onto microscope slides, and secured with fluorescent mounting media (Dako). Slides were visualised, and images taken using the Zeiss LSM510 inverted laser scanning confocal microscope with 63x objective, and the ZEN 2008 Light edition software.

Table 2.13.1 – Antibodies used for immunofluorescence

Ab	Antigen/Fluorophore	Species	Company	Dilution
1°	Shh	Goat polyclonal	Santa Cruz Shh (N-19): sc-1194	1 in 200
2°	CY3-Red	Donkey anti-goat	Jackson Immunoresearch 705-165-003	1 in 1000
1°	Pericentrin	Rabbit polyclonal	Abcam ab4448-100	1 in 1000
2°	AF568-Red	Goat anti-rabbit	Invitrogen A11011	1 in 1000
1°	Acetylated α-tubulin	Mouse monoclonal	Sigma Aldrich T6793	1 in 1000
2°	AF488-Green	Goat anti-mouse	Invitrogen A11029	1 in 1000

2.13.3 Counting and measuring cilia

Cilia were visualised by immunofluorescence, and z-stacks taken using the Zeiss LSM510 laser scanning confocal microscope with 63x objective, and the ZEN 2008 Light edition software. Z-stacks involve the acquisition of multiple images through the visual

field, which are then combined in the processing tools of the Zen program to form a maximum intensity projection. Cilia were counted blind, from equally sized areas in each z-stack. The length of cilia was determined using the Zen program processing tools. Cells requiring serum starvation were grown in 100% optimum I (Gibco) for 24-60 hours prior to fixation.

2.13.4 3βHSD Assay

Cells grown on cover slips were washed in DPBS, and the media changed to that without phenol red. Solutions one and two (see below, made fresh each time) were added to a final concentration of 1x, along with 1% DMSO. The plate was gently rocked, and left for 30-90 minutes, until some of the cells turned blue/purple. They were then washed twice in ice cold PBS, and fixed in 4% PFA for 15 minutes on ice. The cover slips were mounted on slides using glycerol, and visualised and imaged using the Leica DMR light microscope with 20x objective, Leica DC200 digital camera, and Leica DCViewer software.

A 50x stock of solution one contains 12.5mg/ml NBT (nitroblue tetrazolium) and 2.5mg/ml DHEA (Dehydroepiandrosterone) in 70% Dimethylformamide (BDH Chemicals), while a 50x stock of solution two contains 14mg/ml nicotinamide and 30mg/ml βNAD (β nicotinamide adenine dinucleotide hydrate) in H_2O (Chiappe et al, 2002; Marrone & Sebring, 1989).

2.14 Histology

2.14.1 Paraffin embedding

After harvesting, adrenals from mice, age 16-20 weeks, were fixed in 4% PFA overnight at 4°C. They were then washed in H_2O, 50%, 70%, 90% and 100% ethanol for 1 hour each, and left overnight in 100% ethanol at 4°C. The adrenals were washed twice in xylene for 1-2 minutes, and soaked in liquid paraffin for 24 hours at 56°C. The paraffin containing the specimens was then poured into plastic block-moulds and left at room temperature to set.

2.14.2 Sectioning and Mounting

7-10µm thick sections were cut from adrenals embedded in paraffin blocks using the Leitz 1512 microtome, and mounted on TESPA treated slides (3-triethoxysilylpropylamine; VWR) by the floating-out technique (Sack, 1963). Briefly, a small amount of water was placed on the slides, and ribbons of serial sections laid flat on the water. They were heated to approximately 8°C, and the water removed by pipetting from a corner or edge, leaving the sections to bond with the adhesive coating (TESPA). The slides were then dried overnight at 37°C to increase the adhesion, and ensure the sections would not dissociate during further treatments.

2.14.3 Deparaffinisation

As paraffin is insoluble in water, most staining techniques require it to be removed. To deparaffinise, sections were washed three times in xylene, twice in 100% ethanol, once in 90%, 70% and 50% ethanol, and then rehydrated by washing twice in H_2O. Each wash lasted 10 minutes.

2.14.4 Haematoxylin & Eosin staining

Slides were placed in haematoxylin for 2 minutes (Lamb Laboratories), followed by 2 minutes in running H_2O. They were then dipped in acidic alcohol (75% ethanol, 0.04% HCl) for 1 minute, and placed under running H_2O for a further 2 minutes. After dipping the slides in ammonia solution (0.084% ammonium hydroxide) for 1 minute, they were subject to 5 minutes under running H_2O, 1 minute in 80% ethanol, 15 seconds in Eosin (Lamb Laboratories), two 1 minute washes in 95% ethanol, two 1 minute washes in 100% ethanol, and three 10 minute washes in xylene. Excess xylene was wiped from the back and edges of the slides, and they were covered with glass slips using DPX mounting media (Lamb Laboratories) to preserve the staining. They were visualised and imaged using the Leica DMR Light microscope with 10x and 40x objectives, Leica DC200 digital camera, and Leica DCViewer software.

2.14.5 DAPI staining to quantify capsule density

Adrenal sections were cut at equal thickness, and mounted on TESPA treated slides. They were deparaffinised and washed in PBS-triton (0.1%) for 10 minutes. One drop of DAPI (4',6-diamidino-2-phenylindole, 1 in 5000) was then added to each section for 1 minute, and the slides washed again in PBS-triton. Fluorescent mounting media (Dako) was used to preserve the staining under glass slips. Sections were visualised, and z-stacks taken using the Zeiss LSM510 laser scanning confocal microscope with 63x objective, and the ZEN 2008 Light edition software. Capsule density was quantified by blind counting the number of capsular nuclei within equally sized areas of each z-stack.

2.14.6 Immunoperoxidase staining

Sections were deparaffinised with three washes in xylene and one in 100% ethanol, then washed for 1 hour with agitation in 3% hydrogen peroxide in methanol (Fisher Scientific) to block endogenous peroxidase activity. Ethanol washes were continued using 100%, 90%, 70% and 50% solutions, followed by two washes with H_2O to rehydrate. The slides were then boiled for 15 minutes in 10mM sodium citrate buffer - pH6 (BDH Chemicals) to break cross-links formed between proteins during paraffin embedding, and unmask antigens and epitopes. After a 5 minute wash in PBS-triton, the slides were blocked for 30 minutes with 10% normal goat serum, followed by 15 minutes with Avidin D, and 15 minutes with Biotin from the Vector Laboratories Avidin/Biotin blocking kit, to prevent non-specific secondary antibody and tertiary reagent binding. The primary antibody was applied overnight at room temperature (Table 2.14.1), then any unbound antibody was removed by washing three times in PBS-triton. This was followed by 2 hours incubation with a biotinylated secondary antibody, three washes in PBS-triton, 1 hour treatment with the Vectastain ABC tertiary reagent containing a preformed Avidin and Biotinylated horseradish peroxidase (HRP) macromolecular Complex (Vector Laboratories), another three washes in PBS-triton, and finally addition of the DAB (3, 3'-diaminobenzidine) peroxidase substrate containing hydrogen peroxide and nickel (DAB peroxidase substrate kit; Vector laboratories) for 5 minutes. Once a grey/black colour had developed, the sections were dehydrated by washing in 50%, 70%, 90%, and two lots

of 100% ethanol, followed by three 10 minute washes in xylene. DPX mounting media was used to preserve the sections under glass slips, and they were visualised and imaged using the Leica DMR Light microscope with 10x objective, Leica DC200 digital camera, and Leica DCViewer software.

Table 2.14.1 – Antibodies used in immunoperoxidase staining

Ab	Antigen/Detector	Species	Company	Dilution
1°	CYP11A1 (SCC)	Rabbit polyclonal	Millipore AB1244	1 in 1000
2°	Biotinylated	Goat anti-rabbit	Vector Laboratories BA-1000	1 in 500
1°	CYP11B1	Mouse monoclonal	Dr Gomez-Sanchez, University of Mississippi	1 in 20
2°	Biotinylated	Goat anti-mouse	Vector Laboratories BA-9200	1 in 500

2.15 Zebrafish

Embryos were obtained from single pairs of the Queen Mary University strain of zebrafish.

2.15.1 Microinjection

Morpholino Oligomers (Table 2.15.1; Gene Tools, LLC) were re-suspended in Danieau buffer containing 58mM sodium chloride, 0.7mM potassium chloride, 0.4mM magnesium sulphate, 0.6mM calcium nitrate and 5mM HEPES in H_2O. Embryos were then lined up in a petri dish along the edge of a microscope slide, and visualised using the Leica MXFL III stereo dissecting microscope. 5ng of each morpholino was injected into the embryos at the 1-2 cell stage using the Parker Instrumentation Picospritzer III. Embryos were then incubated at 28.5°C in embryo media pH7.2 containing 13.7mM sodium chloride, 0.54mM potassium chloride, 25.2µM disodium hydrogen phosphate, 44.1µM potassium dihydrogen phosphate, 1.3mM calcium chloride, 1mM magnesium sulphate and 10mM HEPES in H_2O, with methyl blue.

24 hours post fertilisation (hpf) PTU (Propylthiouracil) was added to the media at a concentration of 0.003%, to prevent the development of pigmentation and maintain transparency of the embryos. At 24, 27 or 30 hpf the embryos were dechorionated and

staged by counting the number of somites and assessing the head-trunk position. Embryos were visualised, phenotypes recorded and images taken on a Leica MXFL III stereo dissecting microscope fitted with a Leica DC300 camera, using the Leica IM50 software.

Table 2.15.1 – Morpholino sequences

Morpholino	Sequence 5' – 3'	
Control	CCTCTTACCTCAGTTACAATTTATA	Gene Tools, LLC
p53	GCGCCATTGCTTTGCAAGAATTG	Gene Tools, LLC
Target sequence	CAATTCTTGCAAAGCAATGGCGC	
BBS4	TGTTTAACTGGTGCTTACAGCGATC	**(Yen et al, 2006)**
Target sequence	GATCGCTGTAAGCACCAGTTAAACA	
BBS6	GCTTCTTCTTACTAATGCGAGACAT	**(Badano et al, 2006; Yen et al, 2006)**
Target sequence	ATGTCTCGCATTAGTAAGAAGAAGC	

2.15.2 Immunofluorescence

After dechorionation and staging, embryos were fixed in 4% PFA with 0.15mM calcium chloride and 4% sucrose overnight at 4°C. They were then washed three times in PBS for 10 minutes each, and permeabilised in 100% acetone for 5 minutes at -20°C. After a further three washes in PBS, the embryos were blocked for 1 hour in 10% goat serum in PBS with 0.8% triton (PBS-triton), and incubated overnight at 4°C with the primary antibodies (Table 2.15.2). After five 30 minute washes in PBS-triton, incubation with secondary antibodies in PBS-triton containing 1% goat serum was carried out overnight, again at 4°C. The embryos were washed three times in PBS-triton for 10 minutes each, and then incubated in DAPI for 1-2 minutes. This was followed by two washes in PBS-triton and storage at 4°C in 70% glycerol. The embryos were visualised and images taken using the Zeiss LSM510 laser scanning confocal microscope and the ZEN 2008 Light edition software.

Table 2.15.2 – Antibodies used for zebrafish immunofluorescence

Ab	Antigen/Fluorophore	Species	Company	Dilution
1°	Acetylated α-tubulin	Mouse monoclonal	Sigma Aldrich T6793	1 in 500
2°	AF488-Green	Goat anti-mouse	Invitrogen A11029	1 in 500

2.15.3 Counting and measuring cilia

Cilia were visualised by immunofluorescence, and z-stacks taken using the Zeiss LSM510 laser scanning confocal microscope with 63x objective and the ZEN 2008 Light edition software. Cilia were counted blind, from equally sized areas, in similar positions within the tail region of each embryo. The length of cilia was determined using the Zen program processing tools.

2.15.4 Whole mount ISH

After dechorionation and staging, embryos were fixed in 4% PFA (BDH Chemicals) overnight at 4°C. They were then washed in PBS with 0.1% Tween20 (PBS-tween), and dehydrated in 100% methanol for 30 minutes. They were stored overnight in 100% methanol at -20°C.

Rehydration of the embryos was achieved by washing in 75%, 50% and 25% methanol in PBS for 5 minutes each, followed by four washes in PBS-tween. They were then treated with 10µg/ml proteinase K in PBS-tween for 20 minutes at room temperature to permeabilise the cell membranes. The embryos were fixed again in 4% PFA for 20 minutes, and washed four times in PBS-tween. Prior to incubation with the zebrafish *in situ* ff1b probe (Dr Bon-chu Chung, Academia Sinica, Taiwan), the embryos were placed in a hybridisation buffer for 2-5 hours at 65°C. The hybridisation buffer contained 50% formamide, 25% 5x SSC (sodium saline citrate), 50µg/ml yeast tRNA, 50µg/ml heparin and 0.1% tween in sterile water, buffered to pH6.5 with 1M citric acid. The ff1b probe was then added to the buffer at a concentration of 0.4µg/ml and left overnight at 65°C. Embryos were washed three times in 25% formamide/75% 2x SSC with tween, and twice in 100% 2x SSC with tween, all at 65°C, 10 minutes per wash. They were then washed three times for 20 minutes each in 0.2x SSC with tween, also at 65°C. This was followed by four 5 minute washes in PBS-tween at room temperature. The embryos

were blocked in a solution containing 5% sheep serum and 2mg/ml BSA in PBS-tween for 2 hours, followed by incubation with an anti-DIG (Digoxigenin) alkaline phosphatase conjugated antibody (1 in 5000) at 4°C overnight.

After eight 15 minute washes in PBS-tween, and three 5 minute washes in BCL buffer containing 100mM Tris HCL pH9.5, 50mM magnesium chloride, 100mM sodium chloride and 0.1% tween in H_2O, the embryos were incubated for 24-30 hours in Roche BM Purple; AP substrate precipitating solution, protected from light. Once the staining had developed they were washed for 10 minutes in PBS-tween, and fixed at room temperature in 4% PFA for 20 minutes. They were then stored in 70% glycerol at 4°C. Staining was visualised and images taken on a Leica MZFL III stereo dissecting microscope fitted with a Leica DC300 camera, using the Leica IM50 software.

2.16 Data Analysis

All data were analysed using Microsoft Office Excel 2010 and SPSS version 12. One-way ANOVAs (Analysis of variance) were implemented, with the appropriate pre-planned and post-hoc comparisons including the Bonferroni correction for multiple comparisons (Brace et al, 2006). Pre-planned tests are those between factors that are expected to differ, and are already decided upon before carrying out an experiment. Post-hoc tests are comparisons not foreseen, that may reveal interesting connections between data sets. Graphs were producing using SPSS version 12, paint.NETv3.36 and Inkscape version 0.48.

CHAPTER 3: ESTABLISHING AN *IN VITRO* SYSTEM

3.1 Aims

The main aim of this chapter is to show that the human adrenal carcinoma cell line H295R can be used as a model cell line in which to study the role of hedgehog signalling and primary cilia in adrenal differentiation and function *in vitro*. The expression of Hh pathway components, presence of primary cilia, and responses to agonists and antagonists of the Hh pathway are investigated, along with the capacity of these cells to differentiate.

3.2 H295R cells express components of the Hh pathway and have primary cilia

The cell fate regulator Sonic hedgehog (Shh) plays a key role in adrenal development (Ching & Vilain, 2009; Huang et al, 2010; King et al, 2009). To further study its role in an *in vitro* system it was necessary to determine whether the H295R cell line expresses components of the Hh pathway and can respond to its agonists and antagonists. Figure 3.2.1A shows by PCR, that H295R cells express the key components of the Shh pathway, namely Shh itself, two receptor isoforms Ptch1 and 2, Smo and the Hh pathway transcription factors Gli1, 2 and 3. The identity of the PCR products was verified by sequencing, carried out by the Queen Mary Genome Centre. Immunofluorescence with an anti-Shh antibody also shows that these cells are capable of producing the Shh ligand (Figure 3.2.1C). One cell in this field of view is Shh-positive, while the total number of Shh-expressing cells is approximately 5%. By combining these two techniques, showing both RNA and protein expression, it can be concluded that Hh pathway components are present in H295R cells.

cDNA derived from human adrenal cortex RNA (Clontech) was also tested for the expression of Hh pathway components by PCR. As in H295R cells, expression of Shh, Ptch1, Smo and Gli1, 2 and 3 were observed, although the Ptch2 receptor isoform was undetected (Figure 3.2.1B). This shows that Hh pathway components are expressed in human adrenocortical cells, and that work done *in vitro* may have transferrable implications for the *in vivo* system.

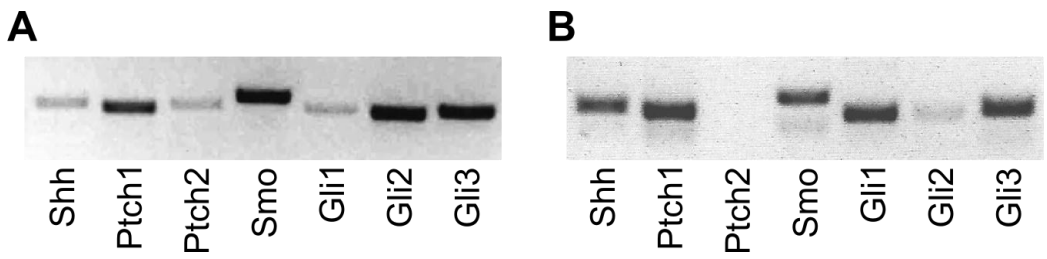

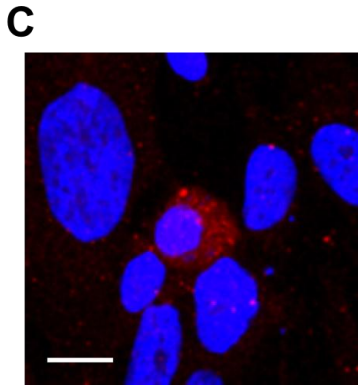

Figure 3.2.1 – H295R cells express components of the Hh pathway
(A-B) Expression of components of the Hh pathway by PCR in H295R cells (A), and the human adrenal cortex (B). 1µl cDNA was used in each reaction lasting 35 cycles, with an annealing temperature of 58°C.
(C) Representative confocal image showing a Shh-expressing H295R cell. Cells were grown on cover slips and after fixation were incubated with an anti-Shh

(C) Representative confocal image showing a Shh-expressing H295R cell. Cells were grown on cover slips and after fixation were incubated with an anti-Shh

It is now generally accepted that proper functioning of the Hh signalling pathway requires primary cilia, with many reports of its pathway components localised there (Corbit et al, 2005; Haycraft et al, 2005; Rohatgi et al, 2007; Satir & Christensen, 2007). To visualise cilia in H295Rs, cells were serum starved prior to fixation, and incubated with antibodies for acetylated α-tubulin and pericentrin (Figure 3.2.2A). Serum starvation helps cells to form cilia by promoting cell cycle arrest (Schneider et al, 2005), as primary cilia form during interphase. Acetylated α-tubulin is a protein that forms the subunits of microtubules, and can be used to visualise primary cilia as their axoneme has a 9+0 microtubule structure. Antibodies for acetylated α-tubulin will also identify other microtubule based structures such as the mitotic spindle during cell division, therefore a second ciliary marker was used to increase accuracy. Pericentrin is a basal body protein that forms a complex with components of the intraflagellar transport system, and is frequently used as a marker of cilium formation (Jurczyk et al, 2004).

The proportion of ciliated cells was estimated by counting cilia from maximum intensity projections (MIPs) of z-stacks, generated by the Zen confocal microscopy program. Using z-stacks, rather than single images, gives a more accurate estimation of the number of cilia in any random field, as it takes into account the third dimension and thus can help visualise cilia oriented perpendicularly to the plane of the image.

Figure 3.2.2B shows the difference between a single image and a MIP of a z-stack taken in the same visual field. Four cilia are clearly identifiable in the MIP, whereas only one can be seen in the single image view.

After 24-60 hours serum starvation, approximately 34-41% of H295R cells were ciliated, with no significant difference in the number of cilia between samples receiving different lengths of serum starvation (Figure 3.2.2C-D). However, increasing serum starvation from 24 to 60 hours did cause a significant increase in cilium length, which was determined using the Zen program processing tools. After 24 hours serum starvation the average cilium length was 1.7µm, with a maximum reading of 4.5µm. In comparison, the average length of cilia measured after 60 hours serum starvation was 3.25µm, with a maximum reading of 8.8µm.

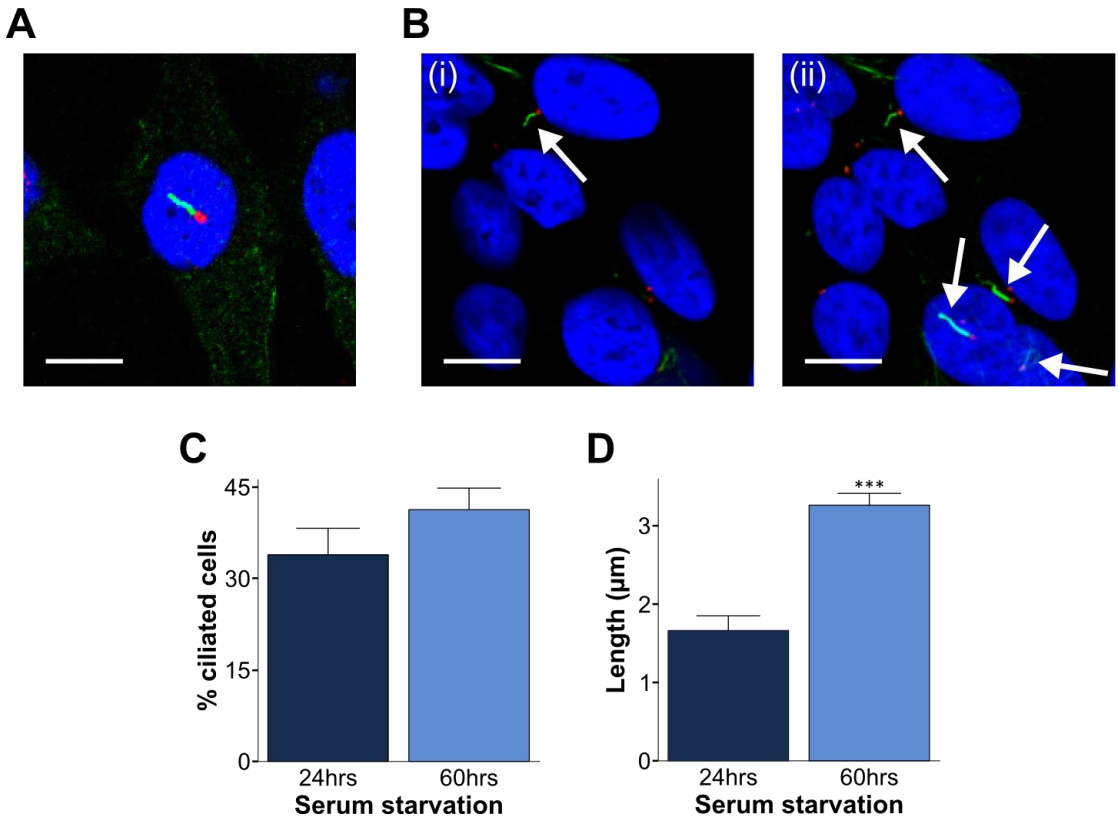

Figure 3.2.2 – H295R cells can form primary cilia
Cells were grown on cover slips and serum starved for 24 or 60 hrs prior to fixing. They were then incubated with an anti-pericentrin antibody marking the basal body (red), and an anti-acetylated α-tubulin antibody marking the ciliary axoneme (green). DAPI was used to stain the nuclei (blue). Cilia were visualised (A) and their number (C) and length (D) determined using the Zeiss LSM510 inverted laser scanning confocal microscope with 63x objective, and ZEN 2008 Light edition software. Scale bar represents 10µm. For each serum starvation, cilia were blindly counted from 3 slides, using 5 maximum intensity projections of z-stacks per slide (N=3). The length of 20 cilia was measured across the 3 slides (N=20). The data were analysed using a one-way ANOVA with post-hoc comparisons. Data collated, error bars indicate SEM. *** p<0.001 compared to 24hrs.
(B) Comparison between taking a single image (i) and a maximum intensity projection of a z-stack (ii). Cilia are indicated by the arrows, scale bar represents 10µm.

3.3 Hh pathway agonists and antagonists

As H295R cells express Hh pathway components and have cilia, an essential structural component for signalling, it was of interest to investigate their responsiveness to Hh pathway agonists and antagonists. Initially, using Shh Light II cells, a number of compounds were assessed for their ability to cause changes in Hh pathway activation via a functional assay. This cell line stably expresses the GLI-responsive firefly luciferase reporter which contains eight Gli1 binding sites upstream of the firefly luciferase gene

(Sasaki et al, 1997), and the constitutively active pRL-TK *Renilla* luciferase expression vector (Promega). As a result of changing Gli1 levels caused by the activation or inhibition of the Hh pathway by agonists or antagonists, transcription from the Gli1 responsive promoter will vary with resultant changes in expression of firefly luciferase. Gli1 levels are frequently used as a marker for Hh pathway activity (Dai et al, 1999). Shh Light II cells were either untreated, or incubated with a vehicle control, or Hh pathway agonists or antagonists, either individually or in combination, and a dual-luciferase assay conducted.

Purmorphamine, ShhN and SAG are all Hh pathway agonists. Purmorphamine and SAG target Smo, and bind within its heptahelical bundle to cause changes in its conformation, and effect Smo activation (Chen et al, 2002b; Sinha & Chen, 2006). This also causes translocation of Smo to the primary cilium, and therefore downstream signalling in the absence of Shh (Rohatgi et al, 2007; Wang et al, 2009). ShhN acts at Ptch1, binding and preventing it from inhibiting Smo thereby allowing downstream Hh signalling. Upon binding, the Shh-Ptch1 complex is internalised and translocates out of the cilium (Rohatgi et al, 2007). Figure 3.3.1 shows that all three agonists cause a significant two-fold increase in the firefly luciferase activity of Shh Light II cells compared to their respective controls.

Cyclopamine, vismodegib (GDC-0449) and Sant1 are Hh pathway antagonists that target Smo. They also bind within its heptahelical domain, but in different locations both to the agonists, and to each other (Chen et al, 2002a; Chen et al, 2002b; Yauch et al, 2009). They cause changes in Smo conformation resulting in its inactivation, and loss of downstream signalling. Tomatidine is a structural analogue of cyclopamine that does not inhibit Hh signalling (Mukherjee et al, 2006). It is used as a control for cyclopamine toxicity. Of the three antagonists, Sant1 was the only one when used individually to cause a significant decrease in the luciferase activity of Shh Light II cells compared to the controls (Figure 3.3.1). However, when combined with purmorphamine, cyclopamine and vismodegib also caused a significant decrease in luciferase activity when compared to purmorphamine treatment alone. This result was reproduced when cells were treated with tomatidine in combination with

purmorphamine, a finding that was unexpected given that tomatidine should not inhibit Hh signalling.

Another compound; forskolin (Fsk), stimulates activation of adenylate cyclase and PKA. This leads to Gli phosphorylation and proteolytic processing to form transcriptional repressors (Pan & Wang, 2007). Although Fsk is reported in the literature to be a non-selective Hh pathway antagonist (Hyman et al, 2009; Taipale et al, 2000), in this case a significant 5.7-fold increase in luciferase activity was observed, suggesting agonist actions (Figure 3.3.1).

Lastly, cycloheximide inhibits protein biosynthesis by blocking translation (Baliga et al, 1969; Chow et al, 1995) and was used as a negative control. It prevents *de novo* luciferase production, resulting in low luciferase activity. It also triggers apoptosis in some cell lines (Lu & Mellgren, 1996). Luciferase activity was significantly reduced in Shh Light II cells treated with cycloheximide (Figure 3.3.1).

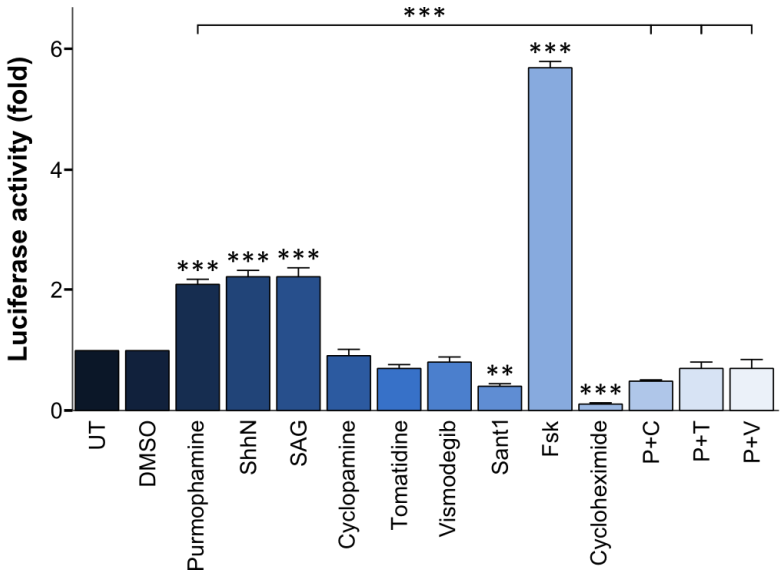

Figure 3.3.1 – Shh Light II luciferase assay

Graph showing relative luciferase activities normalised to renilla. Shh Light II cells were either untreated (UT) or treated with 8µl/ml DMSO, 2µM purmorphamine, 0.35µg/ml ShhN, 200nM SAG, 2µM cyclopamine, 2µM tomatidine, 20nM vismodegib, 2µM Sant1, 10µM forskolin (Fsk), 80µg/ml cycloheximide, 2µM purmorphamine plus 2µM cyclopamine (P+C), 2µM purmorphamine plus 2µM tomatidine (P+T), or 2µM purmorphamine plus 20nM vismodegib (P+V) for 48 hrs. A dual-luciferase reporter assay was then conducted, and the data analysed using a one-way ANOVA with pre-planned and post-hoc comparisons of treatments. N=3, data collated, error bars indicate SEM. ** p<0.01, *** p<0.001 compared to UT or DMSO, unless otherwise indicated.

These results show that the Hh pathway agonists purmorphamine, ShhN and SAG act to increase Gli1 transcription, while the antagonists Sant1, cyclopamine and vismodegib inhibit it, although the effect of cyclopamine may be non-specific given that tomatidine also inhibits. It can therefore be assumed that canonical signalling is occurring in Shh Light II cells in this instance. To investigate the responsiveness of H295Rs to Hh pathway effectors, a transient Gli-luciferase reporter system was implemented. Cells were transfected with either the pGL3-6xGBS firefly luciferase plasmid (Dr Graham Neill, Queen Mary University of London), or the pGL3-empty vector (Promega), and the pRL-CMV renilla plasmid at a ratio of 30:1. The pGL3-6xGBS luciferase plasmid has a synthetic promoter composed of six multimeric Gli1 binding sites upstream of the luciferase gene, while the pGL3-empty vector contains the luciferase gene but no promoter. Similar treatments to those described above were employed, but no significant differences in luciferase activities were found. Real-time qPCR examining Gli1 expression was therefore used as an alternative method for analysing the ability of purmorphamine or cyclopamine to cause changes in Hh pathway activity. Purmorphamine treatment caused an increase, albeit not significant, in Gli1 expression of approximately ten-fold compared to untreated cells (Figure 3.3.2), whereas cyclopamine treatment did not have any effect. These results fit with the documented actions of purmorphamine, as a Hh pathway agonist (Wu et al, 2002).

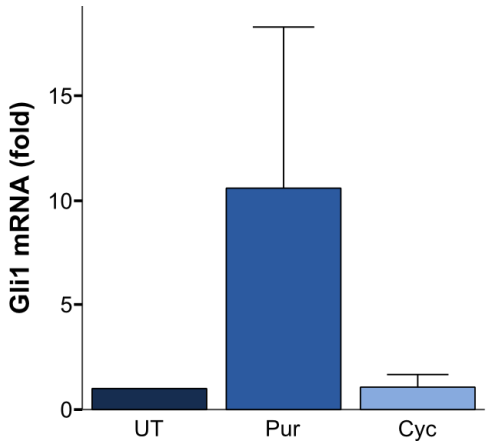

Figure 3.3.2 – Gli1 mRNA expression
Graph showing the relative quantities of Gli1 mRNA in H295R cells. Cells were treated for 24hrs with either 2µM purmorphamine (Pur) or 2µM cyclopamine (Cyc), compared to untreated cells (UT). Quantitative real-time qPCR was carried out measuring Gli1 expression. 18S rRNA expression was used as the loading control. A one-way ANOVA with pre-planned and post-hoc comparisons of the treatments was used to interpret the results. N=3, data collated, error bars indicate SEM.

Before continued use of these compounds in H295R cells, assessment of their cytotoxic status was carried out using both a lactate dehydrogenase (LDH) assay, and fluorescence-activated cell sorting (FACS). H295R cells were either untreated, or incubated with Hh pathway agonists or antagonists, either individually or in combination. The percentage of cytotoxic cells was established by measuring LDH levels, or flow cytometry analysis of propidium iodide incorporation.

LDH is normally present in the cytoplasm of healthy cells, but is released upon the loss of membrane integrity during lysis, necrosis or apoptosis. It converts a tetrazolium salt within the substrate mixture of the Promega cytotoxicity assay kit, into a soluble red formazan product, which can be measured by spectrophotometry (Promega Technical Bulletin TB163). Propidium iodide (PI) is a fluorescent molecule that binds stoichiometrically to double stranded DNA. PI incorporation increases as the cell cycle progresses, and chromosome replication occurs (Abcam Resources; *Propidium iodide staining of cells to assess DNA cell cycle*). For example; cells in the G2 phase contain twice as much DNA as those in G1, and will therefore have a higher level of PI incorporation. Apoptotic cells have a low rate of PI incorporation, as their DNA content is reduced. Hence, flow cytometry analysis of PI incorporation can be used to determine the number of cells within each stage of the cell cycle, and distinguish them from those that are undergoing cell death, possibly as a result of cytotoxicity.

Figure 3.3.3A shows that the percentage of cytotoxic cells, calculated from LDH levels, is significantly increased only in those treated with cycloheximide, an activator of apoptosis. All other samples remain unchanged. This result was replicated by the FACS analysis.

Figure 3.3.3C and D show the flow cytometry plots generated by treatment of cells with either DMSO or cycloheximide respectively. All other treatments resulted in plots identical to those obtained for DMSO. The first plots in the left panel (i) show forward and side scatter, which are representative of cell volume and morphological complexity. The middle panel (ii) shows pulse width plotted against pulse area, to distinguish between single cells and those that are doublets or clumped together. The gating implemented in this plot, labelled as P2, determines which cells are further

analysed, shown in green. All red cells have been excluded. The third panel on the right (iii) then shows the DNA cell cycle histogram, labelled with propidium iodide. The amount of PI increases as the cell cycle progresses, and so P4, P5 and P6 show the number of cells in G1, S phase and G2 respectively. P7 contains polyploidy cells that have escaped G2 and cell division. Cells undergoing apoptosis will be present in P3, with the lowest PI levels. Figure 3.3.3B shows the percentage of cells recorded in P3 for each treatment.

These plots show that the majority of the cells counted, after all treatments excluding cycloheximide, were in the G1 phase (Figure 3.3.3C (iii)). After cycloheximide treatment, the total number of cells sorted was reduced (fewer events recorded in Figure 3.3.3D (i) and (ii)), and the majority of those were undergoing apoptosis in P3 (Figure 3.3.3D (iii)). Also, when compared to the other treatments, the percentage of cells in P3 was significantly greater (Figure 3.3.3B). Together, these results delineate cycloheximide as the only substance tested with any cytotoxic effect on H295R cells, at the concentrations used.

The above data indicate that purmorphamine, ShhN and SAG work via up-regulation of Gli1 expression in Shh Light II cells, and this is most likely the case in H295R cells as well. They also do not have any cytotoxic effects at the concentrations used here, and thus are suitable for use in further experimentation. Results obtained from Hh pathway antagonists seem to show they are capable of inhibiting Gli1 up-regulation, and like the agonists; they do not appear to stimulate apoptosis.

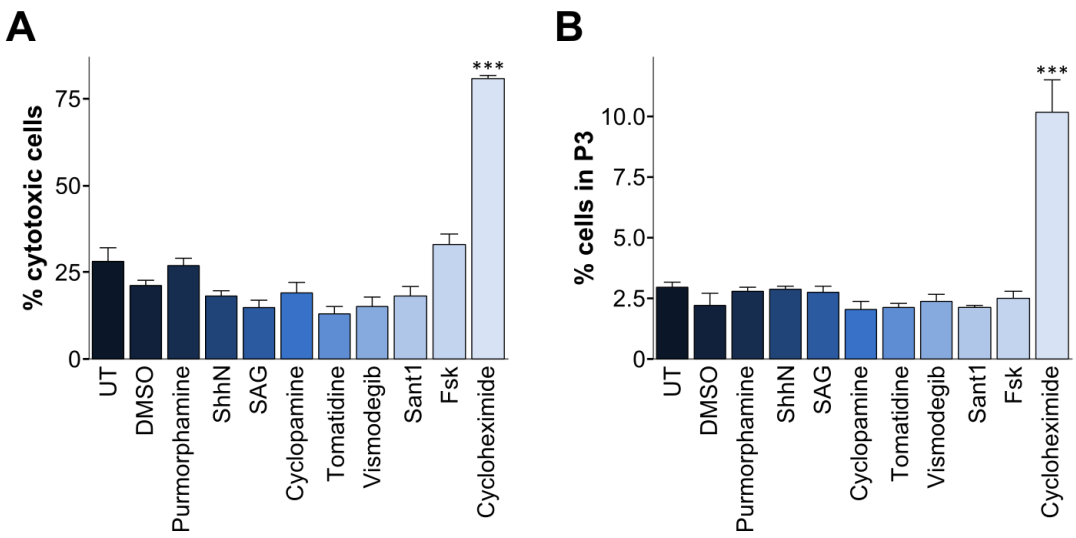

Figure 3.3.3 – Cytotoxicity of Hh pathway agonists and antagonists (this page and following page) **H295R cells were either untreated (UT) or treated with 8µl/ml DMSO, 2µM purmorphamine, 0.35µg/ml ShhN, 200nM SAG, 2µM cyclopamine, 2µM tomatidine, 20nM vismodegib, 2µM Sant1, 10µM forskolin (Fsk), or 80µg/ml cycloheximide for 72hrs. They were then assayed for LDH levels and the percentage of cytotoxic cells calculated (A), or sorted by FACS on the basis of propidium iodide incorporation and the percentage of apoptotic cells in P3 recorded (B). The data were analysed using a one-way ANOVA with pre-planned and post-hoc comparisons of treatments. N=3, data collated, error bars indicate SEM. *** p<0.001 compared to UT.**

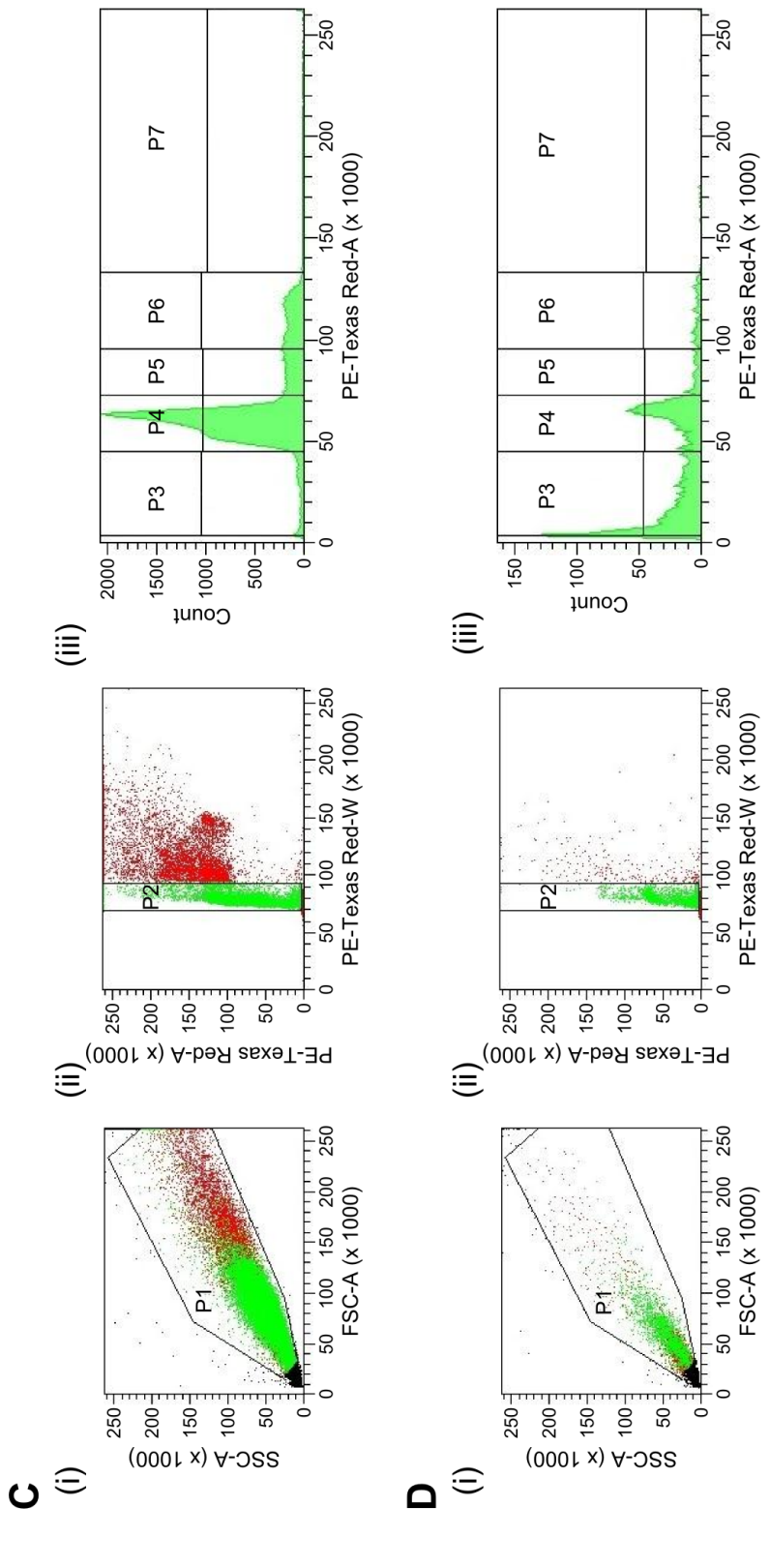

Figure 3.3.3 – Cytotoxicity of Hh pathway agonists and antagonists (continued)
(C-D) Flow cytometry plots generated by DMSO (C) or cycloheximide (D) treatment. (i) Plots showing forward and side scatter; P1. (ii) Plots showing pulse width and pulse area gating; P2. (iii) Plots showing the DNA cell cycle histogram.

3.4 Differentiation of H295R cells

The data shown above demonstrate that H295R cells express Hh pathway components and form primary cilia. This cell line has been widely used as a model adrenal cell line, not only because of its ability to express all human adrenal steroids but also because it can differentiate into cells whose gene expression and steroidogenic output resembles the three human adrenal zones; zG, zF and zR. As part of the renin-angiotensin-aldosterone pathway, angiotensin II stimulates aldosterone production via AT1 receptors in the zG of the adrenal cortex (LeHoux et al, 1997). It also stimulates the differentiation of H295R cells towards a zG-like fate, characterized by increased production of CYP11B2 (aldosterone synthase) and aldosterone (Bird et al, 1993).

In contrast, ACTH, released from the anterior pituitary as part of the HPA axis, stimulates glucocorticoid production. It does this via its receptor, MC2R, which is present on the surface of zF/zR cells, and activates adenylate cyclase to promote the conversion of ATP to cAMP (Aumo et al, 2010; Rainey et al, 2004). Stimulating the cAMP pathway in H295Rs leads to their differentiation towards a zF-like fate, characterised by increased production of CYP11B1 (11β-hydroxylase) (Cobb et al, 1996). Due to the tendency of these cells to lack ACTH-responsiveness, forskolin (Fsk) is used to directly activate adenylate cyclase in this pathway (Denner et al, 1996; Janes et al, 2008). However, chronic Fsk treatment also results in up-regulation of cytochrome b5, which enhances the 17,20 lyase activity of CYP17 and stimulates the production of androstenedione (Auchus et al, 1998; Pandey & Miller, 2005), a functional characteristic of the zR.

Real-time qPCR examining CYP11B1 and CYP11B2 expression in H295R cells treated with AngII or Fsk was carried out. Figure 3.4.1A shows there is an increase in both CYP11B1 and CYP11B2 mRNA levels in samples treated with AngII or Fsk, compared to untreated cells. However, as Fsk stimulates zF-like differentiation, these cells have significantly higher CYP11B1 levels than those treated with AngII or untreated cells (Figure 3.4.1A (i)), indicating that these cells resemble more closely the zF than the others. AngII treatment also produced significantly higher CYP11B2 levels than Fsk

treatment or no treatment at all (Figure 3.4.1A (ii)), indicating that these cells resemble the zG more closely than the others.

Real-time qPCR reports only on the quantity of mRNA within cells, so staining cells to determine the levels of the steroidogenic protein 3βHSD was also conducted. 3βHSD (3-beta-hydroxysteroid dehydrogenase) is required in the first steps of steroidogenesis (Figure 1.1.2) and is therefore needed for the production of glucocorticoids, mineralocorticoids and androgens. Its expression reflects steroid production, and so cells with increased cortisol or aldosterone levels, as in those differentiating, will have more 3βHSD. Figure 3.4.1B shows images of cells stained in purple for the oxidation of DHEA to androstenedione, in the presence of 3βHSD and the coenzyme NAD^+. AngII or Fsk treated samples have more stained cells than the untreated sample, and the colour is more intense. The staining appears in patches of cells, indicating that these are steroidogenic, and therefore likely to produce more aldosterone or cortisol than unstained cells.

As a final method for determining the steroidogenic characteristics of differentiating H295R cells, cortisol and aldosterone levels in the media were assessed by using enzyme-linked immunosorbent assays (ELISA). Cells treated with AngII produced significantly higher levels of aldosterone than the untreated cells (Figure 3.4.1C (i)), while those treated with Fsk produced significantly more cortisol (Figure 3.4.1C (ii)). This indicates that steroid production by H295R cells can be altered in accordance with the literature (Bird et al, 1993; Denner et al, 1996), by treating them with AngII or Fsk.

Together, these data indicate that H295R cells can differentiate towards either a zG or zF-like phenotype under the experimental conditions, measurable by their steroidogenic enzyme expression levels and steroidogenic output. These results recapitulate the findings of others, and ensure that these cells have retained their responsiveness to the differentiation compounds. They also serve to establish that qPCR analysis of CYP11B1 and CYP11B2 expression is a quantifiable functional reporter system for the differentiated state of H295Rs.

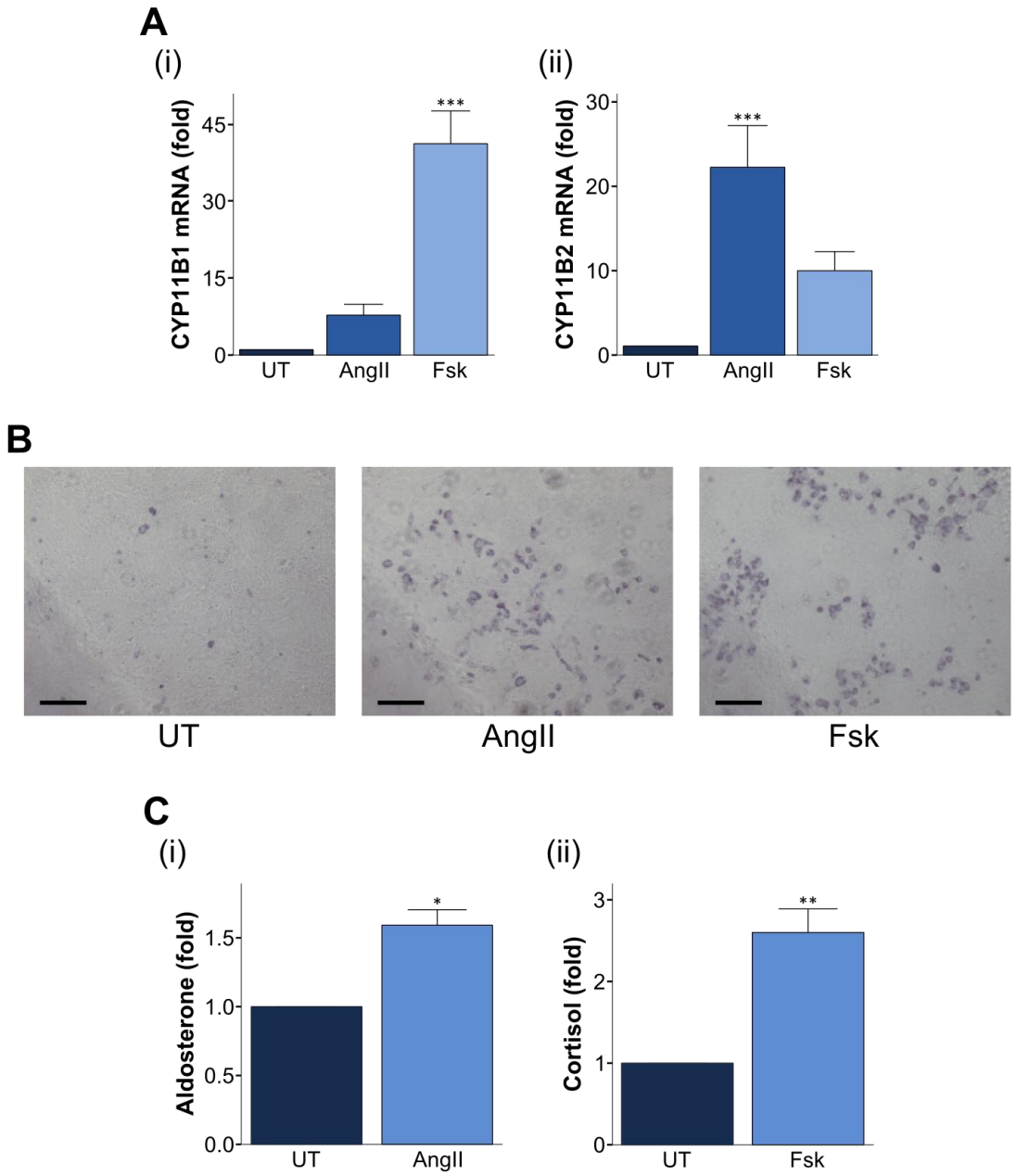

Figure 3.4.1 – Differentiation of H295R cells

(A) Graphs showing the relative quantities of CYP11B1 (i) and CYP11B2 (ii) mRNA in H295R cells. Cells were either untreated (UT), or differentiated over a 72-96hr period with 10µM angiotensin II (AngII) or 10µM forskolin (Fsk). Quantitative real-time qPCR was carried out measuring CYP11B1 or CYP11B2 expression. GAPDH expression was used as the loading control. For each gene, a one-way ANOVA with pre-planned and post-hoc comparisons of treatments was used to interpret the data. N=6, data collated, error bars indicate SEM. *** p<0.001 compared to UT.

(B) Representative light microscopy images of H295R cells with staining for the oxidation of DHEA to androstenedione, in the presence of 3βHSD and the coenzyme NAD^+. Cells were differentiated for 72hrs as in (A), and a 3βHSD assay performed. Images were taken using the Leica DMR light microscope with 20x objective. Scale bar represents 10µm.

(C) Graphs showing relative aldosterone (i) and cortisol (ii) levels in H295R cells. Cells were differentiated for 96hrs as in (A), and aldosterone and cortisol production determined by an ELISA. A one-way ANOVA for each steroid was used to interpret the data. N=3, data collated, error bars indicate SEM. * p<0.05, ** p<0.01 compared to UT.

3.5 Discussion

Evidence has been provided to show that H295R cells and the human adrenal cortex express components of the Hh signalling pathway, including the ligand Shh (Figure 3.2.1A). Immunofluorescence analysis revealed that the Shh protein is also present in some H295Rs (Figure 3.2.1C). As not all H295R cells express Shh, but both the ligand and downstream signalling components are present, we hypothesise that within the population of cells some are Hh-producing cells, while the others are capable of responding to the signal, as occurs *in vivo*. Immunofluorescence staining for Shh with Gli1 or Ptch1 would help to determine if this is the case. It would also show the localisation of Hh pathway components, in and around the cilium, as has previously been reported (Corbit et al, 2005; Haycraft et al, 2005; Rohatgi et al, 2007; Satir & Christensen, 2007). A lack of suitable antibodies has not made this feasible.

Within this mixed population of cells, those that express Shh might have stem cell capabilities. King et al. showed using lineage studies, that Shh-positive cells in the subcapsular region of the developing mouse adrenal can give rise to all steroidogenic cells types of the cortex *in vivo.* They have steroidogenic capacity (SF-1-positive), but are CYP11B1- and CYP11B2-negative, so are considered to be a separate group of cells from the zG or zF (King et al, 2009). They are relatively undifferentiated, and if truly stem cells, will have the capacity to replicate indefinitely, qualities that make them ideal candidates for transformation. They may also be the location of the originating cells, or cancer stem cells (CSCs), of the adrenocortical tumour from which H295Rs were derived.

Hh signalling has been identified as a key player in the maintenance of CSCs in a wide number of haematological and solid malignancies including multiple myeloma (Peacock et al, 2007), myeloid leukaemia (Zhao et al, 2009) and colorectal cancer (Varnat et al, 2009). It is thought to regulate their renewal capabilities (Zhao et al, 2009), and resistance to chemotherapy (Lin & Matsui, 2012), and may also be involved in dictating their cell fate decisions (Merchant & Matsui, 2010; Peacock et al, 2007). Hh pathway components have therefore become a target for the development of novel anticancer drugs. Gli inhibitors are currently in development (Mas & Ruiz i Altaba,

2010), and phase I and II clinical trials are underway for the Smo antagonist Vismodegib (GDC-0449) (Lin & Matsui, 2012). Targeting CSCs in combination with current treatments will likely be the most effective method for eradicating tumours (Naka et al, 2010).

H295R cells mainly produce DHEA and DHEAS, with low cortisol and aldosterone synthesis (Gazdar et al, 1990), characteristics resembling the steroidogenic profile of the foetal adrenal. Therefore some zG/zF cells may also have been incorporated into the carcinoma, accounting for these low cortisol/aldosterone levels. However, the possibility that other zG/zF cells were transformed to an undifferentiated state, losing their zG/zF identity, cannot be excluded.

Further evidence to suggest that the Shh-expressing H295R cells may be cancer stem cells, comes from the fact that ligand dependent cancers such as gastrointestinal tumours, pancreatic cancer and prostate cancer, have been associated with the Hh pathway (Beachy et al, 2004; Lindemann, 2008). For example, in prostate cancer, the Hh ligands Shh and Ihh are expressed in normal prostate tissue, but Ptch1, Smo and Gli1 expression is gained in cancerous cells (Karhadkar et al, 2004). Hh-responsiveness dependent upon ligand expression is acquired, allowing pathway activation and oncogenic transformation. In the mammalian adrenal cortex, Shh is expressed in the subcapsular/zU region, while Gli1 expression, and therefore the correct components for Hh signalling, are limited to the capsule. If the H295R adrenocortical tumour originated in the zU, then Hh pathway activation and Ptch1, Ptch2, Smo and Gli1-3 expression could have been acquired by the progenitor cells for the growth and survival of the tumour, or for maintenance of its microenvironment and its cells in an undifferentiated and proliferative state (Jiang & Hui, 2008). Any capsular cells incorporated into the tumour would have avoided the need for acquisition of Hh responsiveness in those cells.

The above data shows that primary cilia are present on just over one third of H295R cells after serum starvation (Figure 3.2.2), however, cilium formation is a dynamic process, and under the correct conditions every cell should have the capacity to become ciliated. Serum starvation is used to try to make cells quiescent and arrest in

interphase, when cilia formation occurs. Using the mouse fibroblast cell line NIH3T3, Schneider et al. report that after 24 hours serum starvation, over 90% of these cells are ciliated (Schneider et al, 2005). NIH3T3s have a population doubling time of approximately 20 hours (http://bioinformatics.istge.it/cldb/cl3711.html), while H295Rs divide more slowly (doubling time of 2 days), and this may account for the observed differences in cilia number reported. H295Rs are also cancer cells, and malignant transformation involves, in-part, the sequential loss of cell cycle check points. As primary cilia form during interphase, they are likely to be required as part of the G_1 and G_2 check points, allowing DNA replication, and subsequent cell division. Without check points, it might be more difficult to force H295Rs to leave the cell cycle, and they may not need to form cilia when they are dividing.

The average length of cilia present on H295R cells after 24 hours serum starvation was 1.7µm. However, the range of lengths varied quite considerably, with the longest cilium measuring approximately 4.5µm, and was also influenced by the amount of serum starvation the cells received. Cilium length is dependent upon cell type and function, and NIH3T3s have an average cilium length of 6µm after 24 hours serum starvation (Schneider et al, 2005). Fixation and mounting of cultured cells results in their cilia lying at a point somewhere between the horizontal and vertical planes. The measured length will therefore vary with the cosine of the angle from which the cilium protrudes from the focal plane, and this is likely to be responsible, in part, for the wide array in lengths observed. The variation may also be attributed to slow cilium formation, if this is in any way linked to cell cycling speed, and thus more cilia would be measurable at intermediary stages of construction than in faster cycling cells such as NIH3T3s.

Luciferase assays, using Shh Light II cells, yielded results that indicate the agonists used did indeed stimulate Hh pathway activation (Figure 3.3.1). Purmorphamine and SAG act at Smo, while ShhN targets Ptch, showing that activation of the pathway at either of these sites leads to a similar output in Gli activity. Although the ShhN protein used here is derived from recombinant mouse DNA, it is 99% identical to human Shh (R&D

systems data sheet 464-SH), and therefore should also inhibit Ptch in human cell lines, allowing downstream signalling.

When treating Shh Light II cells with the antagonists alone, it was not known if they would be able to inhibit basal Gli promoter activity to a level measurable by the luciferase reporter system. No reduction in luciferase output was recorded after cyclopamine or vismodegib treatment, although a significant decrease was observed in cells exposed to Sant1. All these antagonists target Smo, but are thought to have different binding sites and cause different conformational changes (Chen et al, 2002b; Wang et al, 2009; Wilson et al, 2009). Alternative Smo conformations probably result in different levels of Smo activation or inhibition, to give varying degrees of Hh signalling. Cyclopamine has also been shown to cause Smo ciliary translocation in both NIH3T3s and mouse embryonic fibroblasts, while Sant1 does not (Wang et al, 2009; Wilson et al, 2009). Various studies using Sant1 suggest that it is a more potent inhibitor of agonist stimulated activation of the Hh pathway than the other antagonists (Chen et al, 2002b; Wang et al, 2009; Wilson et al, 2009), and hence this is likely to be the reason why this was the only one to have measurable effects when given alone.

LDH and FACS experiments confirm that there was no significant cytotoxicity after treatment with any of the Hh pathway effectors (Figure 3.3.3). Therefore, the reduction in luciferase activity recorded in response to Sant1 treatment (Figure 3.3.1) was not due to an increase in cell death, and rather an inhibition of signalling.

The antagonists cyclopamine and vismodegib were further tested in combination with purmorphamine treatment. In this situation they produced a significant decrease in luciferase activity when compared to purmorphamine treatment alone (Figure 3.3.1). However, tomatidine also showed this effect, despite being reported to not cause inhibition of Hh signalling in chick neural ectoderm cells (Cooper et al, 1998). The relationship between purmorphamine and tomatidine has not been thoroughly investigated, and so an interaction disrupting the agonist effects of purmorphamine or its target Smo cannot be ruled out as an explanation for these results.

Another compound tested was Forskolin, reported to be a Hh pathway antagonist through its activation of adenylate cyclase, and stimulation of protein kinase A (PKA) production (Hyman et al, 2009; Taipale et al, 2000). However, PKA has been implicated

in both positive and negative regulation of Hh signalling. Formation of Gli transcriptional repressors (GliRs) involves their phosphorylation by PKA, CK1 (Casein Kinase 1) and GSK3β (glycogen synthase kinase 3β) at conserved serine residues in the C-terminus, to allow binding of βTrCP, an E3 ubiquitin ligase, part of the ubiquitin ligase complex (Pan & Wang, 2007; Tempe et al, 2006; Wang & Li, 2006). This results in ubiquitination, and targets the protein for proteasomal processing. In the majority of cases, proteasomal processing (ubiquitin-proteasome proteolytic system) leads to complete degradation of the ubiquitinated target protein. However, in a few cases such as this, processing only leads to partial degradation, and therefore GliR formation (Pan & Wang, 2007). The proteolysis removes the carboxyl-terminal activation domain, so truncated products act as repressors (King et al, 2008). SuFu is a nuclear trafficking protein that forms part of a complex with PKA, CK1 and GSK3β, and may act as a scaffold, permitting Gli phosphorylation. (Jia et al, 2009; Yue et al, 2008).

Conversely, PKA in combination with CK1 in drosophila, or GSK3β in mice, phosphorylates Arginine clusters in the Smo intracellular carboxy-terminal tail. This is thought to allow an activating conformational change (Chen et al, 2004; Wilson et al, 2009; Zhao et al, 2007) and redistribution of Smo from cytoplasmic pools to the cell or ciliary membrane (Jia et al, 2004; Wang et al, 2009). Fsk has also been shown to cause translocation of Smo to a proximal region in primary cilia, although this did not correspond with increased Gli-luciferase reporter activity in MEFs (Wilson et al, 2009). It is therefore a rather complicated system, and the increase in luciferase activity found here after Fsk treatment cannot easily be explained.

While both Ptch1 and Gli1 are factors up-regulated by Hh signalling, Ptch1 expression is also controlled by other factors (Goodrich et al, 1996). Hence, Gli1 expression is a better readout for Hh pathway activity. Using real-time qPCR it was possible to show increased Gli1 mRNA levels in H295R cells treated with purmorphamine (Figure 3.3.2), although it was not significant. This was primarily due to large variability in the strength of the increase, with the range of values spread between two- and twenty five-fold. Repeating this study several more times could result in a significant increase.

The Gli-luciferase reporter system was unsuccessful in H295R cells, possibly due to the inefficiency of transfecting this cell line. Even under optimal conditions of transient transfection only about 30% of cells are transfected (Julia Kowalczyk, personal communication), and thus luciferase activity would generally be below the detectable limit of the luminometer, given that the response of an optimised system, Shh Light II cells, to the agonists is only two-fold. H295R cells also form fewer cilia than NIH3T3s (Schneider et al, 2005), from which the Shh Light II cell line was derived, which may limit the capacity of these cells to respond to the Hh pathway agonists.

A thirty-fold increase in Gli1 expression by qPCR was reported by Kim et al. after stimulation of murine bone marrow stromal cells with 1µM purmorphamine for 48 hours (Kim et al, 2009). This is three times as great as the average ten-fold increase recorded here, and cell type may be an influencing factor. As described above, H295R cells are capable of forming primary cilia, an essential component for Hh signalling, but do so at a slower rate than other cell lines. Therefore, this could impact on the cells ability to respond to purmorphamine, resulting in saturation of Smo at a much lower concentration.

Gli1 mRNA expression after treatment with the Hh pathway antagonist cyclopamine was also tested by real-time qPCR, with no significant deviation in levels from the untreated cells. As with the luciferase assay, it was unclear if treatment alone would cause a measurable decrease in basal Gli1 levels, at the concentration used. More information about the actions of cyclopamine may be gained from testing its ability to inhibit elevated Gli1 activity after agonist stimulation.

While PCR is a quick, easy and reasonably reliable method for determining gene expression, and generally mRNA abundance corresponds moderately with protein abundance, there can be discrepancies between the two types of data. Post-transcriptional and post-translational modifications, RNA and protein stability, and experimental error can all contribute to the variability, as well as gene/protein length, which may be minimally responsible (Nie et al, 2006; Pascal et al, 2008). mRNAs whose levels change with the different stages of the cell cycle, correspond more closely to final protein content, because there is tight control at the transcriptional level.

Whereas those that have a more consistent expression throughout, tend to be more independent of final protein levels, as regulation is governed at the translation or post-translational stages (Greenbaum et al, 2003). Therefore, wherever possible, both RNA and protein expression should be examined, but either alone can also provide some significant information regarding biological systems.

The lack of availability of specific and reliable Gli1 antibodies has prevented the attainment of western blotting data that corresponds with these qPCR results. Therefore, it cannot be conclusively reported that purmorphamine is activating the canonical Hh pathway in H295R cells. However, it is most likely that this is the case, as all literature, and data obtained thus far, support this hypothesis.

The ability to differentiate H295R cells towards either a zG- or zF-like phenotype, by treatment with angiotensin II or forskolin respectively, has been shown by the qPCR assessment of CYP11B1 and CYP11B2 mRNA levels (Figure 3.4.1A). Increased staining for the oxidation of DHEA to androstenedione, which requires 3βHSD activity, also indicates an increase in steroidogenesis in these cells (Figure 3.4.1B), as well as measuring the final steroidal output by ELISA (Figure 3.4.1C). Reports suggest that anything between 6 and 96 hours treatment with these compounds will cause CYP11B1 and CYP11B2 levels to rise (Cobb et al, 1996; Denner et al, 1996), with subsequently increased cortisol and aldosterone production, a characteristic that defines the differentiated cell type. Further treatment with Fsk will also result in an increase in DHEA and DHEAS levels, indicative of a shift in the steroidogenic pathway towards androgen production like that of the zR (Cobb et al, 1996).

With reference to the initial aims of this chapter, the adrenal carcinoma cell line H295R has been shown to express components of the Hh pathway, have the capacity to form primary cilia, and can be differentiated towards the zonal phenotypes of the mammalian adrenal cortex. They also appear to respond to Hh pathway agonists in a canonical signalling manner. Therefore, this cell line meets the criteria required of a suitable *in vitro* system in which to study the role of hedgehog signalling and primary cilia in adrenal differentiation and function.

CHAPTER 4: THE ROLE OF PRIMARY CILIA IN THE DIFFERENTIATION OF H295R CELLS

4.1 Aims

The previous chapter investigated the adrenocortical H295R cell line and demonstrated that these cells have primary cilia, and can be induced to differentiate under defined conditions into cells characteristic of the different zones of the adrenal cortex. The main aim of this chapter is to investigate whether primary cilia are involved in the differentiation of H295R cells. siRNAs are used to disrupt cilium formation and function, and the resulting effect on differentiation is established by measuring steroidogenic enzyme expression. The roles of the Hh and Wnt signalling pathways in this process are also addressed.

4.2 The effects of siRNA on ciliation

Inhibiting the formation of primary cilia can be used to investigate the role they play in H295R cell differentiation. This can be performed using synthetic siRNAs (short interfering RNAs) of approximately 20-25 nucleotides in length, that bind to a specific mRNA sequence, targeting it for degradation and therefore silencing the corresponding gene. mRNA sequences for genes encoding components of the intraflagellar transport system, or other proteins involved in ciliogenesis, are ideal targets.

Genetic mutations in the intraflagellar transport machinery component IFT88 are proven to hinder the formation of cilia in *Chlamydomonas* (green algae) and mice, resulting in their stunted growth (Pazour et al, 2000). This has also been achieved using siRNA in the mouse stem cell line P19.CL6 (Clement et al, 2009). Bardet-Biedl Syndrome, a known ciliopathy, has been linked to mutations in a number of proteins, including BBS4 and BBS6. These are involved in protein folding and targeting components to the cilium, and while they may not be essential for cilium formation in all cell types, they are required for its function (Kim et al, 2005; Mykytyn et al, 2004). Therefore, IFT88, BBS4 and BBS6 were targeted for knockdown using siRNAs.

In an initial experiment, knockdown of the cilia components was attempted in normally growing H295R cells. After transfection with siIFT88, siBBS4, siBBS6 or an siRNA negative control (ctrl), IFT88, BBS4 or BBS6 mRNA expression was measured by qPCR. As primary cilia form a key structural component of Hh (and other) signalling pathways, the expression of Hh pathway genes was also examined.

Each siRNA was capable of significantly reducing the mRNA levels of its target gene (Figure 4.2.1A-C), with IFT88, BBS4 and BBS6 expression decreased to 48%, 26% and 46% respectively. Cells transfected with siIFT88 also showed a significant reduction in the expression of Hh pathway genes (Figure 4.2.1A), but there was no significant change in their levels after siBBS4 or siBBS6 transfection (Figure 4.2.1B-C). FoxD1 and NR4A1 are Shh targets (Ingram et al, 2002). FoxD1 is a transcription factor, and like Gli1, is expressed in the capsule and a few subcapsular cells of the adrenal cortex (Dr Peter King, unpublished data), while NR4A1 is a nuclear receptor expressed in both the zG and zF (Bassett et al, 2004a). PPIA (peptidylprolyl isomerase A) is a housekeeping gene that should not be regulated by ciliary proteins, nor is it a target of Hh signalling. It is included as a negative control.

To complement the mRNA data, relative protein abundance was also measured by western blotting. Figure 4.2.1D shows that IFT88 and BBS4 protein levels were reduced to 72% and 63% respectively, after transfection with their corresponding siRNAs.

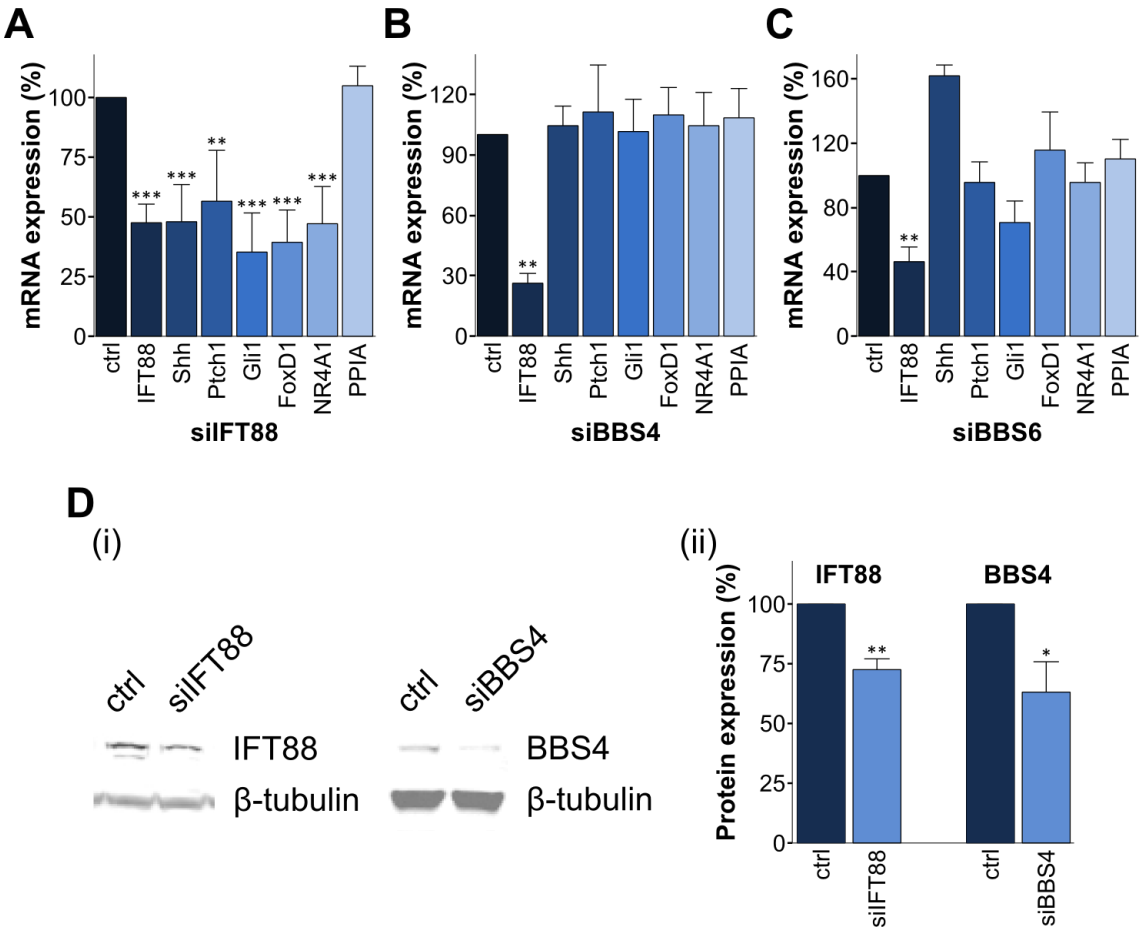

Figure 4.2.1 – Knockdown of ciliary components in H295R cells
(A-C) Graphs showing the mRNA expression of different genes in H295R cells. Cells were harvested 48hrs after transfection with 100nM siIFT88 (A), siBBS4 (B), or siBBS6 (C), and mRNA expression was compared to that of cells transfected with a negative control (ctrl). Quantitative real-time qPCR was carried out measuring IFT88, BBS4 or BBS6 expression, and Shh, Ptch1, Gli1, FoxD1, NR4A1 or PPIA expression. 18S rRNA expression was used as the loading control. The data were analysed using a one-way ANOVA with pre-planned and post-hoc comparisons for each gene. N=6, data collated, error bars indicate SEM. ** p<0.01, *** p<0.001 compared to ctrl.
(D) Images and graph showing protein expression in H295R cells. Cells were harvested 48hrs after transfection with 100nM siIFT88, siBBS4 or a negative control (ctrl), and protein extracts were analysed by western blotting. Anti-IFT88 and anti-BBS4 antibodies were used to detect the targeted proteins. An anti-β-tubulin antibody was used as a loading control. Images of the blots were scanned using the Licor Odyssey infrared scanner (i), and quantified using the Licor Odyssey imaging systems software (ii). The data were analysed using a one-way ANOVA for each gene. N=3, data collated, error bars indicate SEM. * p<0.05, ** p<0.01 compared to ctrl.

Knocking down genes encoding ciliary network proteins can be detrimental to cilium formation, as previously mentioned. Therefore the effect of the knockdowns on the frequency and gross morphology of cilia in H295R cells was examined. After transfection with the siRNAs or negative control, cells were fixed and markers of the ciliary axoneme and basal body were analysed by confocal microscopy. While there was no apparent change in the number of ciliated cells, there was a significant

decrease in the length of cilia after transfection with any of the siRNAs (Figure 4.2.2). It can therefore be said that IFT88, BBS4 and BBS6 are required for normal cilium formation in H295R cells.

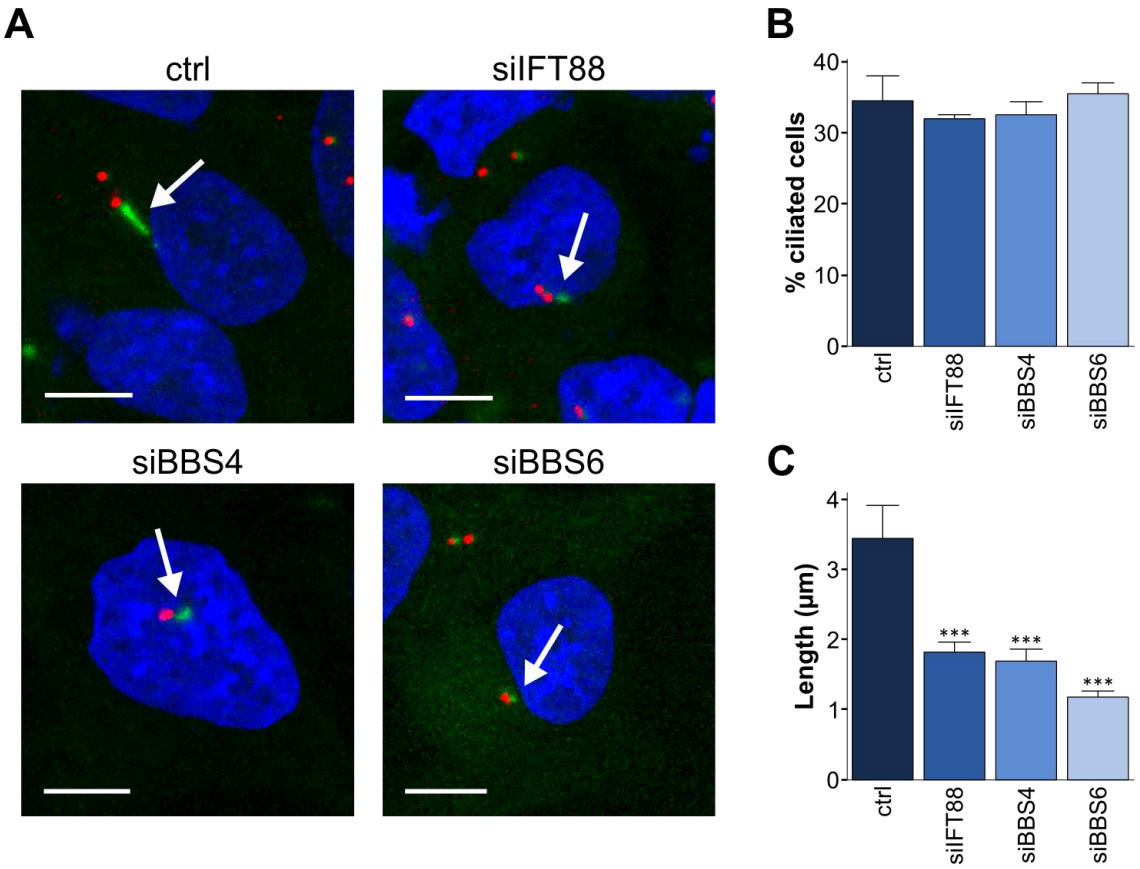

Figure 4.2.2 – The effects of siRNA on ciliation
48hrs after transfection with 100nM ciliary targeting siRNAs or a negative control (ctrl), H295R cells were fixed and stained with antibodies against acetylated α-tubulin (green), and pericentrin (red). DAPI was used to stain the nuclei (blue). Cilia were visualised (A - representative images, cilia are indicated by the arrows) and their number (B) and length (C) determined using the Zeiss LSM510 inverted laser scanning confocal microscope with 63x objective, and the ZEN 2008 Light edition software. Scale bar represents 10µm. For each siRNA, cilia were blindly counted from 3 slides, using 5 maximum intensity projections of z-stacks per slide (N=3). The length of 15 cilia was measured across the 3 slides (N=15). The data were analysed using a one-way ANOVA with post-hoc comparisons. Data collated, error bars indicate SEM. *** p<0.001 compared to ctrl.

4.3 Cilia are required for zG-like differentiation

Having established that IFT88, BBS4 and BBS6 mRNAs were successfully knocked down, with a corresponding reduction in protein abundance for IFT88 and BBS4, as well as a

reduction of cilium length in H295R cells, the effects of these knockdowns on the ability of these cells to differentiate was investigated. H295R cells were transfected with siRNA targeting IFT88, BBS4 and BBS6 or a negative control and treated with angiotensin II (AngII) or forskolin (Fsk). Quantitative real-time qPCR was then carried out measuring IFT88, BBS4 and BBS6 expression to assess the effectiveness of the knockdown, and CYP11B1 and CYP11B2 expression to determine differentiation of the cells by the different agonists.

Figure 4.3.1A shows that successful knockdown of IFT88, BBS4 and BBS6 were again achieved in this experiment, regardless of the inclusion of the differentiation agents in the media. In cells transfected with the negative control and treated with AngII or Fsk, up-regulation of CYP11B1 and CYP11B2 expression, respectively, was observed (Figure 4.3.1B-C), similar to the results shown in chapter 3 (Figure 3.4.1). This demonstrates that the siRNA transfection protocol itself does not affect differentiation.

Analysing expression of the zF marker CYP11B1, demonstrated that cells transfected with the siRNAs show a similar pattern of its mRNA expression to the negative control, with Fsk treated samples having the highest values, and no significant difference between them (Figure 4.3.1). AngII treatment also increased CYP11B1 expression, which is perhaps reduced by transfection of the specific siRNAs. Untreated, siRNA transfected cells show no change in CYP11B1 expression compared with the untreated, siRNA negative control. These results suggest that there is no change in the differentiation of cells towards a zF-like phenotype when transfected with the ciliary gene targeting siRNAs. CYP11B1 expression may, however, be slightly reduced in cells differentiating towards a zG-like phenotype after AngII treatment, in combination with the siRNA transfections.

CYP11B2 expression, a marker of the zG, was greatly increased by AngII treatment in cells transfected with the control siRNA (Figure 4.3.1C). Treatment with all the gene specific siRNAs reduced the level of this increase to approximately half that of the control, although this only reached significance when knocking down IFT88. All cells treated with Fsk showed a marginal increase in CYP11B2 expression compared with untreated cells, regardless of the siRNA transfected, and there was no difference

between CYP11B2 mRNA levels in all untreated samples. These data indicate that AngII treatment does not increase CYP11B2 expression to the same extent in cells transfected with the ciliary gene targeting siRNAs compared to those transfected with the control. Therefore it is likely that differentiation towards a zG-like phenotype is reduced when IFT88, BBS4 or BBS6 are knocked down in the H295R cell line.

The above data indicate that when combining transient transfections with AngII or Fsk treatment, the expected siRNA target genes are successfully down-regulated, and differentiation occurs normally in the negative controls, measured by CYP11B1 and CYP11B2 expression. Therefore, this protocol is appropriate for studying the effects of siRNA targeted knockdown of ciliary network components, causing reduced cilium length and, presumably, function, on H295R cell differentiation. An apparent decrease in CYP11B2 expression in cells transfected with the siRNAs in combination with AngII treatment was found. As each siRNA targets a different ciliary component, together these results imply that there is a role for primary cilia at least as far as AngII signalling is concerned, and potentially in the differentiation of H295R cells towards a zG-like phenotype.

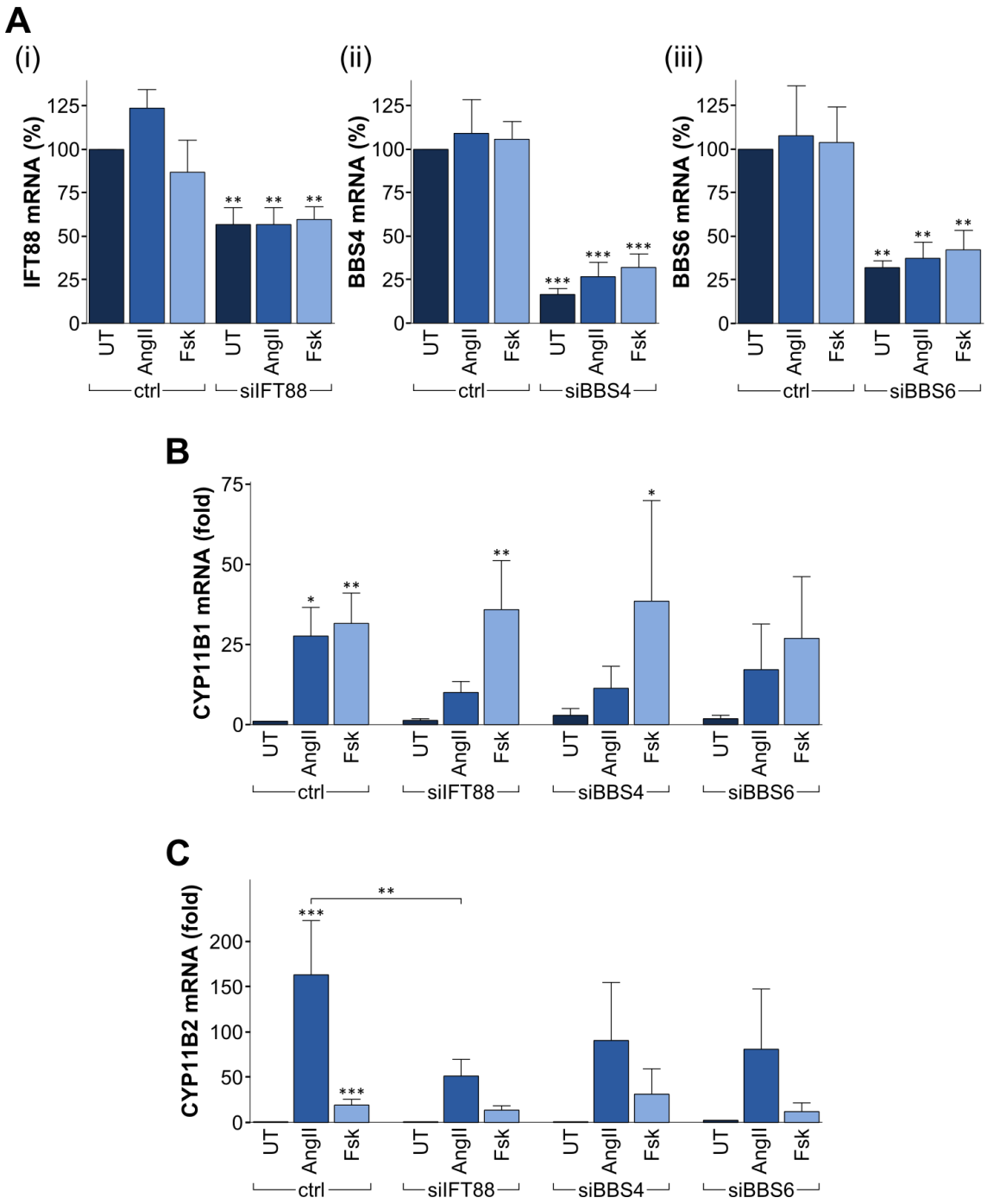

Figure 4.3.1 – The effects of siRNA on differentiation
Graphs showing the relative quantities of IFT88, BBS4 and BBS6 (A), CYP11B1 (B) and CYP11B2 (C) mRNA in H295R cells. Cells were transfected with 100nM siRNA or a negative control (ctrl), and differentiated over a 40hr period. Cells were either untreated (UT), or given 10µM Angiotensin II (AngII) or Forskolin (Fsk). Quantitative real-time qPCR was carried out measuring IFT88, BBS4, BBS6, CYP11B1 or CYP11B2 expression. 18S rRNA expression was used as the loading control. For each gene, a one-way ANOVA with pre-planned and post-hoc comparisons of treatments was used to interpret the data. N=10 for ctrl, N=7 for siIFT88, N=3 for siBBS4 & siBBS6, data collated, error bars indicate SEM. * p<0.05, ** p<0.01, *** p<0.001 compared to UT ctrl, unless otherwise indicated.

4.4 The effects of ShhN on differentiation

The above data indicate that primary cilia may play a key role in the process of differentiating H295R cells towards a zG-like phenotype, possibly via the signalling pathways to which they play host. Hh signalling is a key pathway involved in adrenal development that is also highly reliant upon primary cilia for its correct function. In the mammalian adrenal cortex, Hh-expressing cells lie in the subcapsular region, while Hh responsive (Gli1-positive) cells are present in the overlying capsule, the predicted source of adrenocortical stem cells (Huang et al, 2010; King et al, 2009; Salmon & Zwemer, 1941). It is therefore possible that the differentiation of these stem cells into zG and zF cells may involve the Hh signalling pathway. Gli1 mRNA expression was subsequently measured as a marker of Hh signalling in H295R cells transfected with the ciliary targeting siRNAs, and treated with AngII or Fsk, however its expression was not significantly altered after any of the transfections or treatments (Figure 4.4.1).

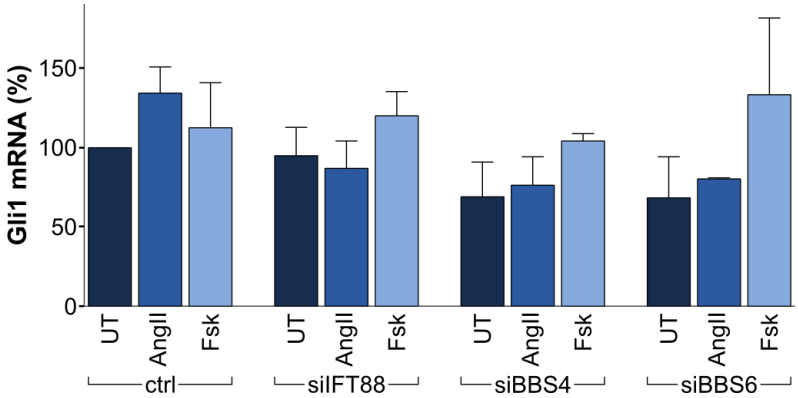

Figure 4.4.1 – Gli1 mRNA expression in differentiating H295R cells
Graph showing the relative quantities of Gli1 mRNA in H295R cells. Cells were transfected with 100nM siRNA or a negative control (ctrl), and differentiated over a 40hr period. Cells were either untreated (UT), or given 10µM Angiotensin II (AngII) or Forskolin (Fsk). Quantitative real-time qPCR was carried out measuring Gli1 expression. 18S rRNA expression was used as the loading control. The data were analysed using a one-way ANOVA with pre-planned and post-hoc comparisons of treatments. N=10 for ctrl, N=7 for siIFT88, N=3 for siBBS4 & siBBS6, data collated error bars indicate SEM.

Although no clear conclusions could be drawn from the Gli1 qPCR results, Shh-positive cells have been shown to give rise to all steroidogenic cell types during development of the mouse adrenal, Shh null adrenals exhibit impaired steroidogenic differentiation (King et al, 2009), and Shh expression is altered during adrenal remodelling (Guasti et al, manuscript in preparation), hence it is possible that Shh regulates adrenal

differentiation, and further studies were conducted to help elucidate its role in this process. H295R cells were either untreated, or given AngII or Fsk, in the presence or absence of ShhN. Quantitative real-time qPCR was then carried out measuring CYP11B1 and CYP11B2 expression to determine differentiation of the cells, and Shh or Gli1 expression to identify changes in Hh pathway activation.

With the addition of ShhN, the small increase in CYP11B1 expression produced by AngII treatment alone was abrogated, as was the significant increase AngII caused in CYP11B2 mRNA levels (Figure 4.4.2A-B). ShhN treatment did not alter the expression of either steroidogenic enzyme when combined with Fsk treatment, or used on its own. These data suggest that the presence of ShhN inhibits differentiation of H295R cells towards a zG-like phenotype, but has no effect on zF differentiation.

All treatment conditions resulted in similar levels of Shh expression, although they were marginally higher in those treated with ShhN (Figure 4.4.2C). Shh is not known to positively regulate its own expression and so activation of this pathway with the addition of ShhN would not be expected to cause a significant increase in Shh expression. It would however be expected to increase the mRNA levels of Gli1. Whilst mRNA levels were slightly increased above background in each condition when ShhN was used, these increases were not significant (Figure 4.4.2D).

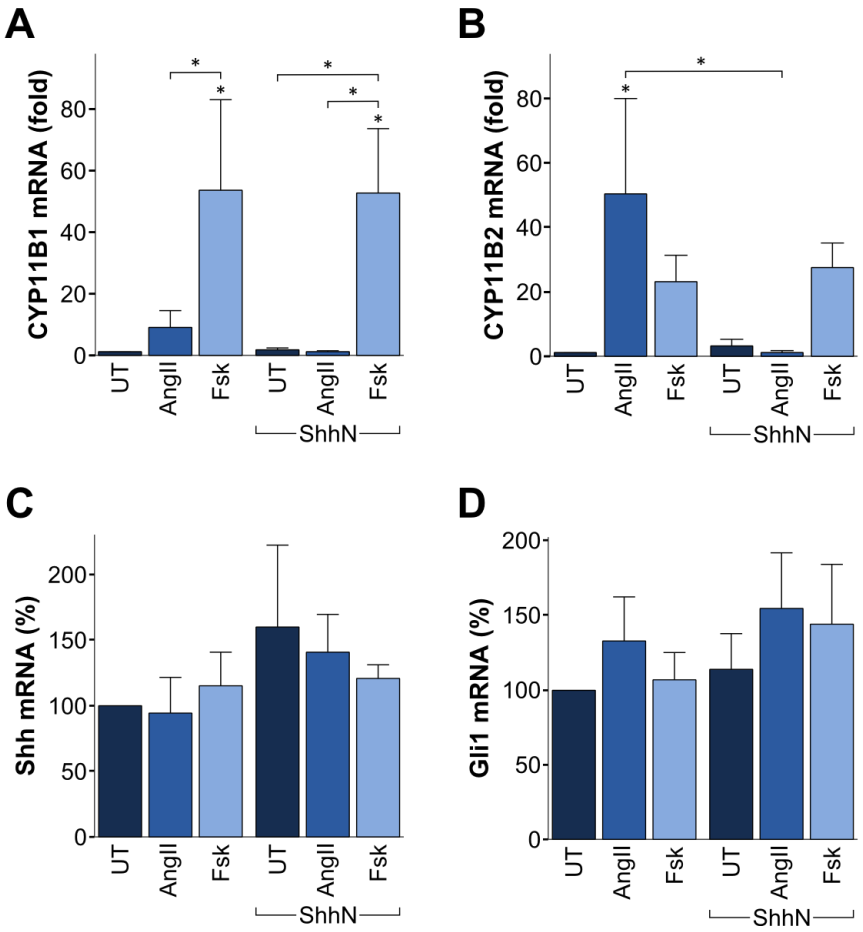

Figure 4.4.2 – The effects of ShhN on differentiation
Graphs showing the relative quantities of CYP11B1 (A), CYP11B2 (B), ShhN (C) and Gli1 (D) mRNA in H295R cells. Cells were treated with 0.35µg/ml ShhN in combination with 10µM Angiotensin II (AngII) or 10µM Forskolin (Fsk) every 24hrs over a 96hr time period. Quantitative real time qPCR was carried out measuring CYP11B1, CYP11B2, ShhN or Gli1 expression. 18S rRNA expression was used as the loading control. A one-way ANOVA with pre-planned and post-hoc comparisons of treatments was implemented for each gene to interpret the data. N=3, data collated, error bars indicate SEM. * $p<0.05$ compared to UT, unless otherwise indicated.

Angiotensin II acts via the AT1 receptor in humans, and AT1a and AT1b receptors in rodents, to increase CYP11B2 synthesis (Bogdarina et al, 2009; Rainey et al, 2004). If Hh signalling via cilia directly influences zG-like differentiation, it may be hypothesised that AT1 is a Shh target gene, and Gli1 could alter AT1 production either directly, by binding the AT1 promoter, or via up-regulation of other transcription factors. To investigate this, H295R cells were co-transfected with a rat AT1b promoter-luciferase reporter plasmid (pGL3-AT1b; Dr Irina Bogdarina, Queen Mary University of London) and a Gli1 expression plasmid (pEGFP-Gli1; Dr Graham Neill, Queen Mary University of London), and stimulated with AngII. A dual-luciferase assay was then performed.

Modulation of the AT1b promoter activity will result in changes in luciferase expression which can be assessed using a luciferase assay. Overexpression of Gli1 caused a small decrease in the AT1b promoter activity in these studies, as did treatment with AngII, both in the presence or absence of over-expressed Gli1 (Figure 4.4.3A), although these reductions were not statistically significant. As these results suggest that Hh signalling, via Gli1, potentially inhibits the transcriptional activity of the AT1b promoter, human AT1 mRNA expression was examined in H295R cells in which cilia had been knocked down.

Cells were transfected with siIFT88 or a negative control, and stimulated to differentiate by adding AngII or Fsk. Quantitative real-time qPCR was then carried out measuring AT1 expression. Figure 4.4.3B shows that treatment with Fsk, with or without siIFT88 transfection, significantly reduced AT1 mRNA expression, as did AngII treatment when combined with siIFT88. However, there was no change in AT1 expression in untreated, siIFT88 transfected cells compared to the untreated control cells, suggesting that reducing Hh signalling by impairing cilium formation and function with siRNAs, has little impact on AT1 expression.

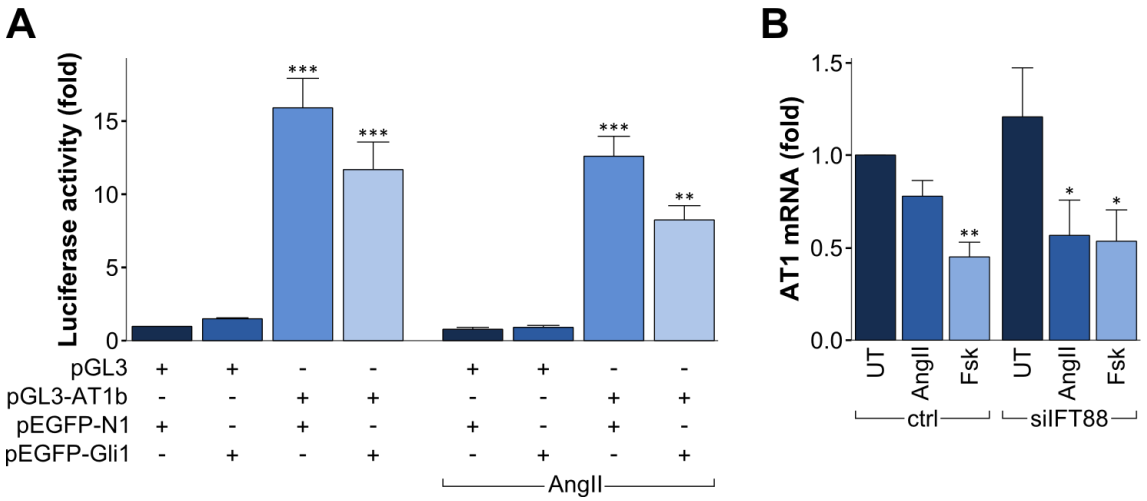

Figure 4.4.3 – AT1 promoter activity and mRNA expression
(A) Graph showing relative luciferase activities normalised to renilla. H295R cells were co-transfected with a rat AT1b promoter-luciferase reporter plasmid (pGL3-AT1b) and a Gli1 expression plasmid (pEGFP-Gli1), or their equivalent empty vector controls (pGL3 & pEGFP-N1), and either untreated, or stimulated with 10µM Angiotensin II (AngII) for the last 16 hours of the transfection. All cells were also transfected with the pRL-CMV renilla control plasmid. After 48hrs a dual-luciferase reporter assay was conducted and the data analysed using a one-way ANOVA with post-hoc comparisons of the transfections. N=3, data collated, error bars indicate SEM. ** p<0.01, *** p<0.001 compared to pGL3, pEGFP-N1 transfected cells without AngII treatment.
(B) Graph showing the relative quantities of AT1 mRNA in H295R cells. Cells were transfected with 100nM siRNA or a negative control (ctrl), and differentiated over a 40hr period. Cells were either untreated (UT), or given 10µM Angiotensin II (AngII) or Forskolin (Fsk). Quantitative real-time qPCR was carried out measuring AT1 expression. 18S rRNA expression was used as the loading control. A one-way ANOVA with pre-planned and post-hoc comparisons of treatments was used to interpret the data. N=3, data collated, error bars indicate SEM. * p<0.05, ** p<0.01 compared to UT ctrl.

Although Hh signalling may not regulate AT1 expression, a significant decrease in CYP11B2 mRNA expression in H295R cells was seen when ShhN treatment was combined with AngII (Figure 4.4.2B). Therefore the ability of ShhN to regulate the activity of the CYP11B2 promoter was investigated. Cells were transfected with a rat CYP11B2 promoter-luciferase reporter plasmid (pGL3-CYP11B2; Dr Artem Bakmanidis, Queen Mary University of London) and treated with AngII and/or ShhN. A dual-luciferase reporter assay was then carried out. AngII treatment significantly increased CYP11B2 luciferase activity, as expected, while ShhN treatment did not (Figure 4.4.4). Combining ShhN with AngII treatment also resulted in an increase in CYP11B2 luciferase activity, but to a lesser extent than AngII treatment alone, suggesting that ShhN may be inhibiting the activity of the CYP11B2 promoter.

The above data suggest that ShhN, at the concentration used, acts to prevent the differentiation of AngII treated H295R cells towards a zG-like phenotype, measurable by reduced steroidogenic enzyme expression. However, it is not clear if it exerts this effect through activation of the canonical Hh signalling pathway, which requires functional primary cilia. It may regulate responsiveness to AngII, and therefore CYP11B2 and aldosterone production.

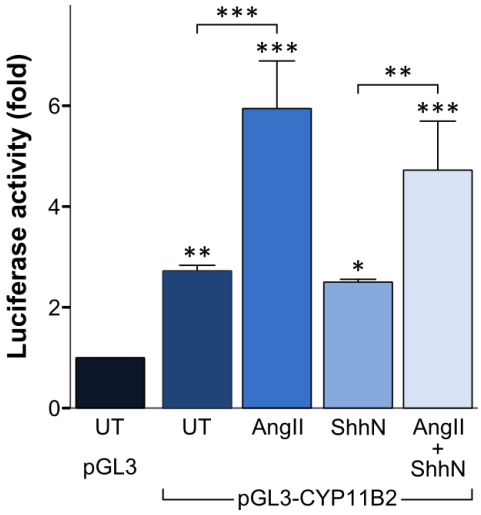

Figure 4.4.4 – CYP11B2 luciferase assay
Graph showing relative luciferase activities normalised to renilla. H295R cells were transfected with a rat CYP11B2 promoter-luciferase reporter plasmid (pGL3-CYP11B2) or the equivalent empty vector control (pGL3), and either untreated (UT), or stimulated with 10µM AngII, 0.35µg/ml ShhN, or both for 32hrs. All cells were also transfected with the pRL-CMV renilla control plasmid. 48hrs after the initial transfection a dual-luciferase reporter assay was conducted and the data analysed using a one-way ANOVA with pre-planned and post-hoc comparisons of the transfections. N=3, data collated, error bars indicate SEM. * p<0.05, ** p<0.01, *** p<0.001 compared to pGL3 transfected, untreated cells, unless otherwise indicated.

4.5 Wnt signalling

It has been shown that primary cilia appear to be required for H295R cells to acquire zG-like phenotypes, but that ShhN is inhibitory to AngII stimulated differentiation. Therefore, other signalling pathways that utilise the cilium may be involved in the mechanism by which primary cilia are involved in this process. Components of the canonical Wnt signalling pathway have been shown to localise to the cilium (Corbit et al, 2005; Satir & Christensen, 2007; Simons et al, 2005), and in some cases, such as in

renal cells, correct regulation of its signalling is dependent upon primary cilia (Eggenschwiler & Anderson, 2007). Wnt signalling is also required during adrenal development. β-catenin is expressed throughout the developing adrenal cortex in mice, which then becomes restricted to the subcapsular cells in the adult, and mice with conditionally inactivated β-catenin have adrenal aplasia by E18.5 (Kim et al, 2008a). Furthermore, constitutive activation of β-catenin in the adrenal can lead to ectopic expression of CYP11B2 near the medulla (Berthon et al, 2010), and deletion of Wnt4 causes loss of the zG (Heikkila et al, 2002). Hence, the relationship between primary cilia and canonical Wnt signalling in H295R cells was investigated.

H295R cells were transfected with a canonical Wnt responsive luciferase reporter plasmid (TOPFlash), or control plasmid (FOPFlash), in combination with one of the siRNAs targeting components involved in cilium formation and function. A dual-luciferase assay was then conducted. The M50 Super 8x TOPFlash luciferase plasmid has a synthetic promoter composed of seven multimeric TCF/LEF binding sites upstream of the luciferase gene, while the promoter of the M51 Super 8x FOPFlash luciferase vector contains six mutated TCF/LEF binding sites (Figure 4.5.1A; Prof Randall Moon, University of Washington). Disruption of the canonical Wnt signalling pathway should result in changes in the amount of β-catenin that translocates to the nucleus and interacts with TCF/LEF (T-cell factor/lymphoid enhancer-binding factor) to activate transcription of the luciferase reporter.

Compared to the FOPFlash negative control, the TOPFlash promoter construct was highly active in H295R cells, indicating significant canonical Wnt signalling in this cell line (Figure 4.5.1B). However, the siRNAs had no effect on the activity of the TOPFlash promoter. It is therefore unlikely that canonical Wnt signalling requires, or is inhibited by, primary cilia in H295R cells, and thus it may not be involved in the effects observed in Figure 4.3.1B above.

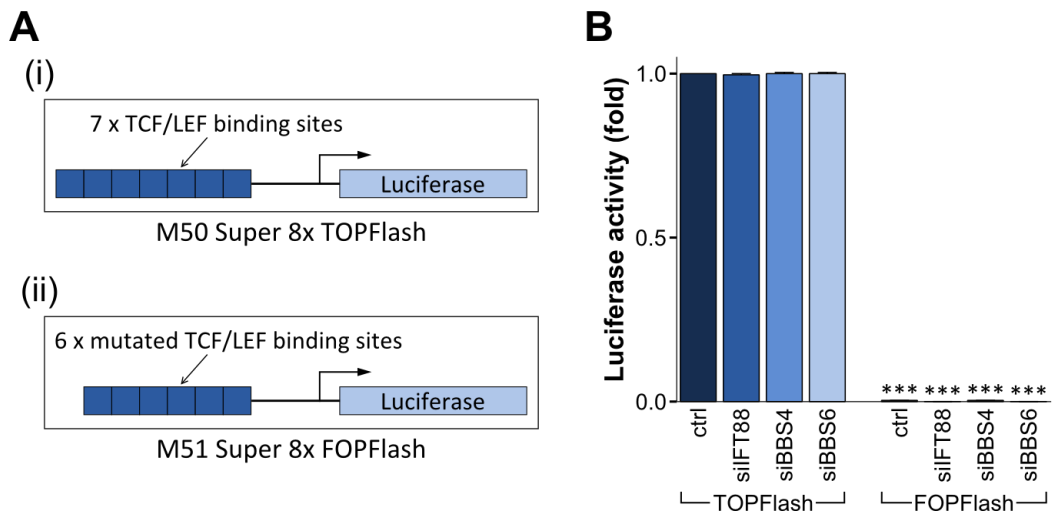

Figure 4.5.1 – Wnt signalling in H295R cells
(A) Schematic diagram depicting the M50 Super 8x TOPFlash (i) and M51 Super 8x FOPFlash (ii) luciferase plasmids.
(B) Graph showing relative luciferase activities normalised to renilla. H295R cells were transfected with a canonical Wnt responsive luciferase reporter plasmid (TOPFlash), or mutated control (FOPFlash) and the pRL-CMV renilla plasmid, either on their own (ctrl) or in combination with 100nM siRNA targeting components involved in cilium formation and function (siIFT88, siBBS4, siBBS6). After 48hrs the cells were harvested and a dual-luciferase assay was conducted. The results were analysed using a one-way ANOVA with pre-planned and post-hoc comparisons. N=3, data collated, error bars indicate SEM. *** p<0.001 compared to ctrl, TOPFlash transfected cells.

4.6 Discussion

Using siRNAs targeting components required for cilium formation and function, it has been possible to knockdown IFT88, BBS4 and BBS6 mRNA expression levels to below fifty per cent in H295R cells (Figure 4.2.1A-C). Although not to a similar degree, a corresponding reduction in protein abundance was also determined using antibodies for IFT88 and BBS4 (Figure 4.2.1D). BBS6 protein levels were not examined due to a lack of suitable antibodies.

Reduced mRNA expression of Hh pathway genes after transfection with siIFT88 shows that Hh signalling is impaired, implying the likely reduction of cilium function (Figure 4.2.1A). Canonical Hh signalling is known to be strictly dependent on the ability of cells to form functional cilia in all systems studied, as many components of the pathway are localised therein (Haycraft et al, 2005). Hh reporter expression was unchanged in BBS4 siRNA transfected cells, and perhaps only slightly disrupted in cells that received BBS6 siRNA (Figure 4.2.1B-C). This most likely reflects the different cellular functions of each of these proteins.

IFT88 is an intraflagellar transport protein that is part of protein complex B within the IFT particles (Tobin & Beales, 2009). Not only is it essential for cilium formation, it is required for localisation of the Gli transcription factors to the tip of the cilium, processing of Gli3 to a transcriptional repressor, and is involved in Gli2 functions (Haycraft et al, 2005). Therefore, IFT88 plays a direct role in transmitting the Hh signal. In contrast, BBS4 and BBS6 have not been directly implicated in Hh pathway transduction. BBS4 is part of the BBSome complex of proteins, which are involved in ciliary membrane biogenesis through mediation of vesicular transport (Nachury et al, 2007), while BBS6 shares structural homology with the group II chaperonins required for folding newly synthesised proteins. A reduction in Hh signalling after knockdown of BBS4 or BBS6 may only occur as a secondary characteristic of impaired cilium formation or function, and hence may not produce as great an effect on the expression of Hh reporters.

Although disruptions in Hh signalling were not clearly apparent with all the siRNAs, this does not mean that other ciliary functions were not disrupted. The percentage of ciliated cells remained unchanged, but the length of cilia was severely reduced after transfection with any of the siRNAs compared to the negative control (Figure 4.2.2c). A reduction in cilium length is highly likely to impact on its function.

Stunted cilia, or their complete absence, are well documented in cells lacking IFT88, however the effect of knocking down BBS genes results in varied phenotypes. BBS1, 4 or 6 null mice have anosmia, due to disrupted formation of sensory cilia in the olfactory epithelium, and develop retinal degeneration, corresponding with a role for these proteins in the maintenance of connecting cilia within the photoreceptor cells (Kulaga et al, 2004; Ross et al, 2005). BBS5, 7 and 8 have also been shown to be required for cilia/flagella assembly in the nematode worm (*C. Elegans*) and green algae (*Chlamydomonas*) (Blacque et al, 2004; Li et al, 2004). However, BBS4 does not appear to be required for cilium formation in the trachea and kidney of BBS4 null mice, but the males have aflagellate spermatozoa (Mykytyn et al, 2004), and knockdown of BBS6 in NIH3T3 cells was reported to cause no change in cilia frequency or gross morphology (Kim et al, 2005). While requirement of the BBS proteins in ciliogenesis is perhaps dependent on cell type, there is a conserved biological requirement for these proteins in cilia maintenance, such as in the Kupffer's vesicle of zebrafish. Yen et al. report progressive loss of these cilia after knockdown of BBS2, 4, 5, 6, 7 or 8 (Yen et al, 2006).

Knockdown of the ciliary network components was successful in combination with treatments to stimulate differentiation of H295Rs, and differentiation occurred normally in the negative controls (Figure 4.3.1). Together, data from CYP11B1 and CYP11B2 mRNA expression provides compelling evidence that cilia are required for the differentiation of H295R cells towards a zG-like phenotype, particularly as the results were reproduced with each siRNA transfection, and each protein knocked down has a different role in the ciliary network. On the contrary, it is unlikely that cilia play as vital a role in zF differentiation, which would therefore appear to be governed by extraciliary signalling pathways. There is currently some debate as to the process of

establishing zF cells during remodelling and maintenance of the adrenal gland. They may differentiate from stem cells directly, or they could arise from zG cells as they migrate centripetally.

Cilia may mediate zG differentiation by allowing cells to respond to the AngII signal, which is transduced via the G-protein coupled receptors AT1 and AT2 on receiving cells. Both are expressed in human adrenal tissues (Tanabe et al, 1998), but AT1 appears to predominate in the cortex, while AT2 has a greater presence in the medulla (Lu et al, 1995). AT1 is coupled to G_q which activates phosphoinositidase C (PI3C) resulting in increased intracellular calcium levels, and regulation of CYP11B2 transcription (Bird et al, 1993). It is thought that AT2 has antagonistic functions to AT1 (Inagami et al, 1999), and is coupled to $G_{i\alpha}$, which inhibits adenylate cyclase, reducing cAMP production (Zhang & Pratt, 1996). AT1 is expressed in H295R cells (Figure 4.4.3B) but it would be interesting to determine whether it is located within the ciliary membrane, thus this could be the mechanism through which cilia are involved in zG specification. This was not carried out due to a lack of suitable antibodies.

While primary cilia seem to be required for zG differentiation, Hh signalling was found to inhibit it (Figure 4.4.2). CYP11B2 expression was abrogated in cells treated with AngII in conjunction with ShhN, but again, zF differentiation was unaffected. If ShhN is exerting its effect via canonical Hh signalling, it would be expected that Gli1 mRNA levels would be increased in all cells treated with ShhN. None of the ShhN treated cells showed a significant increase in Gli1 expression, although the AngII treated ones did have the greatest mRNA levels. Gli1 expression may have initially increased in response to ShhN, but already returned to basal levels at the time the cells were harvested. Ptch1 is also up-regulated by Hh signalling and acts as a suppressor, providing a means of limiting the extent of the signal (King et al, 2008). Its up-regulation in cells exposed to prolonged ShhN treatment could restrict the Gli1 response.

Although up-regulation of Gli1, which only acts as a transcriptional activator, is frequently used as a marker of active Hh signalling (Vokes et al, 2007), the up-regulation of Hh target genes is not only a consequence of binding transcriptional

activators. Hh target genes can also be activated by a reduction in their transcriptional repression by Gli3R or Gli2R. Different concentrations of Hh ligand cause alterations in the ratio between GliAs and GliRs, allowing different genes to be expressed, depending upon their differential responses to de-repression or transactivation, commonly referred to as the Gli code (Briscoe, 2009; Jacob & Briscoe, 2003; Ruiz i Altaba et al, 2007). Therefore, canonical Hh signalling could still be active even in the absence of Gli1 up-regulation.

Different levels of Hh pathway activity are known to influence neuronal cell type specification during development of the neural tube and central nervous system (Ericson et al, 1996; Ericson et al, 1995a; Ericson et al, 1995b), and so changes in expression of Shh could govern adrenal stem/progenitor cell fate. High expression of the ligand, as used here, could result in inhibition of differentiation, while lower level signalling may stimulate and direct it. Certainly Shh expression changes in adrenal remodelling experiments. Mice given the ACE (angiotensin-converting enzyme) inhibitor captopril cannot produce AngII, resulting in an extreme reduction in the size of the zG, with an increase in Shh expression. In contrast, those fed a low sodium diet, which activates the RAA system, have increased CYP11B2 expression, a larger zG than control animals, and there is a decrease in the number of cells expressing Shh (Guasti et al, manuscript in preparation). This may indicate that Shh is inhibitory to zG differentiation from the capsule and its down-regulation is a prerequisite for zG expansion, or it could indicate that the Shh-expressing cells themselves are differentiating into zG cells.

At present it is unclear the exact role that Shh plays during development and in the adult adrenal. It may be involved in differentiation, and evaluating the response of H295R cells treated with AngII and different concentrations of ShhN would be a valuable experiment to carry out. However, it is unlikely to be required for zonation as although smaller in size, the adrenal glands still form with regular concentric steroidogenic enzyme expression in Shh null mice (Ching & Vilain, 2009; Huang et al, 2010; King et al, 2009). In the adult, Shh may be involved in remodelling of the cortex. Lineage tracing studies show that Shh-positive cells are capable of becoming

steroidogenic both during development and in the adult mouse, however Gli1 cells mainly only contribute to the capsule in the adult (Dr Ed Laufer, personal communication), unlike during development when they can give rise to steroidogenic lineages (King et al, 2009). A combination of lineage tracing studies and remodelling experiments would help clarify the contribution of Shh-positive cells to the cortex in the adult.

To help determine the mechanism by which Hh signalling may play a direct role in zG differentiation, the AT1b-luciferase reporter was used in conjunction with over-expressing Gli1 in H295R cells. The rodent AT1a and AT1b receptors are highly homologous to each other, and to the human AT1 receptor. They have near identical signalling mechanisms (Inagami et al, 1999), but vary in their expression. AT1a is present throughout the adrenal cortex, while AT1b is exclusive to the zG (Naruse et al, 1998).

Although high levels of Gli1 appeared to lower AT1b luciferase activity, as did AngII treatment, and a further reduction was seen when the two were combined (Figure 4.4.3A), these reductions were not significant. Bird et al. have previously shown that AngII treatment causes a decrease in AT1 mRNA levels in H295s, via PKC and other calcium sensitive protein kinases (Bird et al, 1994), even though CYP11B2 expression is up-regulated. However, *in vivo*, AngII causes selective down-regulation of the AT1 receptor in vascular tissue, while increasing its expression within the adrenal (Clauser et al, 1996). Fsk and cortisol are also known to down-regulate AT1 (Bird et al, 1994; Dell et al, 1996).

Further analysis of AT1 in H295R cells transfected with siIFT88 suggests that the ability of these cells to form functional cilia does not affect its mRNA expression (Figure 4.4.3B). However, mRNA expression does not always correspond with protein levels, and AT1 could still utilise the primary cilium for signal transduction. At this point it is not possible to conclusively rule out the possibility that Hh signalling influences zG differentiation via AT1 regulation, although the evidence presented here would suggest it is unlikely.

An alternative to regulation at the level of the AngII receptor, is regulation of the transcription factors that transduce the AngII signal. CYP11B2 promoter activity was to some extent reduced in H295R cells treated with ShhN in combination with AngII (Figure 4.4.4; p=0.09). This could result from the direct binding of Gli transcription factors to the promoter, or via the up-regulation of other transcription factors.

AngII has also been shown to increase mRNA and protein levels of the nuclear receptor NR4A1 in H295R cells, and overexpression of NR4A1 increases CYP11B2 transcription (Bassett et al, 2004b). It is therefore thought that NR4A1 is, in-part, responsible for regulation of CYP11B2 expression and aldosterone production in response to AngII or potassium treatment. Furthermore, NR4A1 has been identified as a target gene up-regulated by the Hh signalling pathway in pluripotent mouse mesenchymal cells (Ingram et al, 2002), and thus may be involved in a system whereby Hh signalling positively regulates responsiveness to AngII, for example at lower concentrations of the ligand if there is a graded response.

The data, thus far, indicate that Shh inhibits the differentiation of H295R cells towards a zG-like phenotype, but as primary cilia seem to be required for this differentiation process then this may be via a non-canonical signalling mechanism. There is a growing body of evidence to suggest that such pathways of Hh signalling exist, adding significant complexity to the system. This could involve signalling that does not require Smo or the Gli transcription factors, atypical interactions of Hh pathway components, or their direct interaction with other signalling pathways (Jenkins, 2009).

In many cases, canonical and non-canonical Hh signalling appear to act in parallel or sequentially. For example; commissural axons, which originate in the dorsal neural tube, migrate ventrally towards the floor plate during development of the rudimentary spinal cord. This initial migration process involves canonical Hh signalling, with Shh acting as a chemoattractant (Charron et al, 2003). Shh is expressed in the notochord and ventral floor plate cells of the neural tube, and a decreasing gradient of Shh expression extends dorsally (Wolpert, 2007). A gradient of Shh expression is also present along the caudal-rostral axis of the spinal cord, from high to low (Bourikas et al, 2005). Once the commissural axons reach the floor plate they then turn and migrate

rostrally, with Shh now acting as a chemorepellant. Using chick embryos, Bourikas et al. have shown that Shh may be acting in a non-canonical manner to direct rostral turning of the commissural axons. They found that expression of both Ptch and Smo is not present in these neurons during this time point, and inhibition of Smo activity using cyclopamine or RNAi did not stall or reverse migration in a caudal direction, as was found when Shh was targeted with double stranded RNA, or Shh-blocking antibodies (Bourikas et al, 2005).

Additionally, Ptch has been found to interact with cyclin B1, inhibiting its nuclear translocation and cell cycle progression (Barnes et al, 2001), as a separate function from its role within the Hh pathway, and TGFβ induces up-regulation of Gli1 and Gli2, which does not require upstream Hh signalling components (Dennler et al, 2007). These observations provide further evidence for non-canonical signalling, which most probably does not require functional primary cilia. Therefore, it is hard to say whether in this instance Hh is acting via cilia, and so further investigations would be required.

Wnt signalling is another pathway that is known to rely, in certain tissues, on primary cilia for its function, and is required for development of the adrenal gland. It was therefore investigated as another means by which cilia may be involved in zG differentiation. Initial investigations indicated that it is unlikely that canonical Wnt signalling requires or is inhibited by primary cilia in H295R cells, as knockdown of ciliary network components did not alter the luciferase activity of the M50 Super 8x TOPFlash reporter (Figure 4.5.1B). However, non-canonical Wnt/PCP signalling has also been shown to utilise primary cilia (Ross et al, 2005), and so this could be involved in the mechanism through which cilia are involved in the differentiation of H295R cells towards a zG-like phenotype.

Reflecting on the aims initially set out in this chapter, the evidence suggests that a full length functional primary cilium is required for initiating cell fate decisions in H295Rs that result in the zG phenotype. Shh also appears to be involved in this process, but may or may not require cilia for its actions in this system. Which other signalling pathways act through the cilium is a question that is under intense scrutiny at present,

and these pathways may well be involved in adrenal development in addition to or separate from Hh signalling. It is highly likely that different mechanisms are involved in the regulation of zG versus zF differentiation.

CHAPTER 5: *IN VIVO* MODELS

5.1 Aims

Chapter 4 demonstrated that primary cilia are required for the differentiation of human adrenocortical carcinoma cells into cells characteristic of the zona glomerulosa of the adrenal cortex *in vitro*. The main aim of this chapter is to indicate the likely outcomes of cilia defects on adrenal function *in vivo*, using mouse and zebrafish models of ciliopathies. Adrenals from BBS knockout and wild-type mice are examined and compared to identify any differences in histology. The effects of knocking down BBS genes in zebrafish embryos, on the subsequent establishment of interrenal cells, are also examined.

5.2 Part A - BBS Mice

5.2.1 BBS adrenals have reduced capsule density

Bardet-Biedl syndrome is a ciliopathic disorder characterised by obesity, retinopathy, polydactyly, mental retardation, hypogonadism and renal dysplasia (Tobin & Beales, 2009). Along with other syndromes involving genetic mutations that affect cilium formation and function, it exhibits phenotypes similar to those observed in conditions arising from disrupted Hh signalling. While many features of BBS have been characterised, the variation in patient presentation, combined with a plethora of symptoms, may disguise an as yet un-described adrenal phenotype. Prototypical BBS phenotypes in mice include; obesity, retinal degeneration, aflagellate spermatozoa and olfactory dysfunction, but they do not display polydactyly, renal malformations or situs inversus (Kulaga et al, 2004; Mykytyn et al, 2004; Nishimura et al, 2004; Ross et al, 2005; Zhang et al, 2012).

Mice with homozygous null mutations in one of several BBS genes were used to compare phenotypes and identify common adrenal traits. BBS4 encodes a BBSome protein involved in organisation and trafficking at the basal body and within the cilium (Nachury et al, 2007), while BBS6 and BBS12 encode proteins that resemble group II chaperonins which are involved in folding proteins, possibly those required for

ciliogenesis (Tobin & Beales, 2007). Adrenals from mice, age 16-20 weeks, were obtained from Professor P. Beales (Institute of Child Health, UCL) and Dr V. Marion (Faculté de Médecine, Université de Strasbourg, France).

Expression of steroidogenic enzymes marking the different cortical zones was examined by immunoperoxidase staining with antibodies for CYP11A1 (P450 side chain cleavage) and CYP11B1. Figure 5.2.1 shows that CYP11A1 is expressed throughout the cortex, but not the capsule, and CYP11B1 expression is restricted to zF cells in both wild-type and knockout animals. There is therefore no change in the expression of these steroidogenic enzymes in BBS null mice.

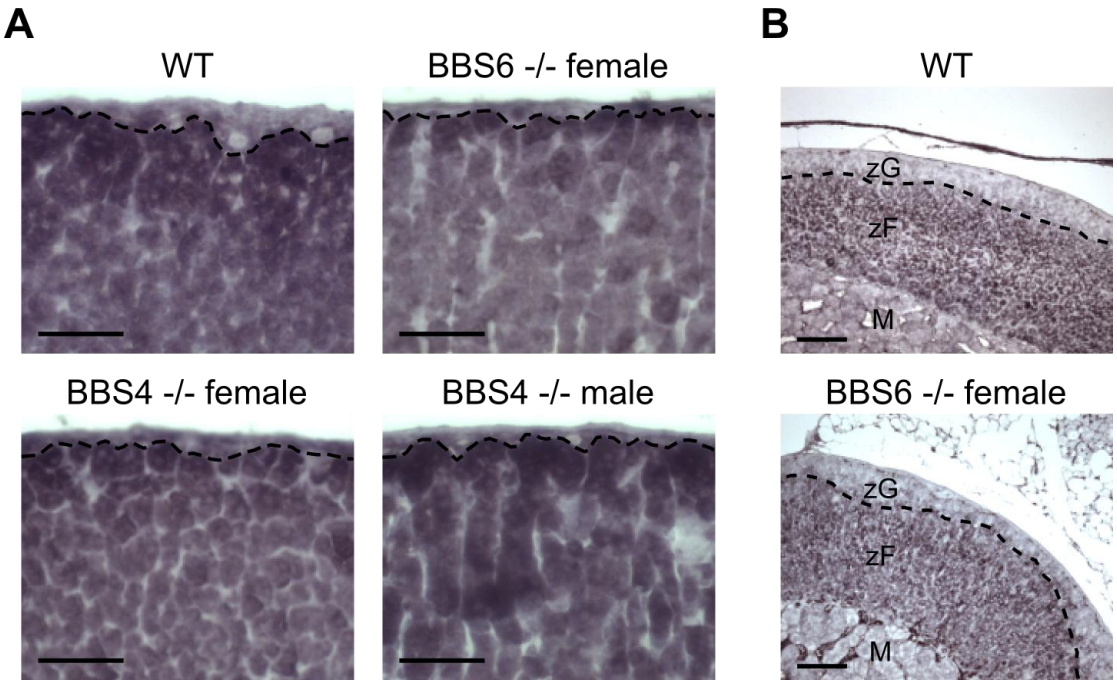

Figure 5.2.1 – CYP11A1 and CYP11B1 expression in BBS adrenals
Representative light microscopy images of paraffin embedded adrenal sections from wild-type (WT) and BBS null mice showing CYP11A1 (A) and CYP11B1 (B) expression by immunoperoxidase staining. Images were taken using the Leica DMR light microscope with 20x and 40x objectives.
(A) Capsule is indicated by the dotted line, scale bar represents 5µm.
(B) zG:zF boundary is indicated by the dotted line, zG; zona glomerulosa, zF; zona fasciculata, M; medulla. Scale bar represents 10µm.

Further analysis using haematoxylin and eosin staining revealed that although steroidogenic enzyme expression may be normal, adrenals from BBS knockout mice have abnormal histology. Several were smaller than those of their wild-type litter mates, with very compact layers (Figure 5.2.2A), and one female BBS6 knockout mouse

had a rather unusual adrenal phenotype. Groups of spindle-shaped cells were identified in the subcapsule, projecting into the zG (Figure 5.2.2B (i) and (ii)). These cells were found to be non-steroidogenic nor zF-like, as shown by their lack of CYP11A1 and CYP11B1 staining respectively (Figure 5.2.2B (iii) and (iv)). This phenotype was limited to a particular area within the adrenal, and was not present in all sections. It was also not observed in the second adrenal from the same animal, or in any other BBS knockout adrenals.

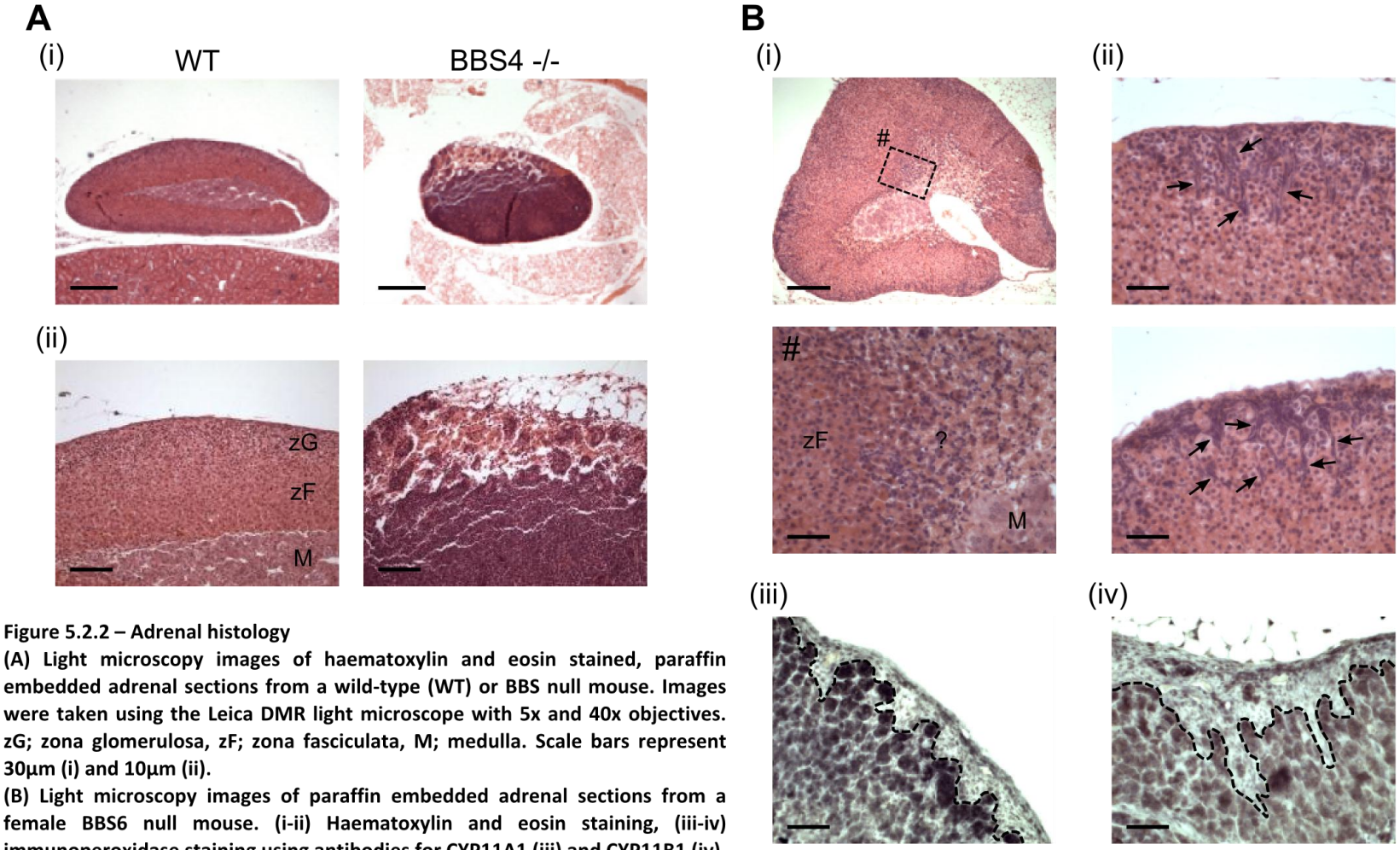

Figure 5.2.2 – Adrenal histology

(A) Light microscopy images of haematoxylin and eosin stained, paraffin embedded adrenal sections from a wild-type (WT) or BBS null mouse. Images were taken using the Leica DMR light microscope with 5x and 40x objectives. zG; zona glomerulosa, zF; zona fasciculata, M; medulla. Scale bars represent 30µm (i) and 10µm (ii).

(B) Light microscopy images of paraffin embedded adrenal sections from a female BBS6 null mouse. (i-ii) Haematoxylin and eosin staining, (iii-iv) immunoperoxidase staining using antibodies for CYP11A1 (iii) and CYP11B1 (iv). Arrows and dotted lines indicate spindle-shaped cells projecting from the subcapsule into the zG. zF; zona fasciculata, M; medulla. Images were taken using the Leica DMR Light microscope with 10x and 40x objectives. Scale bars represent 20 µm (i) and 5µm (#, ii-iv).

While some BBS null adrenals varied in size compared to those obtained from the wild-type mice, the most consistently apparent phenotype seen during histological examination was thinning of the capsule (Figure 5.2.3B). The knockout animals appear to have a capsule approximately 1-3 cells thick, whereas the capsule of the wild-type and heterozygous mice is 4-5 cells thick. The density of the capsular cells was quantified by staining sections with DAPI and counting the number of capsular nuclei within a predetermined area. Nuclei of capsule cells are easily distinguishable from the zG cells because they are thin and oriented in the plane of the capsule. A significant reduction in capsule density was recorded in all adrenals from null mice, compared to their wild-type litter mates (Figure 5.2.3A).

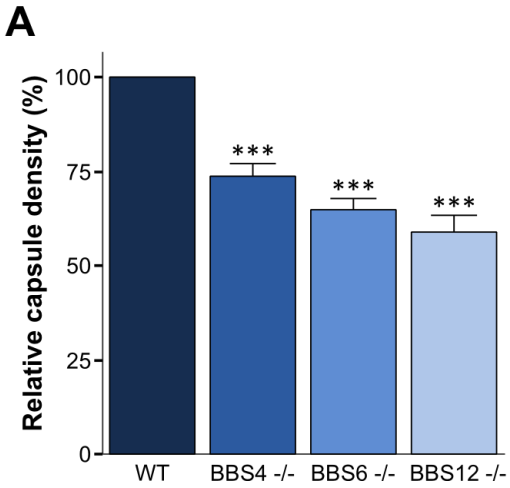

Figure 5.2.3 – Capsule density of BBS adrenals (this page and following page)
(A) Graph showing the relative capsule density of adrenals from BBS null mice compared to their wild-type (WT) counterparts. The capsule was visualised by staining sections with DAPI to mark the nuclei. Images were taken using the Zeiss LSM510 inverted laser scanning confocal microscope with 63x objective, and for each genotype, capsular nuclei were blindly counted from 10 areas of a pre-determined size across 3 sections per adrenal (2 adrenals/genotype) (N=10). Data collated, error bars indicate SEM. *** p<0.001 compared to WT.

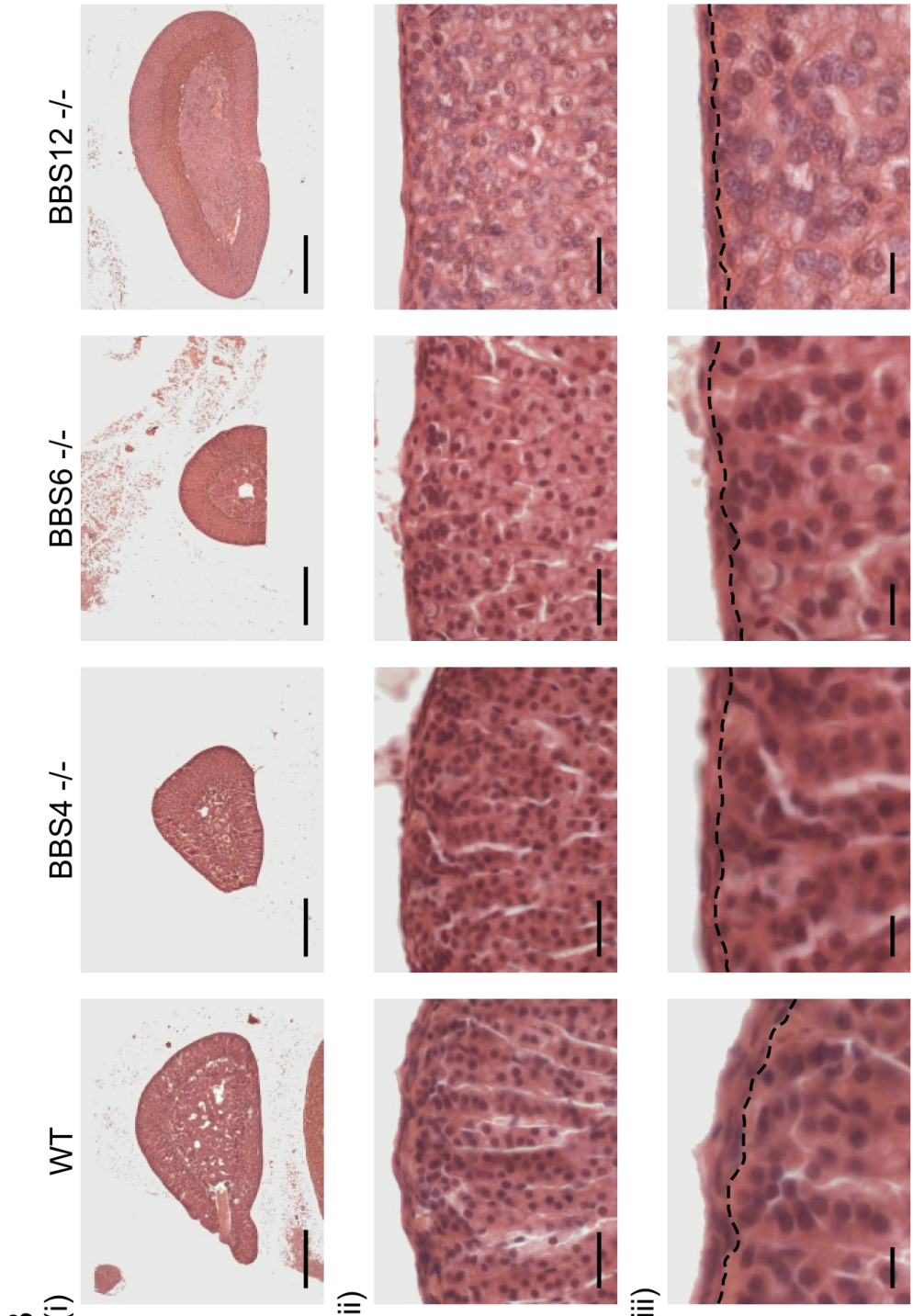

Figure 5.2.3 – Capsule density of BBS adrenals (continued)
(B) Representative light microscopy images of paraffin embedded adrenal sections from wild-type (WT) and BBS null mice stained with haematoxylin and eosin. Capsule is indicated by the dotted line. Images were taken using the Leica DMR light microscope with 5x and 40x objectives. Scale bars represent 50µm (i), 3µm (ii) and 1µm (iii).

5.2.2 BBS12 null mice have increased serum corticosterone following synacthen testing compared to wild-type mice

Following the observation that there are histological differences between the adrenals of BBS null mice compared to the wild-type animals, it was hypothesised that the ability of the adrenal to alter its steroidogenic output in response to different stimuli could be affected. Corticosterone levels were therefore measured in serum obtained from mice after they were injected with synthetic ACTH (synacthen; injections performed by Dr V. Marion, Université de Strasbourg, France). High circulating ACTH levels should stimulate corticosterone production from the adrenal, to maximum levels. Figure 5.2.4 shows that compared to the wild-type mice, BBS12 null mice have significantly higher serum corticosterone levels after synacthen testing.

The above data indicate that adrenals from BBS null mice have an abnormal histological appearance, namely a reduced capsule density. This may have possible implications on the remodelling capabilities of the cortex, as the capsule is a predicted source of adrenocortical stem cells (Huang et al, 2010; King et al, 2009; Salmon & Zwemer, 1941). In response to ACTH stimulation, serum corticosterone levels were greater in BBS12 null mice than in the wild-type animals, suggesting adrenal steroid production may be altered in BBS null mice.

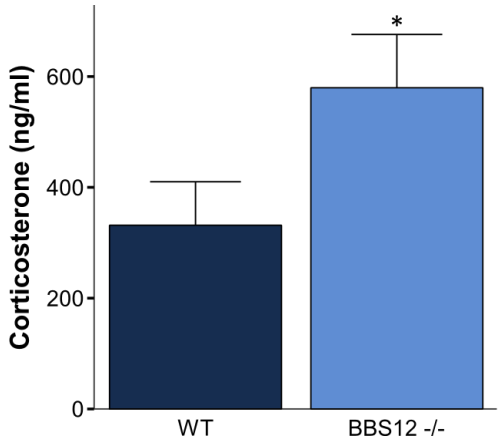

Figure 5.2.4 – Corticosterone ELISA
Graph showing serum corticosterone levels in wild-type (WT) and BBS12 null mice. The concentration of corticosterone in serum obtained from mice one hour after injection with 10mg/kg synacthen was determined by an ELISA, and a one-way ANOVA was used to interpret the data. N=6, data collated, error bars indicate SEM. * p<0.05 compared to WT.

5.3 Part B - Zebrafish

5.3.1 Survival and initial observations

Zebrafish are an increasingly popular model organism for the study of endocrine development and disease. Their external fertilisation, rapid development, and optical clarity are extremely advantageous for developmental studies, and importantly for this thesis, being a vertebrate model they form primary cilia. Most major aspects of the endocrine system and glands are conserved between teleosts and mammals (Liu, 2007), and the developmental processes governing organogenesis are similar (Hsu et al, 2009; McGonnell & Fowkes, 2006). The interrenal is the zebrafish counterpart of the mammalian adrenal cortex, and requires Hh signalling, at least in part, for its correct development (Bergeron et al, 2008). Zebrafish were therefore used to further study the effects of ciliopathies on interrenal development.

The use of morpholinos (MOs) for targeted knockdown of specific genes in frog (*Xenopus laevis*) and zebrafish embryos has become a widely adopted antisense technique, particularly for studying early development. MOs are synthetic antisense oligonucleotides of approximately 25 bases in length that bind to a specific RNA sequence, blocking either a splice site, or initiation of translation. A control MO or ones targeting BBS4 and BBS6, which have previously been characterised (Badano et al, 2006; Yen et al, 2006), were injected into zebrafish embryos at the 1-2 cell stage. Embryos were then incubated at 28.5°C for 24, 27 or 30 hours. A translation blocking MO targeting p53 was included in all injections to reduce off-target neural death. p53 regulates cell cycle and induces apoptosis, and knockdown of this gene has been shown to prevent massive apoptotic responses induced by embryonic microinjection, without affecting normal development (Berghmans et al, 2005).

After dechorionation, initial observations focused on the survival rate of the injected as well as uninjected embryos. Figure 5.3.1 shows that the survival rate for uninjected embryos was approximately 95%. This dropped to around 65% in embryos subjected to injection, but was consistent between the different MOs. Other phenotypes observed in injected embryos include those which lacked either a head or tail, and those that

had clear developmental abnormalities that were not consistent with the phenotypes previously reported for these MOs (Badano et al, 2006). These phenotypes were found in all injected groups of embryos, however, the majority were considered 'normal'.

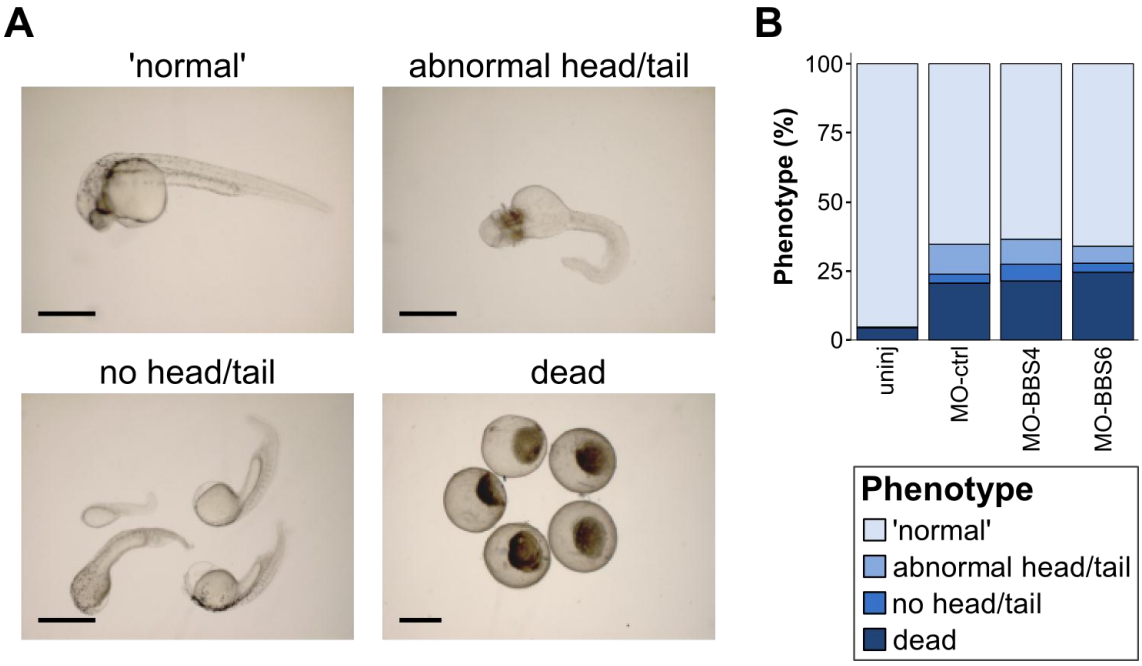

Figure 5.3.1 – Initial observations and survival rate
Zebrafish embryos were injected with morpholinos at the 1-2 cell stage and incubated at 28.5°C for 24, 27 or 30 hours. They were then dechorionated and sorted by phenotype.
(A) Stereo microscopy images of zebrafish embryos showing examples of phenotypes observed and classification used during initial sorting. Images were taken using the Leica MXFL III stereo dissecting microscope. Scale bar represents 400µm.
(B) Graph showing the percentage of each phenotype observed in uninjected embryos (uninj), and those injected with a control morpholino (MO-ctrl), or morpholinos targeting BBS4 (MO-BBS4) and BBS6 (MO-BBS6). For each morpholino and time point, phenotypes were examined in an average of 135 embryos from 3 experimental sets.

5.3.2 Specific morpholino phenotypes

After initially sorting the embryos to remove those that were dead or considered 'abnormal', the remaining 'normal' fish were further categorised according to the phenotypes previously reported for MOs targeting BBS4 and BBS6. Badano et al. characterize morphant embryos as those which have moderate or severe shortening of the body axis, a wavy, kinked or twisted notochord, and to a lesser extent, broadening of the notochord and somites, loss of somatic definition, and defects in tail extension (Badano et al, 2006). Figure 5.3.2A-B shows that all uninjected fish had a straight body

axis, which was also observed in the majority of embryos injected with the control (ctrl). On average, 53% of embryos injected with MO-BBS4 or MO-BBS6 showed severe ventral curvature and shortening of the body axis, which was the most common phenotype recorded. To a lesser extent, bending at the tip of the tail or a moderate curvature of the body length were also found in injected embryos. Kinking of the notochord was evident in MO-BBS4 and MO-BBS6 embryos (Figure 5.3.2c), but was not apparent in MO-ctrl or uninjected fish. Those embryos which displayed both a moderate to severe ventral curvature or shortening of the body axis, and kinking of the notochord were used for further experimentation.

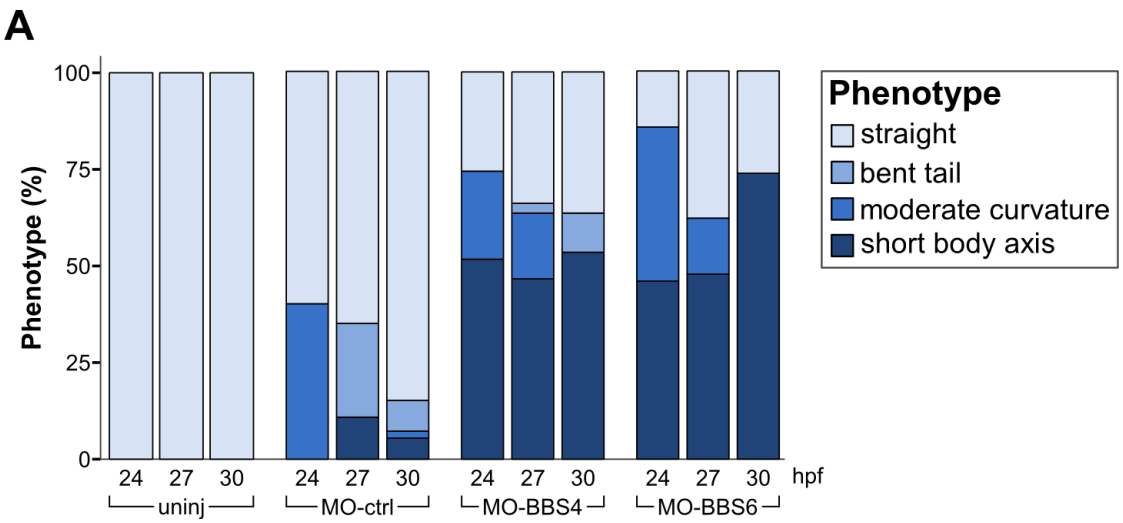

Figure 5.3.2 – Classification of morpholino phenotypes (this page and following page)
Zebrafish embryos injected with morpholinos at the 1-2 cell stage were examined 24, 27 or 30 hours post fertilization (hpf). After initial sorting they were then classified in accordance with previously described phenotypes (Badano et al, 2006).
(A) Graph showing the percentage of each phenotype observed in uninjected embryos (uninj), and those injected with a control morpholino (MO-ctrl), or morpholinos targeting BBS4 (MO-BBS4) and BBS6 (MO-BBS6) at the three time points. For each morpholino and time point, phenotypes were examined in an average of 75 embryos from 3 experimental sets.

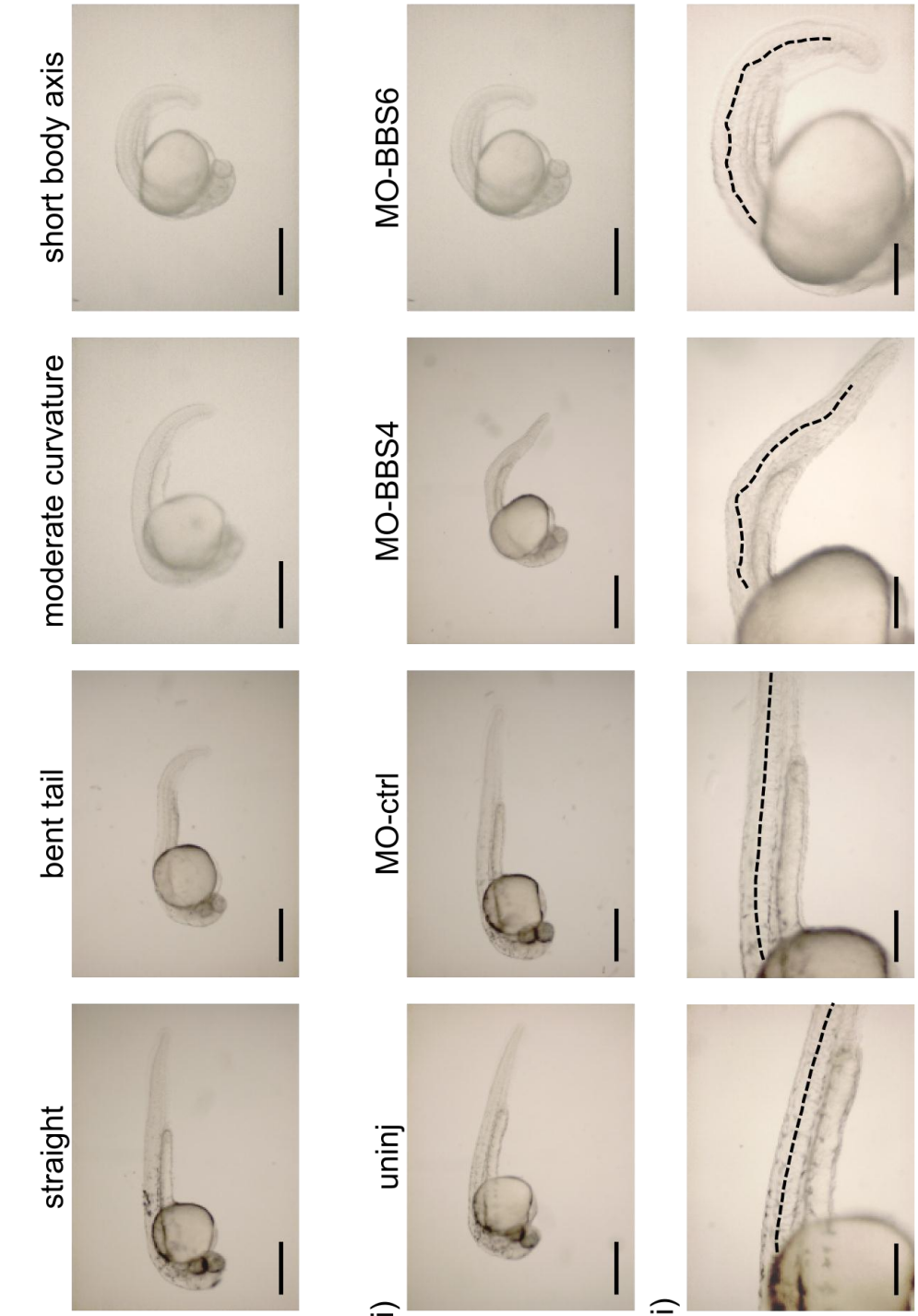

Figure 5.3.2 – Classification of morpholino phenotypes (continued)
(B-C) Representative stereo microscopy images of zebrafish embryos displaying the classified phenotypes (B), and highlighting the shape of the notochord, indicated by the dotted line (C). Images were taken using the Leica MXFL III stereo dissecting microscope. Scale bars represent 400µm (B and C (i)) and 200µm (C (ii)).

Having established the previously characterised zebrafish phenotypes for knockdown of BBS genes using MOs, the resulting effects on ciliation were examined. Confocal microscopy using an antibody for acetylated α-tubulin was carried out to visualise cilia. Figure 5.3.3 shows that there was a small reduction in the number of cilia within a region in the tip of the tail of embryos injected with MO-BBS6, but a greater reduction in those injected with MO-BBS4. However, the length of cilia was significantly reduced in both groups of embryos compared to those injected with the control. A reduction in cilium length, similar to the observations in the previous chapter, suggests that cilium function is likely to be impaired.

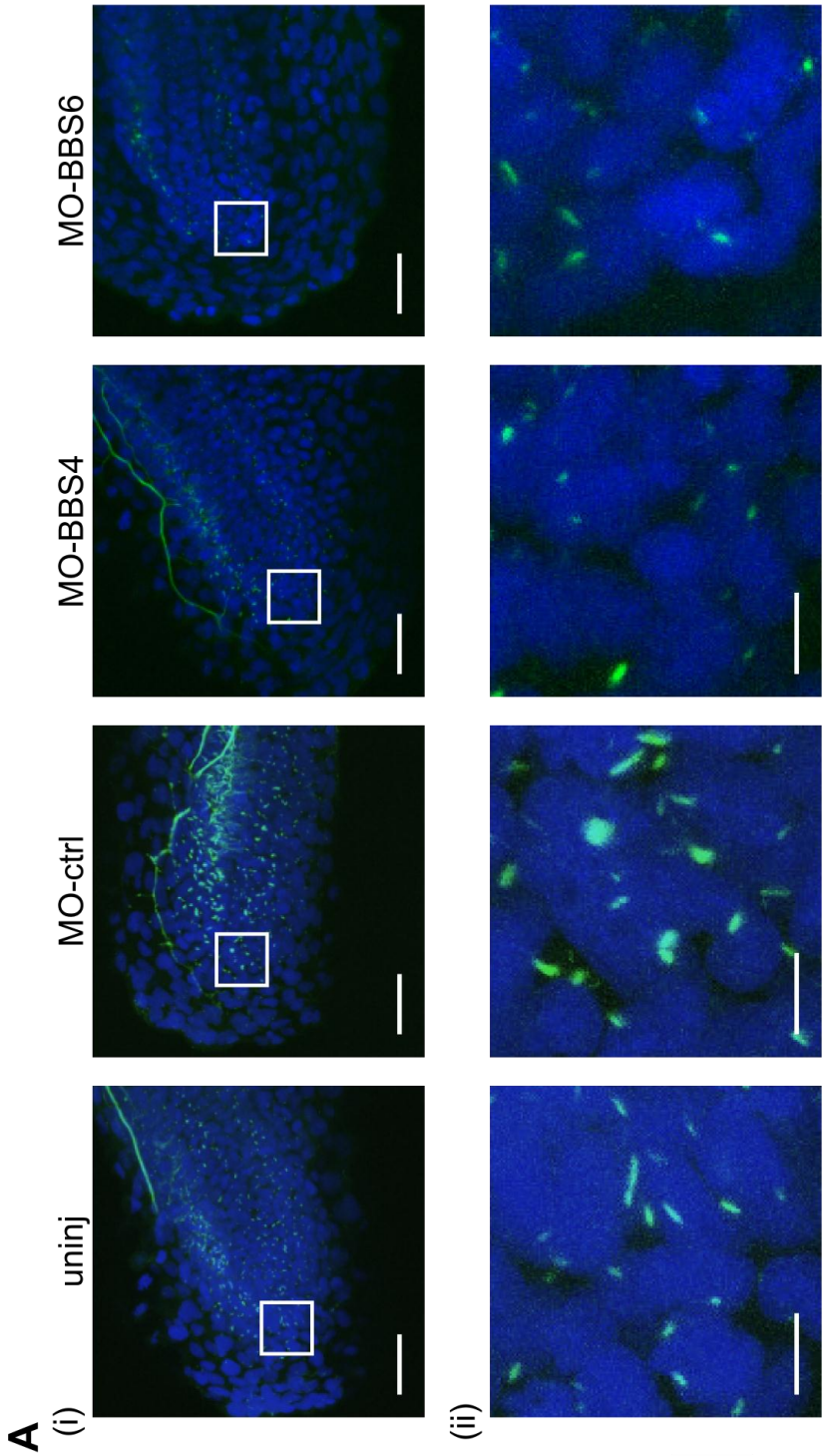

Figure 5.3.3 – The effects of morpholinos on ciliation (this page and following page)
Zebrafish embryos injected with morpholinos at the 1-2 cell stage were collected 24 hours post fertilization (hpf). Cilia were visualised using an anti-acetylated α-tubulin antibody, marking the ciliary axoneme (green). DAPI was used to stain the nuclei (blue).
(A) Representative confocal microscopy images of primary cilia in the zebrafish tail. Images were taken using the Zeiss LSM510 inverted laser scanning confocal microscope with 63x objective. Scale bars represent 10µm (A (i)) and 5µm (A (ii)).

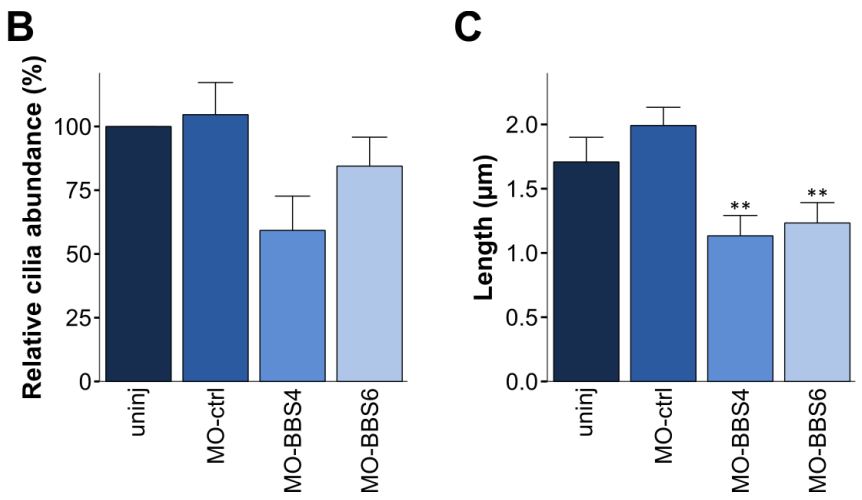

Figure 5.3.3 – The effects of morpholinos on ciliation (continued)
(B-C) Graphs showing the relative abundance of cilia (A), and their length (B), determined using the ZEN 2008 Light edition software. For each morpholino, cilia were blindly counted from 3 embryos, using 3 areas of a pre-determined size within the tail region per embryo (N=3). The length of cilia was measured in 10 areas of a pre-determined size across the 3 embryos (N=10). The data were analysed using a one-way ANOVA with post-hoc comparisons. Data collated, error bars indicate SEM. ** p<0.01 compared to MO-ctrl.

5.3.3 Ff1b expression

MOs targeting BBS4 and BBS6 appear to impact on the ability of cells in the zebrafish embryo to form primary cilia, with a resulting disruption of some aspects of development; including that of the notochord and body axis. After injection at the 1-2 cell stage, embryos were incubated at 28.5°C for 24, 27 or 30 hours, which cover the major time points of interrenal development. The effects of the MOs on the establishment of interrenal cells were investigated by using whole mount *in situ* hybridisation, with an ff1b mRNA targeting probe. Ff1b is the earliest molecular marker specifying interrenal cell lineages and is required for the development of steroidogenic interrenal tissue (Chai et al, 2003).

Figure 5.3.4A-B shows that at 24hpf, ff1b is expressed as two spots in the majority of both uninjected embryos and those injected with the control. By contrast, all embryos injected with MO-BBS4 or MO-BBS6 had no ff1b-expressing cells at that time. As the time points progress, more uninjected and control fish show ff1b expression as a single spot as the two pools of cells merge, slightly to the right of the midline, at the level of the 3rd somite. At 27 and 30hpf some MO-BBS4 and MO-BBS6 injected embryos started to display ff1b expression; however the majority continued to lack its

expression all together. Of those that did express ff1b, the staining appeared to be less distinguished than in the control fish, and the area of staining was reduced in size (Figure 5.3.4c). Measurement of the width of all ff1b spots was carried out at the widest point of the staining, and in all cases the 'spot diameter' was found to increase slightly as the embryos aged. These data suggest that inhibiting cilium formation and, presumably, function, with the use of MOs, results in a delay and reduction in the development of interrenal cells during the development of the zebrafish embryo.

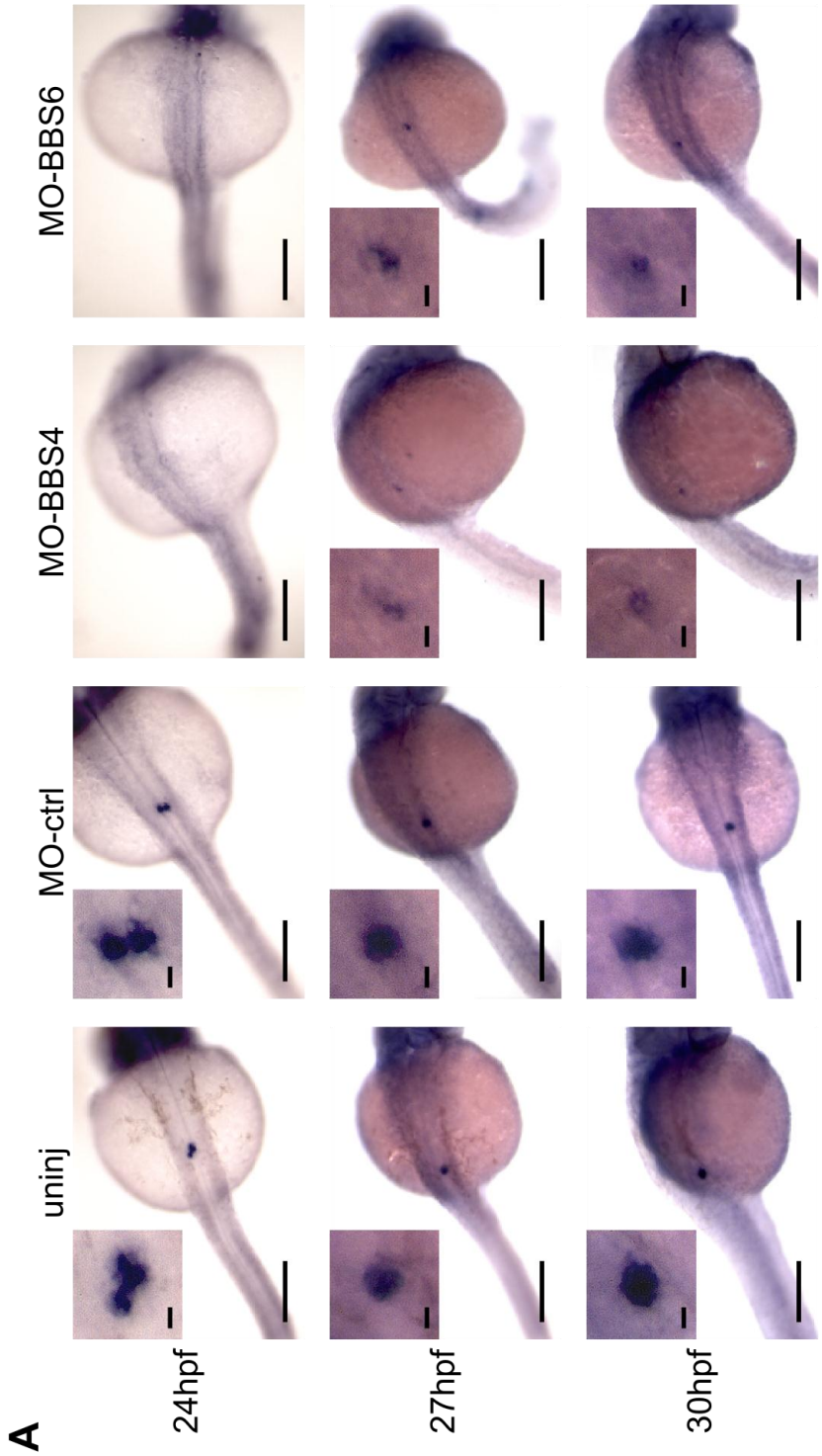

Figure 5.3.4 – The effects of morpholinos on ff1b expression (this page and following page)
Zebrafish embryos injected with morpholinos at the 1-2 cell stage were examined 24, 27 or 30 hours post fertilization (hpf). Those which displayed the classified phenotypes were used for whole mount in situ hybridisation with an ff1b mRNA targeting probe.
(A) Stereo microscopy images showing spots of ff1b expression, taken using the Leica MXFL III stereo dissecting microscope. Scale bars represent 200µm and 15µm (indented images).

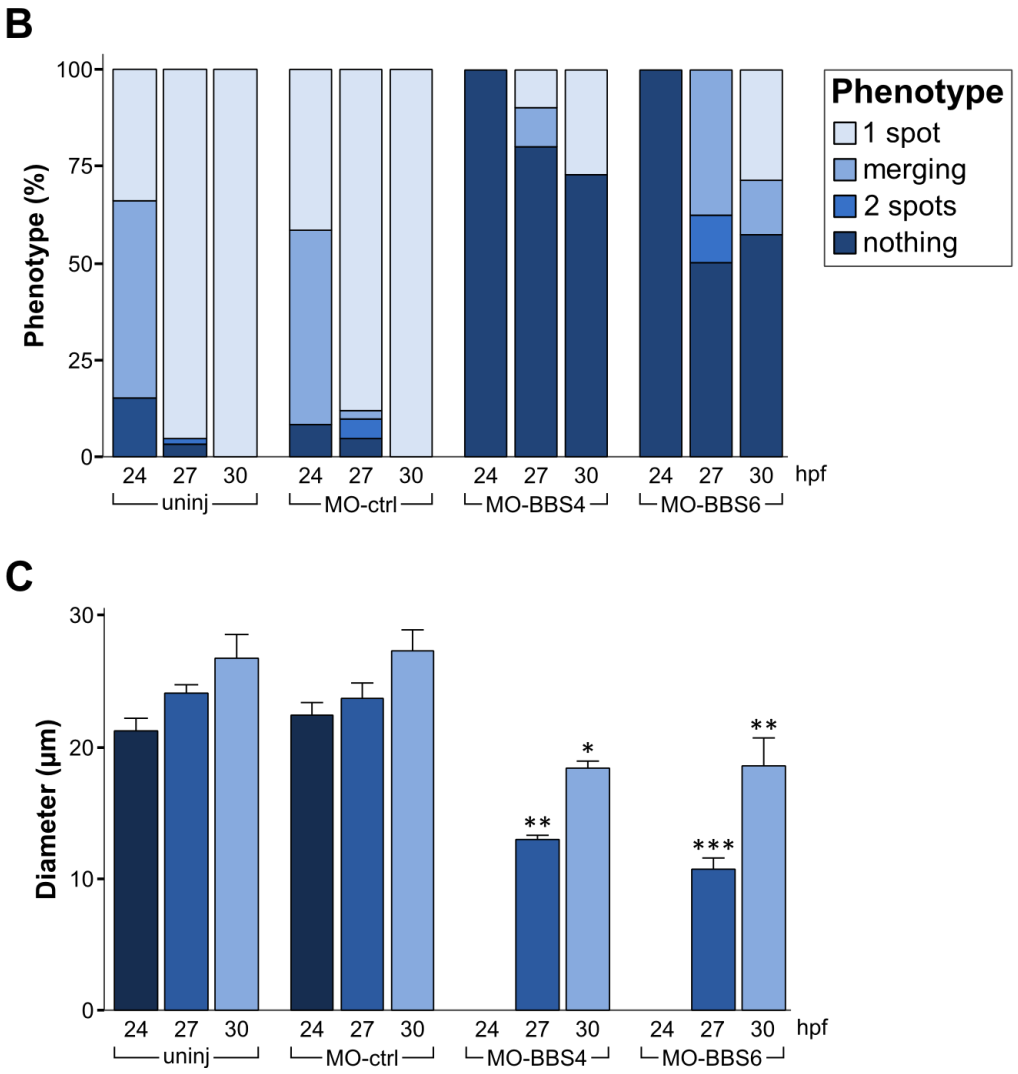

Figure 5.3.4 – The effects of morpholinos on ff1b expression (continued)
(B) Graph showing the percentage of each ff1b expression phenotype observed in uninjected embryos (uninj), and those injected with a control morpholino (MO-ctrl), or morpholinos targeting BBS4 (MO-BBS4) and BBS6 (MO-BBS6) at the three time points. For each morpholino and time point, ff1b expression was examined in 12 embryos from 3 different experimental sets.
(C) Graph showing the diameter of the spots of ff1b expression in uninjected embryos (uninj), and those injected with a control morpholino (MO-ctrl), or morpholinos targeting BBS4 (MO-BBS4) and BBS6 (MO-BBS6) at the three time points. For uninj and MO-ctrl groups 8 spots were measured per time point. For MO-BBS4 and MO-BBS6 groups 4 spots were measured per time point. The data were analysed using a one-way ANOVA with post-hoc comparisons. Data collated, error bars indicate SEM. * p<0.05, ** p<0.01, *** p<0.001 compared to MO-ctrl at corresponding time points.

5.4 Discussion

The above data show that BBS null mice have a reduced adrenal capsule density (Figure 5.2.3), and possibly altered adrenal steroid production (Figure 5.2.4). Some adrenals were also smaller than those from wild-type animals, and one BBS null mouse displayed non-steroidogenic, spindle-shaped cells in the subcapsule and zG (Figure 5.2.2). Using zebrafish it has been shown that interrenal development is delayed and possibly reduced in embryos injected with BBS-targeted MOs.

A key feature of mouse models of adrenal hyperplasia and adrenocortical tumours is the presence of spindle-shaped 'A cells' which project from the capsule/subcapsular region into the zG (Berthon et al, 2010; Bielinska et al, 2003; Hughes et al, 2012; Kim et al, 1997; Parviainen et al, 2007). These cells are non-steroidogenic and express the gonadal transcription factor GATA4, which is normally only present in foetal adrenocortical cells (Viger et al, 1998), where it may be involved in the regulation of SF1 (Tremblay & Viger, 2003). These 'A cells' are also Gli1-positive (Hughes et al, 2012) and it has been hypothesised that they are derived from subcapsular progenitor cells that deviate from their 'normal' differentiation pathway. The phenotype described in Figure 5.2.2B, resembles that of these previously described spindle-shaped 'A cells'. They too are non-steroidogenic and likely to express GATA4.

In mice with gonadectomy-induced adrenocortical tumours, serum luteinising hormone levels are elevated, and GATA4 and LHR (Leutinising Hormone Receptor) expression are increased within the 'A cells' of the adrenal cortex (Bielinska et al, 2006; Bielinska et al, 2003). Progression of tumour formation leads to the development of sex steroid producing 'B cells' within the clusters of 'A cells', and hence it is thought that the subcapsular adrenocortical cells have undergone metaplasia to form tissue resembling gonadal stroma (Bielinska et al, 2006; Bielinska et al, 2003). Hypogonadism is a feature of Bardet-Biedl syndrome and therefore it is possible that ovarian function in the BBS6 KO mouse examined in Figure 5.2.2B was disrupted by the ciliopathy, leading to reduced production of sex hormones, hypogonadism, and subsequent elevated LH levels leading to an adrenal tumour with gonadal features. This may be a

rare occurrence, depending on which organs or systems are affected by the ciliopathy in each individual case. However, it does appear to be a secondary characteristic, and while it is an interesting finding, it is unlikely to reveal a direct role for primary cilia in the adrenal but could indicate the possibility of increased incidence of adrenal hyperplasia in BBS patients. It may be also worth noting that GATA4 expression has been found in some human adrenocortical tumours (Kiiveri et al, 2004).

Genetic ablation of Shh in mice results in small adrenals with thin capsules (Ching & Vilain, 2009; Huang et al, 2010; King et al, 2009). Cortical proliferation and apoptosis are normal, but proliferation in the capsule is reduced (Huang et al, 2010), and it is possible that impaired expansion and growth of the gland results from the decreased capsule density. In accordance with the dual lineage model of adrenocortical development proposed by King et al. (King et al, 2009), cells in these smaller adrenals would arise from an initial Shh-independent primary cell lineage. However, a secondary Shh-dependent cell lineage derived from the capsule, required for growth and expansion of the cortex during development (Huang et al, 2010; King et al, 2009), and possibly maturation and maintenance in the adult, fails to develop. Currently it is not known why the capsule is thin in these KO animals; Shh signals from the periphery of the cortex to the overlying capsular cells and could therefore be acting as a mitogen, as suggested by the reduction in the percentage of Ki67-positive cells in the capsule in Shh KO mice (Huang et al, 2010), could inhibit the differentiation of stem/progenitor cells within the capsule/subcapsule into cortical cells, or could act as a chemoattractant, helping to draw in cells from the surrounding mesenchyme to form the capsule.

Although zonation and differentiation of cortical cells still occurs in conditional Shh KO mice, and are likely to be Shh-independent processes, steroid synthesis may be impaired due to a reduction in the size of the gland. Huang et al. report that plasma corticosterone levels, although normal at 18dpf and 5 days postpartum (P5) in these mice, become significantly reduced by P21 (Huang et al, 2010). Therefore, the ability of the cortex to regulate steroidogenic output by remodelling in response to stress or changes in salt/water balance, is likely to be compromised.

Adrenals examined from BBS KO mice also have a reduced capsule cell density compared to their wild-type littermates (Figure 5.2.3), and this is likely to result from reduced Hh signalling caused by the ciliopathy. Normal zonal steroidogenic enzyme expression was observed (Figure 5.2.1), but the majority were not significantly smaller in size. As a decrease in Hh pathway activity may be an indirect effect resulting from the knockdown of BBS genes, and it is unlikely all signalling is abrogated, it is not surprising that the adrenal phenotype observed is not as severe as that of the conditional Shh KO mice. Even so, as the capsule is thought to be a source of new adrenal cells, and is significantly reduced in size, these mice are likely to have impaired remodelling capabilities, and consequently impaired steroidogenic output, for example increasing aldosterone production in response to low sodium.

Preliminary experiments looking at corticosterone production in response to ACTH stimulation have indicated that adrenal steroidogenic output may be altered in BBS12 null mice (Figure 5.2.4). Synacthen testing resulted in higher serum corticosterone in BBS12 null mice than the wild-type animals, which could point toward greater activity of the zF. Certainly the concentration of corticosterone measured from wild-type mice after ACTH injection is comparable to levels seen previously using this technique (Meimaridou et al, 2012), however basal corticosterone levels were not recorded, and thus BBS null mice may have higher basal circulating corticosterone levels. If that is the case, synacthen testing could result in an equivalent increase in corticosterone compared to the wild-type mice, or if basal levels are dramatically increased, adrenal steroidogenic output may be unaltered after ACTH stimulation.

A possible explanation for increased serum corticosterone in BBS null mice stems from their obese phenotype. These mice have more adipose tissue, thought to be a result of leptin resistance or insensitivity, combined with increased adipogenesis (Marion et al, 2009), and it has been shown that 11β-HSD1 (11β-hydroxysteroid dehydrogenase type 1) expression and activity can be increased in adipose tissue in both mouse models of obesity, and obese humans (Livingstone et al, 2009; Wake et al, 2007). 11β-HSD1 enhances the bioavailability of corticosterone by reducing inert 11-dehydrocorticosterone, thereby counteracting the effects of 11β-HSD2 (11β-

hydroxysteroid dehydrogenase type 2) (Seckl & Walker, 2001). This could therefore cause the increased serum levels seen here, rather than an increase in adrenal corticosterone production. If adrenal corticosterone was increased it should be associated with zF hypertrophy or hyperplasia, which we did not find, as seen in mouse models and humans with Cushing's disease (Helseth et al, 1992). Basal serum corticosterone and aldosterone levels should now be measured, as well as 11β-HSD1 activity, and circulating levels of other components of the HPA axis and RAA system to identify any differences.

Phenotypes for the targeted knockdown of BBS4 and BBS6 genes in zebrafish using MOs have previously been characterised (Badano et al, 2006; Tayeh et al, 2008; Yen et al, 2006). However, investigations looking at the inclusion of an interrenal phenotype have not been implemented. MO microinjections resulted in the generation of embryos with moderate or severe shortening of the body axis (Figure 5.3.2B), and a kinked notochord (Figure 5.3.2C), thus recapitulating the previous studies. Injected embryos had a reasonable survival rate, which did not vary between MOs (Figure 5.3.1). A reduction in protein expression, either by whole mount immunohistochemistry or western blotting, was not carried out due to a lack of suitable antibodies. However, Badano et al. found that co-injection with BBS4 or BBS6 RNA rescued these phenotypes, indicating that they are specific for the MOs (Badano et al, 2006).

Knockdown of BBS4 and BBS6 also caused a reduction in the number and length of cilia in the zebrafish tail (Figure 5.3.3). This corresponds with the report by Yen et al. that there are fewer cilia in the Kupffer's vesicle, and they are significantly shorter by the 10-13 somites stage after injection with BBS targeting MOs (Yen et al, 2006). Kupffer's vesicle is the zebrafish equivalent of the mammalian embryonic node, involved in the generation of left-right asymmetry during development (Essner et al, 2005). Therefore cilia formation and/or maintenance requires BBS proteins in zebrafish, and cilia function is expected to be disrupted in embryos injected with MO-BBS4 or MO-BBS6.

During zebrafish development, ff1b expression is first detected around 20-22hpf, specifying two pools of interrenal cells which then migrate medially and fuse to form one group of cells by 28hpf (Liu, 2007). Ff1b expression was either absent or delayed in zebrafish injected with MOs targeting BBS4 or BBS6 (Figure 5.3.4). In the delayed phenotype, the area of expression was also considerably reduced, and the staining was not as defined, indicating that cilia are required for, or involved in, the establishment of ff1b-positive interrenal cells during embryogenesis. Just as SF-1 is essential for adrenal development in mammals (Luo et al, 1994), ff1b is thought to be absolutely required for the development of steroidogenic interrenal tissue in teleosts (Chai et al, 2003), and therefore in the absence of functional cilia, this process is likely to be disrupted.

In mammals, Hh signalling is closely regulated by cilia. Studies looking at zebrafish with non-functional cilia have revealed that they are required for maximal Hh pathway activation, but not low level signalling (Huang & Schier, 2009). Thus, the delayed or absent specification of interrenal cells in MO-BBS4 or MO-BBS6 injected embryos could be attributed to a reduction in high level Hh signalling, caused by disrupted cilium formation and function. Although murine SF-1 expression is not governed by Hh signalling (Huang et al, 2010), expression of both ff1b (in the interrenal gland) and WT1 (in the pronephric primordium) were found to be reduced in *smu* (slow-muscle omitted) and *dtr* (detour) mutant zebrafish (Bergeron et al, 2008), in which Smo and Gli1 respectively are inactivated. WT1 is however a determining factor for ff1b expression (Hsu et al, 2003), so Hh signalling may either directly or indirectly determine its expression. It may also be worth mentioning that *yot* (you-too; C-terminally truncated Gli2), *smu*, *dtr* and *syu* (sonic-you; deleted Shh) mutant zebrafish all have ventral spinal curvature (Brand et al, 1996), and some have neural tube defects, further suggesting that the phenotypes seen in MO-BBS fish could be a result of impaired Hh signalling.

Given that some MO-BBS injected fish were still able to form interrenal tissue, albeit to a reduced extent, this could indicate that cilia, via Hh signalling, may only be partially required for interrenal gland development or there is a threshold. In mice, a primary adrenal cell lineage forms in the absence of Shh, but specification of a second cell

lineage, and growth, expansion and maintenance of the gland in the adult is Shh-dependant (Huang et al, 2010; King et al, 2009). Hence, the requirement of cilia could correspond with a requirement for Hh signalling.

Alternatively, PCP signalling is perturbed in both BBS null mice and zebrafish injected with BBS targeting MOs (Ross et al, 2005), and this non-canonical Wnt pathway could be involved in adrenal/interrenal development. Zebrafish lacking the non-canonical Wnt, Wnt5, have a shortened tail and body axis, with similarity to the observed BBS phenotypes (Ross et al, 2005; Westfall et al, 2003), and Wnt4 may play a role in the process of distinguishing adrenal from gonadal cells in the murine adrenogonadal primordium (Heikkila et al, 2002). Wnt4 mutant mice also have reduced expression of CYP11B2 in the cortex, with a corresponding decrease in serum aldosterone, indicating that Wnt4 is required for zG development (Heikkila et al, 2002). Although, Wnt4 can act via both the non-canonical and canonical Wnt pathways (Du et al, 1995; Lyons et al, 2004), so either could be the mechanism by which it is acting. In zebrafish, along with Wnt11, Wnt4 is required for the convergence of several organ precursors at the midline (Matsui et al, 2005), which could include interrenal cells, as midline migration is a key step in the development of this gland.

Animal models provide us with the ability to study human diseases *in vivo*. The mammalian mouse model is genetically more similar to humans than zebrafish are, however this latter vertebrate model organism has the advantages of being cheaper, having easily accessible embryos, and a shorter generation time (Eisen & Smith, 2008). By combining the study of both models, the data shown in this chapter indicate that there is a conserved requirement of primary cilia for normal adrenal/interrenal gland development across vertebrate species. Addressing the initial aims of this chapter, these *in vivo* studies suggest that adrenal function could be impaired in patients with ciliopathic disorders.

CHAPTER 6: GENERAL DISCUSSION

H295Rs are the most useful adrenal cell line available at present. They express all enzymes required for steroidogenesis, produce cortisol, aldosterone and DHEA, the major steroidal outputs from the human adrenal, and are responsive to angiotensin II and forskolin. They express many components required for Hh signalling, including having the capacity to form primary cilia, and are likely to respond to Hh pathway agonists in a canonical signalling manner. Differentiation of these cells towards the zonal phenotypes of the mammalian adrenal cortex is measurable by real-time qPCR of their steroidogenic enzyme expression levels. They are therefore a valuable tool for *in vitro* experimentation.

Using siRNA it was possible to knockdown IFT88, BBS4 or BBS6 in H295R cells, with accompanying reductions in cilium length. Knockdown of these ciliary network components preceding stimulation of differentiation indicate a requirement for primary cilia in the acquisition of zG-like phenotypes. On the contrary, differentiation in the presence of ShhN identified that high Hh pathway ligand concentrations, and presumed canonical signalling, inhibit zG-like phenotypes. Primary cilia are therefore feasibly required for initiating cell fate decisions in H295R cells that result in the zG phenotype, which may involve different levels of Hh pathway activation. Other pathways that utilise the cilium for signal transduction are also anticipated to be involved in this process, although canonical Wnt signalling is an unlikely candidate.

Murine ciliopathy models of BBS have a thinner capsule, indicative of inadequate Hh signalling, which is required for normal growth of the capsule and adrenal cortex during development and in the adult. In zebrafish, knockdown of BBS genes using morpholinos resulted in a decrease in the number and length of cilia, and absence, or delayed and reduced specification, of interrenal cells. Together these *in vivo* studies imply there is a requirement for primary cilia in adrenal/interrenal gland development, which is conserved between vertebrate species. As we know from previous mouse studies (Ching & Vilain, 2009; Huang et al, 2010; King et al, 2009), Hh signalling is absolutely required during adrenal development, and as suggested *in vitro,* it may too be responsible in-part for the phenotypes seen here, and/or non-canonical Wnt/PCP signalling. One possibility that emerges from these zebrafish studies is that, following further analysis and comparison of pathways, this could become a model organism for

adrenal development and function, leading to the reduction in, and replacement of, genetic mouse models in future research.

Acknowledging the main aims of this thesis, through *in vitro* and *in vivo* experimentation, it has been shown that primary cilia are very likely to be involved in adrenal development and function. The role of Sonic Hedgehog signalling in these processes has also been to some extent further characterised. These findings will help advance the current understanding of adrenocortical development, and may impact on patient care, as adrenal function could be compromised in patients with ciliopathic disorders.

The next logical step in this investigation would be to measure basal circulating steroid levels in BBS mice, to identify if the increased serum corticosterone after synacthen administration compared to wild-type animals truly exists. Synacthen testing of BBS patients to screen for adrenal pathologies could also be conducted. BBS affects many organ systems and presents itself differently between patients; therefore diagnostic phenotypes of adrenal malfunction may be masked by a wide range of other symptoms.

Further research *in vitro* could explore the effects of varying ShhN concentrations on zG differentiation, as well as the use of other Hh pathway agonists, or over expression of Gli1. siRNA targeting Hh pathway components would perhaps counteract these effects clearly implicating canonical Hh signalling as the mechanism involved in this process. Non-canonical Hh signalling could also be investigated in H295R cells. Using lentiviral technology; generation of an H295R knockdown or inducible knockdown cell line, for ciliary network components, would help facilitate research on the mechanisms through which primary cilia are involved in adrenal development and differentiation.
Breeding BBS knockout mice with those containing a Gli1 binding site-GFP reporter, to allow easy visualisation of active Hh signalling, would provide a system in which to determine if primary cilia and Hh signalling are involved in remodelling of the adrenal *in vivo*. Mice would be provided with a sodium-restricted diet, or captopril via the

drinking water to inhibit ACE (angiotensin-converting enzyme), thus stimulating or repressing zG activity respectively. Plasma aldosterone and corticosterone content could be examined, as well as adrenal zonation by *in situ* hybridisation with steroidogenic markers.

Morpholino studies in the zebrafish could be widened to investigate the expression patterns of steroidogenic enzymes and Hh pathway components. Photoactivatable MOs could also be used to control specific knockdown spatially and temporally, and determine if the interrenal phenotypes are a primary of secondary characteristic of globally impaired ciliogenesis. Alternatively, interrenal development could be analysed in zebrafish mutants such as *ift172*$^{hi2211Tg/+}$, *ift57*$^{hi3417Tg/+}$, *ift81*$^{hi409Tg/+}$ and *ift88*$^{tz288/+}$.

Primary cilia are beginning to impact greatly on endocrine research, as well as within the cancer and developmental biology fields. The development and maintenance of the different adrenocortical zones and their correct steroidal output are extremely important for health, controlling the stress response and blood pressure, disorders of which are an increasingly important clinical problem. Adrenal hyperplastic disorders typically result from steroidogenic enzyme mutations, with the most common caused by 21-hydroxylase deficiency (CYP21, OMIM 20190), occurring in approximately 1/15,000 live births. Adrenal hypoplasia (OMIM 300200) results from incorrect development of adrenocortical cells. Both of these conditions are lethal without lifelong hormone replacement therapy.

Identifying the key pathways and mechanisms involved in adrenal ontogenesis will help to increase our current understanding of this process. This will hopefully enhance the progression towards gene therapy and regeneration technologies for patients with adrenal failure, congenital steroid deficiency, or in the post-operative management of patients with endocrine tumours. These would be a welcome alternative to lifelong therapeutic intervention by hormone replacement, which is still associated with reduced quality of life and significantly increased mortality, can have the side effects of psychological disturbances and does not address secondary issues present occasionally, such as infertility.

The data presented in this thesis not only confirm and extend our understanding of the role of Shh signalling in the adrenal, but also advocate that primary cilia are required for correct adrenal development, possibly via the Hh (and other) signalling pathways. Further elucidation of the signalling pathways that utilise primary cilia in the development of the adrenal gland, will progress our understanding of adrenocortical development and remodelling, and will hopefully lead to improved management of adrenal dysfunction. Determining a functional adrenal deficit caused by ciliopathies will stimulate clinical investigations into as yet unassigned cases of adrenal insufficiency, as well as prompt a review of the clinical management of patients affected by these conditions. Ultimately, identifying that adrenal defects are a characteristic of ciliopathies will have a huge impact on patient care.

REFERENCES

Li-Cors Odyssey Infrared Imaging System - Biocompare Buyer's Guide For Life Scientists. Vol. 2009.

Aguilera G, Schirar A, Baukal A, Catt KJ (1980) Angiotensin II receptors. Properties and regulation in adrenal glomerulosa cells. *Circ Res* **46:** I118-127

Akin L, Kurtoglu S, Kendirici M, Akin MA (2010) Familial glucocorticoid deficiency type 2: a case report. *J Clin Res Pediatr Endocrinol* **2:** 122-125

Almeida MQ, Soares IC, Ribeiro TC, Fragoso MC, Marins LV, Wakamatsu A, Ressio RA, Nishi MY, Jorge AA, Lerario AM, Alves VA, Mendonca BB, Latronico AC (2010) Steroidogenic factor 1 overexpression and gene amplification are more frequent in adrenocortical tumors from children than from adults. *J Clin Endocrinol Metab* **95:** 1458-1462

An M, Luo R, Henion PD (2002) Differentiation and maturation of zebrafish dorsal root and sympathetic ganglion neurons. *J Comp Neurol* **446:** 267-275

Arlt W, Allolio B (2003) Adrenal insufficiency. *Lancet* **361:** 1881-1893

Arnold J (1866) Ein Beitrag zu der feiner Stuktur und dem Chemismus der Nebennieren. *Virchows Archiv Fuer Pathologische Anatomie und Physiologie und fuer Klinische Medizin* **35:** 64-107

Auchus RJ, Lee TC, Miller WL (1998) Cytochrome b5 augments the 17,20-lyase activity of human P450c17 without direct electron transfer. *J Biol Chem* **273:** 3158-3165

Aumo L, Rusten M, Mellgren G, Bakke M, Lewis AE (2010) Functional Roles of Protein Kinase A (PKA) and Exchange Protein Directly Activated by 3',5'-Cyclic Adenosine 5'-Monophosphate (cAMP) 2 (EPAC2) in cAMP-Mediated Actions in Adrenocortical Cells. *Endocrinology***:** en.2009-1139

Babu PS, Bavers DL, Beuschlein F, Shah S, Jeffs B, Jameson JL, Hammer GD (2002) Interaction between Dax-1 and steroidogenic factor-1 in vivo: increased adrenal responsiveness to ACTH in the absence of Dax-1. *Endocrinology* **143:** 665-673

Badano JL, Leitch CC, Ansley SJ, May-Simera H, Lawson S, Lewis RA, Beales PL, Dietz HC, Fisher S, Katsanis N (2006) Dissection of epistasis in oligogenic Bardet-Biedl syndrome. *Nature* **439:** 326-330

Baliga BS, Pronczuk AW, Munro HN (1969) Mechanism of cycloheximide inhibition of protein synthesis in a cell-free system prepared from rat liver. *J Biol Chem* **244:** 4480-4489

Barnes EA, Kong M, Ollendorff V, Donoghue DJ (2001) Patched1 interacts with cyclin B1 to regulate cell cycle progression. *EMBO J* **20:** 2214-2223

Bassett MH, Suzuki T, Sasano H, De Vries CJ, Jimenez PT, Carr BR, Rainey WE (2004a) The orphan nuclear receptor NGFIB regulates transcription of 3beta-hydroxysteroid dehydrogenase. implications for the control of adrenal functional zonation. *J Biol Chem* **279:** 37622-37630

Bassett MH, Suzuki T, Sasano H, White PC, Rainey WE (2004b) The orphan nuclear receptors NURR1 and NGFIB regulate adrenal aldosterone production. *Mol Endocrinol* **18:** 279-290

Beachy PA, Karhadkar SS, Berman DM (2004) Tissue repair and stem cell renewal in carcinogenesis. *Nature* **432:** 324-331

Beales PL, Elcioglu N, Woolf AS, Parker D, Flinter FA (1999) New criteria for improved diagnosis of Bardet-Biedl syndrome: results of a population survey. *J Med Genet* **36:** 437-446

Begleiter ML, Harris DJ (1980) Holoprosencephaly and endocrine dysgenesis in brothers. *Am J Med Genet* **7:** 315-318

Bergeron SA, Milla LA, Villegas R, Shen MC, Burgess SM, Allende ML, Karlstrom RO, Palma V (2008) Expression profiling identifies novel Hh/Gli-regulated genes in developing zebrafish embryos. *Genomics* **91:** 165-177

Berghmans S, Murphey RD, Wienholds E, Neuberg D, Kutok JL, Fletcher CD, Morris JP, Liu TX, Schulte-Merker S, Kanki JP, Plasterk R, Zon LI, Look AT (2005) tp53 mutant zebrafish develop malignant peripheral nerve sheath tumors. *Proc Natl Acad Sci U S A* **102:** 407-412

Berthon A, Sahut-Barnola I, Lambert-Langlais S, de Joussineau C, Damon-Soubeyrand C, Louiset E, Taketo MM, Tissier F, Bertherat J, Lefrancois-Martinez AM, Martinez A, Val P (2010) Constitutive beta-catenin activation induces adrenal hyperplasia and promotes adrenal cancer development. *Hum Mol Genet* **19:** 1561-1576

Bielinska M, Kiiveri S, Parviainen H, Mannisto S, Heikinheimo M, Wilson DB (2006) Gonadectomy-induced adrenocortical neoplasia in the domestic ferret (Mustela putorius furo) and laboratory mouse. *Vet Pathol* **43:** 97-117

Bielinska M, Parviainen H, Porter-Tinge SB, Kiiveri S, Genova E, Rahman N, Huhtaniemi IT, Muglia LJ, Heikinheimo M, Wilson DB (2003) Mouse Strain Susceptibility to Gonadectomy-Induced Adrenocortical Tumor Formation Correlates with the Expression of GATA-4 and Luteinizing Hormone Receptor. *Endocrinology* **144:** 4123-4133

Bird I, Hanley N, Word R, Mathis J, McCarthy J, Mason J, Rainey W (1993) Human NCI-H295 adrenocortical carcinoma cells: a model for angiotensin- II-responsive aldosterone secretion. *Endocrinology* **133:** 1555-1561

Bird IM, Mason JI, Rainey WE (1994) Regulation of type 1 angiotensin II receptor messenger ribonucleic acid expression in human adrenocortical carcinoma H295 cells. *Endocrinology* **134:** 2468-2474

Bitgood MJ, McMahon AP (1995) Hedgehog and Bmp genes are coexpressed at many diverse sites of cell-cell interaction in the mouse embryo. *Dev Biol* **172:** 126-138

Bitgood MJ, Shen L, McMahon AP (1996) Sertoli cell signaling by Desert hedgehog regulates the male germline. *Current Biology* **6:** 298-304

Blacque OE, Reardon MJ, Li C, McCarthy J, Mahjoub MR, Ansley SJ, Badano JL, Mah AK, Beales PL, Davidson WS, Johnsen RC, Audeh M, Plasterk RH, Baillie DL, Katsanis N, Quarmby LM, Wicks SR, Leroux MR (2004) Loss of C. elegans BBS-7 and BBS-8 protein function results in cilia defects and compromised intraflagellar transport. *Genes Dev* **18:** 1630-1642

Bogdarina IG, King PJ, Clark AJL (2009) Characterization of the angiotensin (AT1b) receptor promoter and its regulation by glucocorticoids. *J Mol Endocrinol* **43:** 73-80

Borkowski AJ, Levin S, Delcroix C, Mahler A, Verhas V (1967) Blood cholesterol and hydrocortisone production in man: quantitative aspects of the utilization of circulating cholesterol by the adrenals at rest and under adrenocorticotropin stimulation. *J Clin Invest* **46:** 797-811

Bose HS, Sugawara T, Strauss JF, 3rd, Miller WL (1996) The pathophysiology and genetics of congenital lipoid adrenal hyperplasia. *N Engl J Med* **335:** 1870-1878

Bose J, Grotewold L, Ruther U (2002) Pallister-Hall syndrome phenotype in mice mutant for Gli3. *Hum Mol Genet* **11:** 1129-1135

Bourikas D, Pekarik V, Baeriswyl T, Grunditz A, Sadhu R, Nardo M, Stoeckli ET (2005) Sonic hedgehog guides commissural axons along the longitudinal axis of the spinal cord. *Nat Neurosci* **8:** 297-304

Brace N, Kemp R, Snelgar R (2006) *SPSS for psychologists : a guide to data analysis using SPSS for Windows : versions 12 and 13*, 3rd ed. edn. Basingstoke: Palgrave Macmillan.

Brailov I, Bancila M, Brisorgueil MJ, Miquel MC, Hamon M, Verge D (2000) Localization of 5-HT(6) receptors at the plasma membrane of neuronal cilia in the rat brain. *Brain Res* **872:** 271-275

Brand M, Heisenberg CP, Warga RM, Pelegri F, Karlstrom RO, Beuchle D, Picker A, Jiang YJ, Furutani-Seiki M, van Eeden FJ, Granato M, Haffter P, Hammerschmidt M, Kane DA, Kelsh RN, Mullins MC, Odenthal J, Nusslein-Volhard C (1996) Mutations affecting development of the midline and general body shape during zebrafish embryogenesis. *Development* **123:** 129-142

Bridgham JT, Carroll SM, Thornton JW (2006) Evolution of hormone-receptor complexity by molecular exploitation. *Science* **312:** 97-101

Briscoe J (2009) Making a grade: Sonic Hedgehog signalling and the control of neural cell fate. *EMBO J* **28:** 457-465

Brown JD (1997) A rapid, non-toxic protocol for sequence-ready plasmid DNA. *Technical Tips Online* **1:** 1281

Buglino JA, Resh MD (2008) Hhat is a palmitoylacyltransferase with specificity for N-palmitoylation of Sonic Hedgehog. *J Biol Chem* **283:** 22076-22088

Bumcrot D, Takada R, McMahon A (1995) Proteolytic processing yields two secreted forms of sonic hedgehog [published erratum appears in Mol Cell Biol 1995 May;15(5):2904]. *Mol Cell Biol* **15:** 2294-2303

Carrasco GA, Van de Kar LD (2003) Neuroendocrine pharmacology of stress. *Eur J Pharmacol* **463:** 235-272

Caspary T, Larkins CE, Anderson KV (2007) The Graded Response to Sonic Hedgehog Depends on Cilia Architecture. *Developmental Cell* **12:** 767-778

Chai C, Chan WK (2000) Developmental expression of a novel Ftz-F1 homologue, ff1b (NR5A4), in the zebrafish Danio rerio. *Mech Dev* **91:** 421-426

Chai C, Liu YW, Chan WK (2003) Ff1b is required for the development of steroidogenic component of the zebrafish interrenal organ. *Dev Biol* **260:** 226-244

Chamoun Z, Mann RK, Nellen D, von Kessler DP, Bellotto M, Beachy PA, Basler K (2001) Skinny hedgehog, an acyltransferase required for palmitoylation and activity of the hedgehog signal. *Science* **293:** 2080-2084

Charron F, Stein E, Jeong J, McMahon AP, Tessier-Lavigne M (2003) The morphogen sonic hedgehog is an axonal chemoattractant that collaborates with netrin-1 in midline axon guidance. *Cell* **113:** 11-23

Chen JK, Taipale J, Cooper MK, Beachy PA (2002a) Inhibition of Hedgehog signaling by direct binding of cyclopamine to Smoothened. *Genes & Development* **16:** 2743-2748

Chen JK, Taipale J, Young KE, Maiti T, Beachy PA (2002b) Small molecule modulation of Smoothened activity. *Proceedings of the National Academy of Sciences of the United States of America* **99:** 14071-14076

Chen MH, Li YJ, Kawakami T, Xu SM, Chuang PT (2004) Palmitoylation is required for the production of a soluble multimeric Hedgehog protein complex and long-range signaling in vertebrates. *Genes Dev* **18:** 641-659

Chester-Jones I, Ingleton PM, Phillips JG (1987) *Fundamentals of comparative vertebrate endocrinology*, New York ; London: Plenum.

Chiappe ME, Lattanzi ML, Colman-Lerner AA, Baranao JL, Saragueta P (2002) Expression of 3 beta-hydroxysteroid dehydrogenase in early bovine embryo development. *Mol Reprod Dev* **61:** 135-141

Chida D, Nakagawa S, Nagai S, Sagara H, Katsumata H, Imaki T, Suzuki H, Mitani F, Ogishima T, Shimizu C, Kotaki H, Kakuta S, Sudo K, Koike T, Kubo M, Iwakura Y (2007) Melanocortin 2 receptor is required for adrenal gland development, steroidogenesis, and neonatal gluconeogenesis. *Proc Natl Acad Sci U S A* **104:** 18205-18210

Ching S, Vilain E (2009) Targeted disruption of Sonic Hedgehog in the mouse adrenal leads to adrenocortical hypoplasia. *Genesis* **47:** 628-637

Chow SC, Peters I, Orrenius S (1995) Reevaluation of the role of de novo protein synthesis in rat thymocyte apoptosis. *Exp Cell Res* **216:** 149-159

Christensen ST, Pedersen LB, Schneider L, Satir P (2007) Sensory cilia and integration of signal transduction in human health and disease. *Traffic* **8:** 97-109

Chrousos GP (1995) The hypothalamic-pituitary-adrenal axis and immune-mediated inflammation. *N Engl J Med* **332:** 1351-1362

Chung TT, Chan LF, Metherell LA, Clark AJ (2010) Phenotypic characteristics of familial glucocorticoid deficiency (FGD) type 1 and 2. *Clin Endocrinol (Oxf)* **72:** 589-594

Ciruna B, Weidinger G, Knaut H, Thisse B, Thisse C, Raz E, Schier AF (2002) Production of maternal-zygotic mutant zebrafish by germ-line replacement. *Proc Natl Acad Sci U S A* **99:** 14919-14924

Clark AJ, McLoughlin L, Grossman A (1993) Familial glucocorticoid deficiency associated with point mutation in the adrenocorticotropin receptor. *Lancet* **341:** 461-462

Clark AJ, Weber A (1998) Adrenocorticotropin insensitivity syndromes. *Endocr Rev* **19:** 828-843

Clauser E, Curnow K, Davies E, Conchon S, Teutsch B, Vianello B, Monnot C, Corvol P (1996) Angiotensin II receptors: protein and gene structures, expression and potential pathological involvements. *Eur J Endocrinol* **134:** 403-411

Clement CA, Kristensen SG, Mollgard K, Pazour GJ, Yoder BK, Larsen LA, Christensen ST (2009) The primary cilium coordinates early cardiogenesis and hedgehog signaling in cardiomyocyte differentiation. *J Cell Sci* **122:** 3070-3082

Cobb VJ, Williams BC, Mason JI, Walker SW (1996) Forskolin treatment directs steroid production towards the androgen pathway in the NCI-H295R adrenocortical tumour cell line. *Endocr Res* **22:** 545-550

Cohen AI, Bloch E, Celozzi E (1957) In vitro response of functional experimental adrenal tumors to corticotropin ACTH. *Proc Soc Exp Biol Med* **95:** 304-309

Collier JG, Robinson BF, Vane JR (1973) Reduction of pressor effects of angiotensin I in man by synthetic nonapeptide (B.P.P. 9a or SQ 20,881) which inhibits converting enzyme. *Lancet* **1:** 72-74

Cooper MK, Porter JA, Young KE, Beachy PA (1998) Teratogen-Mediated Inhibition of Target Tissue Response to Shh Signaling. *Science* **280:** 1603-1607

Corbit KC, Aanstad P, Singla V, Norman AR, Stainier DYR, Reiter JF (2005) Vertebrate Smoothened functions at the primary cilium. *Nature* **437:** 1018-1021

Corcoran RB, Scott MP (2006) Oxysterols stimulate Sonic hedgehog signal transduction and proliferation of medulloblastoma cells. *Proc Natl Acad Sci U S A* **103:** 8408-8413

Couette B, Jalaguier S, Hellal-Levy C, Lupo B, Fagart J, Auzou G, Rafestin-Oblin ME (1998) Folding requirements of the ligand-binding domain of the human mineralocorticoid receptor. *Mol Endocrinol* **12:** 855-863

Dai P, Akimaru H, Tanaka Y, Maekawa T, Nakafuku M, Ishii S (1999) Sonic Hedgehog-induced activation of the Gli1 promoter is mediated by GLI3. *J Biol Chem* **274:** 8143-8152

de Kloet ER (1995) Steroids, stability and stress. *Front Neuroendocrinol* **16:** 416-425

Dell GC, Morley SD, Mullins JJ, Williams BC, Walker SW (1996) Multiple signal transduction systems regulate angiotensin II type 1 (AT1) receptor mRNA expression in bovine adrenocortical cells. *Endocr Res* **22:** 363-368

Demeure MJ, Bussey KJ, Kirschner LS (2011) Targeted therapies for adrenocortical carcinoma: IGF and beyond. *Horm Cancer* **2:** 385-392

Denner K, Rainey WE, Pezzi V, Bird IM, Bernhardt R, Mathis JM (1996) Differential regulation of 11 beta-hydroxylase and aldosterone synthase in human adrenocortical H295R cells. *Mol Cell Endocrinol* **121:** 87-91

Dennler S, AndrÃ© J, Alexaki I, Li A, Magnaldo T, ten Dijke P, Wang X-J, Verrecchia F, Mauviel A (2007) Induction of Sonic Hedgehog Mediators by Transforming Growth Factor-Î²: Smad3-Dependent Activation of Gli2 and Gli1 Expression In vitro and In vivo. *Cancer Research* **67:** 6981-6986

Du SJ, Purcell SM, Christian JL, McGrew LL, Moon RT (1995) Identification of distinct classes and functional domains of Wnts through expression of wild-type and chimeric proteins in Xenopus embryos. *Mol Cell Biol* **15:** 2625-2634

Dubourg C, Bendavid C, Pasquier L, Henry C, Odent S, David V (2007) Holoprosencephaly. *Orphanet J Rare Dis* **2:** 8

Dworakowska D, Grossman AB (2011) The molecular pathogenesis of corticotroph tumours. *European Journal of Clinical Investigation***:** no-no

Dwyer JR, Sever N, Carlson M, Nelson SF, Beachy PA, Parhami F (2007) Oxysterols are novel activators of the hedgehog signaling pathway in pluripotent mesenchymal cells. *J Biol Chem* **282:** 8959-8968

Eggenschwiler JT, Anderson KV (2007) Cilia and developmental signaling. *Annu Rev Cell Dev Biol* **23:** 345-373

Eisen JS, Smith JC (2008) Controlling morpholino experiments: don't stop making antisense. *Development* **135:** 1735-1743

Ekker SC (2000) Morphants: a new systematic vertebrate functional genomics approach. *Yeast* **17:** 302-306

El Wakil A, Lalli E (2011) The Wnt/beta-catenin pathway in adrenocortical development and cancer. *Mol Cell Endocrinol* **332:** 32-37

Else T, Hammer GD (2005) Genetic analysis of adrenal absence: agenesis and aplasia. *Trends Endocrinol Metab* **16:** 458-468

Ericson J, Morton S, Kawakami A, Roelink H, Jessell TM (1996) Two critical periods of Sonic Hedgehog signaling required for the specification of motor neuron identity. *Cell* **87:** 661-673

Ericson J, Muhr J, Jessell TM, Edlund T (1995a) Sonic hedgehog: a common signal for ventral patterning along the rostrocaudal axis of the neural tube. *Int J Dev Biol* **39:** 809-816

Ericson J, Muhr J, Placzek M, Lints T, Jessell TM, Edlund T (1995b) Sonic hedgehog induces the differentiation of ventral forebrain neurons: a common signal for ventral patterning within the neural tube. *Cell* **81:** 747-756

Essner JJ, Amack JD, Nyholm MK, Harris EB, Yost HJ (2005) Kupffer's vesicle is a ciliated organ of asymmetry in the zebrafish embryo that initiates left-right development of the brain, heart and gut. *Development* **132:** 1247-1260

Etheridge LA, Crawford TQ, Zhang S, Roelink H (2010) Evidence for a role of vertebrate Disp1 in long-range Shh signaling. *Development* **137:** 133-140

Fallo F, Pezzi V, Barzon L, Mulatero P, Veglio F, Sonino N, Mathis JM (2002) Quantitative assessment of CYP11B1 and CYP11B2 expression in aldosterone-producing adenomas. *Eur J Endocrinol* **147:** 795-802

Fuller PJ, Young MJ (2005) Mechanisms of Mineralocorticoid Action. *Hypertension* **46:** 1227-1235

Gaujoux S, Grabar S, Fassnacht M, Ragazzon B, Launay P, Libé R, Chokri I, Audebourg A, Royer B, Sbiera S, Vacher-Lavenu MC, Dousset B, Bertagna X, Allolio B, Bertherat J, Tissier F (2011) β-catenin activation is associated with specific clinical and pathologic characteristics and a poor outcome in adrenocortical carcinoma. *Clin Cancer Res* **17:** 328-336

Gazdar AF, Oie HK, Shackleton CH, Chen TR, Triche TJ, Myers CE, Chrousos GP, Brennan MF, Stein CA, La Rocca RV (1990) Establishment and Characterization of a Human Adrenocortical Carcinoma Cell Line That Expresses Multiple Pathways of Steroid Biosynthesis. *Cancer Res* **50:** 5488-5496

Gilmour KM (2005) Mineralocorticoid receptors and hormones: fishing for answers. *Endocrinology* **146:** 44-46

Ginzinger DG (2002) Gene quantification using real-time quantitative PCR: An emerging technology hits the mainstream. *Experimental Hematology* **30:** 503-512

Giordano TJ, Kuick R, Else T, Gauger PG, Vinco M, Bauersfeld J, Sanders D, Thomas DG, Doherty G, Hammer G (2009) Molecular classification and prognostication of adrenocortical tumors by transcriptome profiling. *Clin Cancer Res* **15:** 668-676

Goodrich LV, Johnson RL, Milenkovic L, McMahon JA, Scott MP (1996) Conservation of the hedgehog/patched signaling pathway from flies to mice: induction of a mouse patched gene by Hedgehog. *Genes Dev* **10:** 301-312

Gottschau M (1883) Struktur und Embryonale Entwickelung der Nebennieren bei Saugetieren. *Archiv fur Anatomie und Entwickelungsgeschichte Anatomisher Abteilung* **9:** 412-458

Grassi Milano E, Basari F, Chimenti C (1997) Adrenocortical and adrenomedullary homologs in eight species of adult and developing teleosts: morphology, histology, and immunohistochemistry. *Gen Comp Endocrinol* **108:** 483-496

Greenbaum D, Colangelo C, Williams K, Gerstein M (2003) Comparing protein abundance and mRNA expression levels on a genomic scale. *Genome Biol* **4:** 117

Greep RO, Deane HW (1949) Histological, cytochemical and physiological observations on the regeneration of the rat's adrenal gland following enucleation. *Endocrinology* **45:** 42-56

Guasti L, Paul A, Laufer E, King P (2011) Localization of Sonic hedgehog secreting and receiving cells in the developing and adult rat adrenal cortex. *Mol Cell Endocrinol* **336:** 117-122

Gummow BM, Winnay JN, Hammer GD (2003) Convergence of Wnt signaling and steroidogenic factor-1 (SF-1) on transcription of the rat inhibin alpha gene. *J Biol Chem* **278:** 26572-26579

Hatano O, Takakusu A, Nomura M, Morohashi K (1996) Identical origin of adrenal cortex and gonad revealed by expression profiles of Ad4BP/SF-1. *Genes Cells* **1:** 663-671

Haycraft CJ, Banizs B, Aydin-Son Y, Zhang Q, Michaud EJ, Yoder BK (2005) Gli2 and Gli3 Localize to Cilia and Require the Intraflagellar Transport Protein Polaris for Processing and Function. *PLoS Genetics* **1:** e53

Heikkila M, Peltoketo H, Leppaluoto J, Ilves M, Vuolteenaho O, Vainio S (2002) Wnt-4 deficiency alters mouse adrenal cortex function, reducing aldosterone production. *Endocrinology* **143:** 4358-4365

Helseth A, Siegal GP, Haug E, Bautch VL (1992) Transgenic mice that develop pituitary tumors. A model for Cushing's disease. *Am J Pathol* **140:** 1071-1080

Hsu H-J, Hsu N-C, Hu M-C, Chung B-C (2006) Steroidogenesis in zebrafish and mouse models. *Molecular and Cellular Endocrinology* **248:** 160-163

Hsu H-J, Lin G, Chung B-c (2003) Parallel early development of zebrafish interrenal glands and pronephros: differential control by wt1 and ff1b. *Development* **130:** 2107-2116

Hsu H-J, Lin J-C, Chung B-c (2009) Zebrafish cyp11a1 and hsd3b genes: Structure, expression and steroidogenic development during embryogenesis. *Molecular and Cellular Endocrinology* **312:** 31-34

Huang C-CJ, Miyagawa S, Matsumaru D, Parker KL, Yao HH-C (2010) Progenitor Cell Expansion and Organ Size of Mouse Adrenal Is Regulated by Sonic Hedgehog. *Endocrinology* **151:** 1119-1128

Huang P, Schier AF (2009) Dampened Hedgehog signaling but normal Wnt signaling in zebrafish without cilia. *Development* **136:** 3089-3098

Hughes CR, Guasti L, Meimaridou E, Chuang C-H, Schimenti JC, King PJ, Costigan C, Clark AJL, Metherell LA (2012) MCM4 mutation causes adrenal failure, short stature, and natural killer cell deficiency in humans. *The Journal of Clinical Investigation* **122:** 814-820

Hui CC, Angers S (2011) Gli proteins in development and disease. *Annu Rev Cell Dev Biol* **27:** 513-537

Hyman JM, Firestone AJ, Heine VM, Zhao Y, Ocasio CA, Han K, Sun M, Rack PG, Sinha S, Wu JJ, Solow-Cordero DE, Jiang J, Rowitch DH, Chen JK (2009) Small-molecule inhibitors reveal multiple strategies for Hedgehog pathway blockade. *Proc Natl Acad Sci U S A* **106:** 14132-14137

Ikeda Y, Swain A, Weber TJ, Hentges KE, Zanaria E, Lalli E, Tamai KT, Sassone-Corsi P, Lovell-Badge R, Camerino G, Parker KL (1996) Steroidogenic factor 1 and Dax-1 colocalize in multiple cell lineages: potential links in endocrine development. *Mol Endocrinol* **10:** 1261-1272

Inagami T, Kambayashi Y, Ichiki T, Tsuzuki S, Eguchi S, Yamakawa T (1999) Angiotensin receptors: molecular biology and signalling. *Clin Exp Pharmacol Physiol* **26:** 544-549

Ingham PW, McMahon AP (2001) Hedgehog signaling in animal development: paradigms and principles. *Genes Dev* **15:** 3059-3087

Ingle DJ, Higgins, G.M. (1938) Regeneration of the adrenal gland following enucleation. *American Journal of Medical Sciences* **196:** 232-239

Ingram WJ, Wicking CA, Grimmond SM, Forrest AR, Wainwright BJ (2002) Novel genes regulated by Sonic Hedgehog in pluripotent mesenchymal cells. *Oncogene* **21:** 8196-8205

Ito M, Yu R, Jameson JL (1997) DAX-1 inhibits SF-1-mediated transactivation via a carboxy-terminal domain that is deleted in adrenal hypoplasia congenita. *Mol Cell Biol* **17:** 1476-1483

Jacob J, Briscoe J (2003) Gli proteins and the control of spinal-cord patterning. *EMBO Rep* **4:** 761-765

Janes ME, Chu KM, Clark AJ, King PJ (2008) Mechanisms of adrenocorticotropin-induced activation of extracellularly regulated kinase 1/2 mitogen-activated protein kinase in the human H295R adrenal cell line. *Endocrinology* **149:** 1898-1905

Jenkins D (2009) Hedgehog signalling: emerging evidence for non-canonical pathways. *Cell Signal* **21:** 1023-1034

Jia J, Kolterud Å, Zeng H, Hoover A, Teglund S, Toftgård R, Liu A (2009) Suppressor of Fused inhibits mammalian Hedgehog signaling in the absence of cilia. *Developmental Biology* **330:** 452-460

Jia J, Tong C, Wang B, Luo L, Jiang J (2004) Hedgehog signalling activity of Smoothened requires phosphorylation by protein kinase A and casein kinase I. *Nature* **432:** 1045-1050

Jiang J, Hui CC (2008) Hedgehog signaling in development and cancer. *Dev Cell* **15:** 801-812

Johnson JA, Davis JO (1973) Angiotensin. II. Important role in the maintenance of arterial blood pressure. *Science* **179:** 906-907

Jurczyk A, Gromley A, Redick S, San Agustin J, Witman G, Pazour GJ, Peters DJ, Doxsey S (2004) Pericentrin forms a complex with intraflagellar transport proteins and polycystin-2 and is required for primary cilia assembly. *J Cell Biol* **166:** 637-643

Karhadkar SS, Bova GS, Abdallah N, Dhara S, Gardner D, Maitra A, Isaacs JT, Berman DM, Beachy PA (2004) Hedgehog signalling in prostate regeneration, neoplasia and metastasis. *Nature* **431:** 707-712

Karlstrom RO, Tyurina OV, Kawakami A, Nishioka N, Talbot WS, Sasaki H, Schier AF (2003) Genetic analysis of zebrafish gli1 and gli2 reveals divergent requirements for gli genes in vertebrate development. *Development* **130:** 1549-1564

Keegan CE, Hammer GD (2002) Recent insights into organogenesis of the adrenal cortex. *Trends in Endocrinology and Metabolism* **13:** 200-208

Kempna P, Fluck CE (2008) Adrenal gland development and defects. *Best Pract Res Clin Endocrinol Metab* **22:** 77-93

Kiiveri S, Liu J, Heikkila P, Arola J, Lehtonen E, Voutilainen R, Heikinheimo M (2004) Transcription factors GATA-4 and GATA-6 in human adrenocortical tumors. *Endocr Res* **30:** 919-923

Kim AC, Hammer GD (2007) Adrenocortical cells with stem/progenitor cell properties: Recent advances. *Molecular and Cellular Endocrinology* **265-266:** 10-16

Kim AC, Reuter AL, Zubair M, Else T, Serecky K, Bingham NC, Lavery GG, Parker KL, Hammer GD (2008a) Targeted disruption of beta-catenin in Sf1-expressing cells impairs development and maintenance of the adrenal cortex. *Development* **135:** 2593-2602

Kim J, Krishnaswami SR, Gleeson JG (2008b) CEP290 interacts with the centriolar satellite component PCM-1 and is required for Rab8 localization to the primary cilium. *Hum Mol Genet* **17:** 3796-3805

Kim JC, Ou YY, Badano JL, Esmail MA, Leitch CC, Fiedrich E, Beales PL, Archibald JM, Katsanis N, Rattner JB, Leroux MR (2005) MKKS/BBS6, a divergent chaperonin-like protein linked to the obesity disorder Bardet-Biedl syndrome, is a novel centrosomal component required for cytokinesis. *J Cell Sci* **118:** 1007-1020

Kim JS, Kubota H, Kiuchi Y, Doi K, Saegusa J (1997) Subcapsular cell hyperplasia and mast cell infiltration in the adrenal cortex of mice: comparative study in 7 inbred strains. *Exp Anim* **46:** 303-306

Kim W-K, Meliton V, Park KW, Hong C, Tontonoz P, Niewiadomski P, Waschek JA, Tetradis S, Parhami F (2009) Negative Regulation of Hedgehog Signaling by Liver X Receptors. *Mol Endocrinol* **23:** 1532-1543

King P, Paul A, Laufer E (2009) Shh signaling regulates adrenocortical development and identifies progenitors of steroidogenic lineages. *Proc Natl Acad Sci U S A* **106:** 21185-21190

King PJ, Guasti L, Laufer E (2008) Hedgehog signalling in endocrine development and disease. *J Endocrinol* **198:** 439-450

Komiya Y, Habas R (2008) Wnt signal transduction pathways. *Organogenesis* **4:** 68-75

Kreidberg JA, Sariola H, Loring JM, Maeda M, Pelletier J, Housman D, Jaenisch R (1993) WT-1 is required for early kidney development. *Cell* **74:** 679-691

Kretzschmar K, Watt FM (2012) Lineage tracing. *Cell* **148:** 33-45

Kulaga HM, Leitch CC, Eichers ER, Badano JL, Lesemann A, Hoskins BE, Lupski JR, Beales PL, Reed RR, Katsanis N (2004) Loss of BBS proteins causes anosmia in humans and defects in olfactory cilia structure and function in the mouse. *Nat Genet* **36:** 994-998

Kuo MW, Postlethwait J, Lee WC, Lou SW, Chan WK, Chung BC (2005) Gene duplication, gene loss and evolution of expression domains in the vertebrate nuclear receptor NR5A (Ftz-F1) family. *Biochem J* **389:** 19-26

Laufer E, Kesper Dr, Vortkamp A, King P (2012) Sonic hedgehog signaling during adrenal development. *Molecular and Cellular Endocrinology* **351:** 19-27

Lee FlorenceÂ Y, Faivre EmilyÂ J, Suzawa M, Lontok E, Ebert D, Cai F, Belsham DeniseÂ D, Ingraham HollyÂ A (2011) Eliminating SF-1 (NR5A1) Sumoylation InÂ Vivo Results in Ectopic Hedgehog Signaling and Disruption of Endocrine Development. *Developmental Cell* **21:** 315-327

Lehmann T, Wrzesinski T (2012) The molecular basis of adrenocortical cancer. *Cancer Genet* **205:** 131-137

LeHoux J-G, Bird IM, Briere N, Martel D, Ducharme L (1997) Influence of Dietary Sodium Restriction on Angiotensin II Receptors in Rat Adrenals. *Endocrinology* **138:** 5238-5247

Levens NR (1990) Control of renal function by intrarenal angiotensin II in the dog. *J Cardiovasc Pharmacol* **16 Suppl 4:** S65-69

Li JB, Gerdes JM, Haycraft CJ, Fan Y, Teslovich TM, May-Simera H, Li H, Blacque OE, Li L, Leitch CC, Lewis RA, Green JS, Parfrey PS, Leroux MR, Davidson WS, Beales PL, Guay-Woodford LM, Yoder BK, Stormo GD, Katsanis N, Dutcher SK (2004) Comparative genomics identifies a flagellar and basal body proteome that includes the BBS5 human disease gene. *Cell* **117:** 541-552

Lienkamp S, Ganner A, Walz G (2012) Inversin, Wnt signaling and primary cilia. *Differentiation* **83:** S49-55

Lin L, Hindmarsh PC, Metherell LA, Alzyoud M, Al-Ali M, Brain CE, Clark AJ, Dattani MT, Achermann JC (2007) Severe loss-of-function mutations in the adrenocorticotropin receptor (ACTHR, MC2R) can be found in patients diagnosed with salt-losing adrenal hypoplasia. *Clin Endocrinol (Oxf)* **66:** 205-210

Lin SR, Lee YJ, Tsai JH (1994) Mutations of the p53 gene in human functional adrenal neoplasms. *J Clin Endocrinol Metab* **78:** 483-491

Lin TL, Matsui W (2012) Hedgehog pathway as a drug target: Smoothened inhibitors in development. *Onco Targets Ther* **5:** 47-58

Lindemann RK (2008) Stroma-initiated hedgehog signaling takes center stage in B-cell lymphoma. *Cancer Res* **68:** 961-964

Liu J, Heikkila P, Meng QH, Kahri AI, Tikkanen MJ, Voutilainen R (2000) Expression of low and high density lipoprotein receptor genes in human adrenals. *Eur J Endocrinol* **142:** 677-682

Liu YW (2007) Interrenal organogenesis in the zebrafish model. *Organogenesis* **3:** 44-48

Livingstone DE, Grassick SL, Currie GL, Walker BR, Andrew R (2009) Dysregulation of glucocorticoid metabolism in murine obesity: comparable effects of leptin resistance and deficiency. *J Endocrinol* **201:** 211-218

Logan CY, Nusse R (2004) The Wnt signaling pathway in development and disease. *Annu Rev Cell Dev Biol* **20:** 781-810

Lombes M, Kenouch S, Souque A, Farman N, Rafestin-Oblin ME (1994) The mineralocorticoid receptor discriminates aldosterone from glucocorticoids independently of the 11 beta-hydroxysteroid dehydrogenase. *Endocrinology* **135:** 834-840

Low G, Dhliwayo H, Lomas DJ (2012) Adrenal neoplasms. *Clin Radiol* **67:** 988-1000

Lu Q, Mellgren RL (1996) Calpain inhibitors and serine protease inhibitors can produce apoptosis in HL-60 cells. *Arch Biochem Biophys* **334:** 175-181

Lu X, Grove KL, Zhang W, Speth RC (1995) Pharmacological characterization of angiotensin II AT(2) receptor subtype heterogeneity in the rat adrenal cortex and medulla. *Endocrine* **3:** 255-261

Lunt SC, Haynes T, Perkins BD (2009) Zebrafish ift57, ift88, and ift172 intraflagellar transport mutants disrupt cilia but do not affect hedgehog signaling. *Dev Dyn* **238:** 1744-1759

Luo X, Ikeda Y, Parker KL (1994) A cell-specific nuclear receptor is essential for adrenal and gonadal development and sexual differentiation. *Cell* **77:** 481-490

Luo X, Ikeda Y, Schlosser DA, Parker KL (1995) Steroidogenic factor 1 is the essential transcript of the mouse Ftz-F1 gene. *Mol Endocrinol* **9:** 1233-1239

Lyons JP, Mueller UW, Ji H, Everett C, Fang X, Hsieh JC, Barth AM, McCrea PD (2004) Wnt-4 activates the canonical beta-catenin-mediated Wnt pathway and binds Frizzled-6 CRD: functional implications of Wnt/beta-catenin activity in kidney epithelial cells. *Exp Cell Res* **298:** 369-387

Löhr H, Hammerschmidt M (2011) Zebrafish in endocrine systems: recent advances and implications for human disease. *Annu Rev Physiol* **73:** 183-211

Ma R, Li WP, Rundle D, Kong J, Akbarali HI, Tsiokas L (2005) PKD2 functions as an epidermal growth factor-activated plasma membrane channel. *Mol Cell Biol* **25:** 8285-8298

Mandel H, Shemer R, Borochowitz ZU, Okopnik M, Knopf C, Indelman M, Drugan A, Tiosano D, Gershoni-Baruch R, Choder M, Sprecher E (2008) SERKAL syndrome: an

autosomal-recessive disorder caused by a loss-of-function mutation in WNT4. *Am J Hum Genet* **82:** 39-47

Marik PE (2007) Mechanisms and clinical consequences of critical illness associated adrenal insufficiency. *Current Opinion in Critical Care* **13:** 363-369

Marion V, Stoetzel C, Schlicht D, Messaddeq N, Koch M, Flori E, Danse JM, Mandel JL, Dollfus H (2009) Transient ciliogenesis involving Bardet-Biedl syndrome proteins is a fundamental characteristic of adipogenic differentiation. *Proc Natl Acad Sci U S A* **106:** 1820-1825

Marrone BL, Sebring RJ (1989) Quantitative cytochemistry of 3 beta-hydroxysteroid dehydrogenase activity in avian granulosa cells during follicular maturation. *Biol Reprod* **40:** 1007-1011

Marshall WF, Nonaka S (2006) Cilia: tuning in to the cell's antenna. *Curr Biol* **16:** R604-614

Mas C, Ruiz i Altaba A (2010) Small molecule modulation of HH-GLI signaling: current leads, trials and tribulations. *Biochem Pharmacol* **80:** 712-723

Matsui T, Raya A, Kawakami Y, Callol-Massot C, Capdevila J, Rodriguez-Esteban C, Izpisua Belmonte JC (2005) Noncanonical Wnt signaling regulates midline convergence of organ primordia during zebrafish development. *Genes Dev* **19:** 164-175

May SR, Ashique AM, Karlen M, Wang B, Shen Y, Zarbalis K, Reiter J, Ericson J, Peterson AS (2005) Loss of the retrograde motor for IFT disrupts localization of Smo to cilia and prevents the expression of both activator and repressor functions of Gli. *Dev Biol* **287:** 378-389

McCormick SD (2001) Endocrine Control of Osmoregulation in Teleost Fish. *American Zoologist* **41:** 781-794

McCormick SD, Regish A, O'Dea MF, Shrimpton JM (2008) Are we missing a mineralocorticoid in teleost fish? Effects of cortisol, deoxycorticosterone and aldosterone on osmoregulation, gill Na+,K+ -ATPase activity and isoform mRNA levels in Atlantic salmon. *Gen Comp Endocrinol* **157:** 35-40

McGonnell IM, Fowkes RC (2006) Fishing for gene function--endocrine modelling in the zebrafish. *J Endocrinol* **189:** 425-439

Meimaridou E, Kowalczyk J, Guasti L, Hughes CR, Wagner F, Frommolt P, Nurnberg P, Mann NP, Banerjee R, Saka HN, Chapple JP, King PJ, Clark AJL, Metherell LA (2012) Mutations in NNT encoding nicotinamide nucleotide transhydrogenase cause familial glucocorticoid deficiency. *Nat Genet* **44:** 740-742

Merchant AA, Matsui W (2010) Targeting Hedgehog--a cancer stem cell pathway. *Clin Cancer Res* **16:** 3130-3140

Mesiano S, Jaffe RB (1997) Developmental and functional biology of the primate fetal adrenal cortex. *Endocr Rev* **18:** 378-403

Mesiano S, Mellon SH, Jaffe RB (1993) Mitogenic action, regulation, and localization of insulin-like growth factors in the human fetal adrenal gland. *J Clin Endocrinol Metab* **76:** 968-976

Metherell LA, Chapple JP, Cooray S, David A, Becker C, Rüschendorf F, Naville D, Begeot M, Khoo B, Nürnberg P, Huebner A, Cheetham ME, Clark AJ (2005) Mutations in MRAP, encoding a new interacting partner of the ACTH receptor, cause familial glucocorticoid deficiency type 2. *Nat Genet* **37:** 166-170

Miller ED (1981) The role of the renin-angiotensin-aldosterone system in circulatory control and hypertension. *Br J Anaesth* **53:** 711-718

Miller WL, Auchus RJ, Geller DH (1997) The regulation of 17,20 lyase activity. *Steroids* **62:** 133-142

Mitani F, Mukai K, Miyamoto H, Suematsu M, Ishimura Y (1999) Development of functional zonation in the rat adrenal cortex. *Endocrinology* **140:** 3342-3353

Mitani F, Mukai K, Miyamoto H, Suematsu M, Ishimura Y (2003) The undifferentiated cell zone is a stem cell zone in adult rat adrenal cortex. *Biochim Biophys Acta* **1619:** 317-324

Mitani F, Suzuki H, Hata J, Ogishima T, Shimada H, Ishimura Y (1994) A novel cell layer without corticosteroid-synthesizing enzymes in rat adrenal cortex: histochemical detection and possible physiological role. *Endocrinology* **135:** 431-438

Mizusaki H, Kawabe K, Mukai T, Ariyoshi E, Kasahara M, Yoshioka H, Swain A, Morohashi K (2003) Dax-1 (dosage-sensitive sex reversal-adrenal hypoplasia congenita critical region on the X chromosome, gene 1) gene transcription is regulated by wnt4 in the female developing gonad. *Mol Endocrinol* **17:** 507-519

Moore AW, McInnes L, Kreidberg J, Hastie ND, Schedl A (1999) YAC complementation shows a requirement for Wt1 in the development of epicardium, adrenal gland and throughout nephrogenesis. *Development* **126:** 1845-1857

Morley SD, Viard I, Chung BC, Ikeda Y, Parker KL, Mullins JJ (1996) Variegated expression of a mouse steroid 21-hydroxylase/beta- galactosidase transgene suggests centripetal migration of adrenocortical cells. *Mol Endocrinol* **10:** 585-598

Mornet E, Dupont J, Vitek A, White PC (1989) Characterization of two genes encoding human steroid 11 beta-hydroxylase (P-450(11) beta). *J Biol Chem* **264:** 20961-20967

Morohashi K (1997) The ontogenesis of the steroidogenic tissues. *Genes Cells* **2:** 95-106

Mountjoy KG, Bird IM, Rainey WE, Cone RD (1994) ACTH induces up-regulation of ACTH receptor mRNA in mouse and human adrenocortical cell lines. *Molecular and Cellular Endocrinology* **99:** R17-R20

Mukherjee S, Frolova N, Sadlonova A, Novak Z, Steg A, Page GP, Welch DR, Lobo-Ruppert SM, Ruppert JM, Johnson MR, Frost AR (2006) Hedgehog signaling and response to cyclopamine differ in epithelial and stromal cells in benign breast and breast cancer. *Cancer Biol Ther* **5:** 674-683

Muscatelli F, Strom TM, Walker AP, Zanaria E, Recan D, Meindl A, Bardoni B, Guioli S, Zehetner G, Rabl W, et al. (1994) Mutations in the DAX-1 gene give rise to both X-linked adrenal hypoplasia congenita and hypogonadotropic hypogonadism. *Nature* **372:** 672-676

Mykytyn K, Mullins RF, Andrews M, Chiang AP, Swiderski RE, Yang B, Braun T, Casavant T, Stone EM, Sheffield VC (2004) Bardet-Biedl syndrome type 4 (BBS4)-null mice implicate Bbs4 in flagella formation but not global cilia assembly. *Proceedings of the National Academy of Sciences of the United States of America* **101:** 8664-8669

Nachury MV, Loktev AV, Zhang Q, Westlake CJ, Peränen J, Merdes A, Slusarski DC, Scheller RH, Bazan JF, Sheffield VC, Jackson PK (2007) A Core Complex of BBS Proteins Cooperates with the GTPase Rab8 to Promote Ciliary Membrane Biogenesis. *Cell* **129:** 1201-1213

Naka K, Hoshii T, Hirao A (2010) Novel therapeutic approach to eradicate tyrosine kinase inhibitor resistant chronic myeloid leukemia stem cells. *Cancer Sci* **101:** 1577-1581

Nandi JB-E (1962) *The Structure of the Interrenal Gland in Teleost Fishes. [With illustrations.]*: University of California Press: Berkeley & Los Angeles.

Naruse M, Tanabe A, Sugaya T, Naruse K, Yoshimoto T, Seki T, Imaki T, Demura R, Murakami K, Demura H (1998) Deferential roles of angiotensin receptor subtypes in adrenocortical function in mice. *Life Sci* **63:** 1593-1598

Nie L, Wu G, Zhang W (2006) Correlation between mRNA and protein abundance in Desulfovibrio vulgaris: A multiple regression to identify sources of variations. *Biochemical and Biophysical Research Communications* **339:** 603-610

Nikoshkov A, Falorni A, Lajic S, Laureti S, Wedell A, Lernmark K, Luthman H (1999) A conformation-dependent epitope in Addison's disease and other endocrinological

autoimmune diseases maps to a carboxyl-terminal functional domain of human steroid 21-hydroxylase. *J Immunol* **162:** 2422-2426

Ninkovic J, Stigloher C, Lillesaar C, Bally-Cuif L (2008) Gsk3beta/PKA and Gli1 regulate the maintenance of neural progenitors at the midbrain-hindbrain boundary in concert with E(Spl) factor activity. *Development* **135:** 3137-3148

Nishimura DY, Fath M, Mullins RF, Searby C, Andrews M, Davis R, Andorf JL, Mykytyn K, Swiderski RE, Yang B, Carmi R, Stone EM, Sheffield VC (2004) Bbs2-null mice have neurosensory deficits, a defect in social dominance, and retinopathy associated with mislocalization of rhodopsin. *Proc Natl Acad Sci U S A* **101:** 16588-16593

Nusslein-Volhard C, Wieschaus E (1980) Mutations affecting segment number and polarity in Drosophila. *Nature* **287:** 795-801

Ogishima T, Suzuki H, Hata J, Mitani F, Ishimura Y (1992) Zone-specific expression of aldosterone synthase cytochrome P-450 and cytochrome P-45011 beta in rat adrenal cortex: histochemical basis for the functional zonation. *Endocrinology* **130:** 2971-2977

Oparil S, Sanders CA, Haber E (1970) In-vivo and in-vitro conversion of angiotensin I to angiotensin II in dog blood. *Circ Res* **26:** 591-599

Oskarsson A, Ulleras E, Plant KE, Hinson JP, Goldfarb PS (2006) Steroidogenic gene expression in H295R cells and the human adrenal gland: adrenotoxic effects of lindane in vitro. *J Appl Toxicol* **26:** 484-492

Pan Y, Bai CB, Joyner AL, Wang B (2006) Sonic hedgehog signaling regulates Gli2 transcriptional activity by suppressing its processing and degradation. *Mol Cell Biol* **26:** 3365-3377

Pan Y, Wang B (2007) A Novel Protein-processing Domain in Gli2 and Gli3 Differentially Blocks Complete Protein Degradation by the Proteasome. *J Biol Chem* **282:** 10846-10852

Pandey AV, Miller WL (2005) Regulation of 17,20 lyase activity by cytochrome b5 and by serine phosphorylation of P450c17. *J Biol Chem* **280:** 13265-13271

Parker KL, Chaplin DD, Wong M, Seidman JG, Smith JA, Schimmer BP (1985) Expression of murine 21-hydroxylase in mouse adrenal glands and in transfected Y1 adrenocortical tumor cells. *Proc Natl Acad Sci U S A* **82:** 7860-7864

Parmar J, Key RE, Rainey WE (2008) Development of an Adrenocorticotropin-Responsive Human Adrenocortical Carcinoma Cell Line. *J Clin Endocrinol Metab* **93:** 4542-4546

Parviainen H, Kiiveri S, Bielinska M, Rahman N, Huhtaniemi IT, Wilson DB, Heikinheimo M (2007) GATA transcription factors in adrenal development and tumors. *Mol Cell Endocrinol* **265-266:** 17-22

Pascal LE, True LD, Campbell DS, Deutsch EW, Risk M, Coleman IM, Eichner LJ, Nelson PS, Liu AY (2008) Correlation of mRNA and protein levels: cell type-specific gene expression of cluster designation antigens in the prostate. *BMC Genomics* **9:** 246

Pazour GJ, Dickert BL, Vucica Y, Seeley ES, Rosenbaum JL, Witman GB, Cole DG (2000) Chlamydomonas IFT88 and its mouse homologue, polycystic kidney disease gene tg737, are required for assembly of cilia and flagella. *J Cell Biol* **151:** 709-718

Peacock CD, Wang Q, Gesell GS, Corcoran-Schwartz IM, Jones E, Kim J, Devereux WL, Rhodes JT, Huff CA, Beachy PA, Watkins DN, Matsui W (2007) Hedgehog signaling maintains a tumor stem cell compartment in multiple myeloma. *Proc Natl Acad Sci U S A* **104:** 4048-4053

Perrone RD, Bengele HH, Alexander EA (1986) Sodium retention after adrenal enucleation. *Am J Physiol* **250:** E1-12

Pezzi V, Clyne CD, Ando S, Mathis JM, Rainey WE (1997) Ca(2+)-regulated expression of aldosterone synthase is mediated by calmodulin and calmodulin-dependent protein kinases. *Endocrinology* **138:** 835-838

Phelan JK, McCabe ERB (2001) Mutations in NR0B1 (DAX1) and NR5A1 (SF1) responsible for adrenal hypoplasia congenita. *Human Mutation* **18:** 472-487

Pierson RW, Jr. (1967) Metabolism of steroid hormones in adrenal cortex tumor cultures. *Endocrinology* **81:** 693-707

Porter JA, Young KE, Beachy PA (1996) Cholesterol modification of hedgehog signaling proteins in animal development. *Science* **274:** 255-259

Rainey WE, Carr BR, Sasano H, Suzuki T, Mason JI (2002) Dissecting human adrenal androgen production. *Trends Endocrinol Metab* **13:** 234-239

Rainey WE, Saner K, Schimmer BP (2004) Adrenocortical cell lines. *Mol Cell Endocrinol* **228:** 23-38

Reid SG, Fritsche R, Jönsson AC (1995) Immunohistochemical localization of bioactive peptides and amines associated with the chromaffin tissue of five species of fish. *Cell Tissue Res* **280:** 499-512

Reincke M, Karl M, Travis WH, Mastorakos G, Allolio B, Linehan HM, Chrousos GP (1994) p53 mutations in human adrenocortical neoplasms: immunohistochemical and molecular studies. *J Clin Endocrinol Metab* **78:** 790-794

Rhen T, Cidlowski JA (2005) Antiinflammatory action of glucocorticoids--new mechanisms for old drugs. *N Engl J Med* **353:** 1711-1723

Rogerson FM, Fuller PJ (2000) Mineralocorticoid action. *Steroids* **65:** 61-73

Rohatgi R, Milenkovic L, Scott MP (2007) Patched1 Regulates Hedgehog Signaling at the Primary Cilium. *Science* **317:** 372-376

Rohatgi R, Scott MP (2007) Patching the gaps in Hedgehog signalling. *Nat Cell Biol* **9:** 1005-1009

Ross AJ, May-Simera H, Eichers ER, Kai M, Hill J, Jagger DJ, Leitch CC, Chapple JP, Munro PM, Fisher S, Tan PL, Phillips HM, Leroux MR, Henderson DJ, Murdoch JN, Copp AJ, Eliot MM, Lupski JR, Kemp DT, Dollfus H, Tada M, Katsanis N, Forge A, Beales PL (2005) Disruption of Bardet-Biedl syndrome ciliary proteins perturbs planar cell polarity in vertebrates. *Nat Genet* **37:** 1135-1140

Roy S (2012) Cilia and Hedgehog: when and how was their marriage solemnized? *Differentiation* **83:** S43-48

Ruiz i Altaba A, Mas C, Stecca B (2007) The Gli code: an information nexus regulating cell fate, stemness and cancer. *Trends Cell Biol* **17:** 438-447

Rupprecht R, Arriza JL, Spengler D, Reul JM, Evans RM, Holsboer F, Damm K (1993) Transactivation and synergistic properties of the mineralocorticoid receptor: relationship to the glucocorticoid receptor. *Mol Endocrinol* **7:** 597-603

Sack OW (1963) Floating-Out Technics for Rapid Placement of Ribbons of Serial Sections on Slides. *Biotechnic and Histochemistry* **38:** 315 - 320

Sadovsky Y, Crawford PA, Woodson KG, Polish JA, Clements MA, Tourtellotte LM, Simburger K, Milbrandt J (1995) Mice deficient in the orphan receptor steroidogenic factor 1 lack adrenal glands and gonads but express P450 side-chain-cleavage enzyme in the placenta and have normal embryonic serum levels of corticosteroids. *Proc Natl Acad Sci U S A* **92:** 10939-10943

Sakaue M, Hoffman BB (1991) Glucocorticoids induce transcription and expression of the alpha 1B adrenergic receptor gene in DTT1 MF-2 smooth muscle cells. *J Clin Invest* **88:** 385-389

Salmon TN, Zwemer RL (1941) A study of the life history of cortico-adrenal gland cells of the rat by means of trypan blue injections. *The Anatomical Record* **80:** 421-429

Samandari E, Kempna P, Nuoffer J-M, Hofer G, Mullis PE, Fluck CE (2007) Human adrenal corticocarcinoma NCI-H295R cells produce more androgens than NCI-H295A

cells and differ in 3{beta}-hydroxysteroid dehydrogenase type 2 and 17,20 lyase activities. *J Endocrinol* **195:** 459-472

Santos N, Reiter JF (2008) Building it up and taking it down: the regulation of vertebrate ciliogenesis. *Dev Dyn* **237:** 1972-1981

Sapolsky RM (2000) Stress hormones: good and bad. *Neurobiol Dis* **7:** 540-542

Sapolsky RM, Romero LM, Munck AU (2000) How do glucocorticoids influence stress responses? Integrating permissive, suppressive, stimulatory, and preparative actions. *Endocr Rev* **21:** 55-89

Sasaki H, Hui C, Nakafuku M, Kondoh H (1997) A binding site for Gli proteins is essential for HNF-3beta floor plate enhancer activity in transgenics and can respond to Shh in vitro. *Development* **124:** 1313-1322

Satir P, Christensen ST (2007) Overview of Structure and Function of Mammalian Cilia. *Annual Review of Physiology* **69:** 377-400

Schneider L, Cammer M, Lehman J, Nielsen SK, Guerra CF, Veland IR, Stock C, Hoffmann EK, Yoder BK, Schwab A, Satir P, Christensen ST (2010) Directional cell migration and chemotaxis in wound healing response to PDGF-AA are coordinated by the primary cilium in fibroblasts. *Cell Physiol Biochem* **25:** 279-292

Schneider L, Clement CA, Teilmann SC, Pazour GJ, Hoffmann EK, Satir P, Christensen ST (2005) PDGFRalphaalpha signaling is regulated through the primary cilium in fibroblasts. *Curr Biol* **15:** 1861-1866

Scornik OA, Paladini AC (1964) Angiotensin Blood Levels in Hemorrhagic Hypotension and Other Related Conditions. *Am J Physiol* **206:** 553-556

Scriver CR (1995) *The metabolic and molecular bases of inherited disease*, 7th ed. edn. New York ; London: McGraw-Hill, Health Professions Division.

Seckl JR, Walker BR (2001) Minireview: 11beta-hydroxysteroid dehydrogenase type 1- a tissue-specific amplifier of glucocorticoid action. *Endocrinology* **142:** 1371-1376

Selye H (1998) A Syndrome Produced by Diverse Nocuous Agents. *J Neuropsychiatry Clin Neurosci* **10:** 230a-231

Sen Gupta P, Prodromou NV, Chapple JP (2009) Can faulty antennae increase adiposity? The link between cilia proteins and obesity. *J Endocrinol* **203:** 327-336

Simon DP, Hammer GD (2012) Adrenocortical stem and progenitor cells: Implications for adrenocortical carcinoma. *Molecular and Cellular Endocrinology* **351:** 2-11

Simons M, Gloy J, Ganner A, Bullerkotte A, Bashkurov M, Kronig C, Schermer B, Benzing T, Cabello OA, Jenny A, Mlodzik M, Polok B, Driever W, Obara T, Walz G (2005) Inversin, the gene product mutated in nephronophthisis type II, functions as a molecular switch between Wnt signaling pathways. *Nat Genet* **37:** 537-543

Simpson E, Lauber M, Demeter M, Means G, Mahendroo M, Kilgore M, Mendelson C, Waterman M (1992) Regulation of expression of the genes encoding steroidogenic enzymes in the ovary. *J Steroid Biochem Mol Biol* **41:** 409-413

Sinars CR, Cheung-Flynn J, Rimerman RA, Scammell JG, Smith DF, Clardy J (2003) Structure of the large FK506-binding protein FKBP51, an Hsp90-binding protein and a component of steroid receptor complexes. *Proc Natl Acad Sci U S A* **100:** 868-873

Singla V, Reiter JF (2006) The primary cilium as the cell's antenna: signaling at a sensory organelle. *Science* **313:** 629-633

Sinha S, Chen JK (2006) Purmorphamine activates the Hedgehog pathway by targeting Smoothened. *Nat Chem Biol* **2:** 29-30

Skelton FR (1959) Adrenal regeneration and adrenal-regeneration hypertension. *Physiol Rev* **39:** 162-182

Staels B, Hum DW, Miller WL (1993) Regulation of steroidogenesis in NCI-H295 cells: a cellular model of the human fetal adrenal. *Mol Endocrinol* **7:** 423-433

Stone DM, Hynes M, Armanini M, Swanson TA, Gu Q, Johnson RL, Scott MP, Pennica D, Goddard A, Phillips H, Noll M, Hooper JE, de Sauvage F, Rosenthal A (1996) The tumour-suppressor gene patched encodes a candidate receptor for Sonic hedgehog. *Nature* **384:** 129-134

Taipale J, Chen JK, Cooper MK, Wang B, Mann RK, Milenkovic L, Scott MP, Beachy PA (2000) Effects of oncogenic mutations in Smoothened and Patched can be reversed by cyclopamine. *Nature* **406:** 1005-1009

Taipale J, Cooper MK, Maiti T, Beachy PA (2002) Patched acts catalytically to suppress the activity of Smoothened. *Nature* **418:** 892-896

Tanabe A, Naruse M, Arai K, Naruse K, Yoshimoto T, Seki T, Imaki T, Miyazaki H, Zeng ZP, Demura R, Demura H (1998) Gene expression and roles of angiotensin II type 1 and type 2 receptors in human adrenals. *Horm Metab Res* **30:** 490-495

Tao YJ, Zheng W (2011) Chaperones and the maturation of steroid hormone receptor complexes. *Oncotarget* **2:** 104-106

Tayeh MK, Yen HJ, Beck JS, Searby CC, Westfall TA, Griesbach H, Sheffield VC, Slusarski DC (2008) Genetic interaction between Bardet-Biedl syndrome genes and implications for limb patterning. *Hum Mol Genet* **17:** 1956-1967

Tempe D, Casas M, Karaz S, Blanchet-Tournier M-F, Concordet J-P (2006) Multisite Protein Kinase A and Glycogen Synthase Kinase 3{beta} Phosphorylation Leads to Gli3 Ubiquitination by SCF{beta}TrCP. *Mol Cell Biol* **26:** 4316-4326

Thomas M, Yang L, Hornsby PJ (2000) Formation of functional tissue from transplanted adrenocortical cells expressing telomerase reverse transcriptase. *Nat Biotechnol* **18:** 39-42

To TT, Hahner S, Nica G, Rohr KB, Hammerschmidt M, Winkler C, Allolio B (2007) Pituitary-Interrenal Interaction in Zebrafish Interrenal Organ Development. *Molecular Endocrinology* **21:** 472-485

Tobian L, Tomboulian A, Janecek J (1959) The effect of high perfusion pressures on the granulation of juxtaglomerular cells in an isolated kidney. *J Clin Invest* **38:** 605-610

Tobin JL, Beales PL (2007) Bardet-Biedl syndrome: beyond the cilium. *Pediatr Nephrol* **22:** 926-936

Tobin JL, Di Franco M, Eichers E, May-Simera H, Garcia M, Yan J, Quinlan R, Justice MJ, Hennekam RC, Briscoe J, Tada M, Mayor R, Burns AJ, Lupski JR, Hammond P, Beales PL (2008) Inhibition of neural crest migration underlies craniofacial dysmorphology and Hirschsprung's disease in Bardet-Biedl syndrome. *Proc Natl Acad Sci U S A* **105:** 6714-6719

Tobin JLP, Beales PLBMDF (2009) The nonmotile ciliopathies. *Genetics in Medicine* **11:** 386-402

Tremblay JJ, Viger RS (2003) Novel roles for GATA transcription factors in the regulation of steroidogenesis. *J Steroid Biochem Mol Biol* **85:** 291-298

Vainio SJ, Uusitalo MS (2000) A road to kidney tubules via the Wnt pathway. *Pediatr Nephrol* **15:** 151-156

Val P, Martinez-Barbera J-P, Swain A (2007) Adrenal development is initiated by Cited2 and Wt1 through modulation of Sf-1 dosage. *Development* **134:** 2349-2358

Van de Kar LD, Blair ML (1999) Forebrain pathways mediating stress-induced hormone secretion. *Front Neuroendocrinol* **20:** 1-48

Varnat F, Duquet A, Malerba M, Zbinden M, Mas C, Gervaz P, Ruiz i Altaba A (2009) Human colon cancer epithelial cells harbour active HEDGEHOG-GLI signalling that is

essential for tumour growth, recurrence, metastasis and stem cell survival and expansion. *EMBO Mol Med* **1:** 338-351

Viger RS, Mertineit C, Trasler JM, Nemer M (1998) Transcription factor GATA-4 is expressed in a sexually dimorphic pattern during mouse gonadal development and is a potent activator of the Mullerian inhibiting substance promoter. *Development* **125:** 2665-2675

Vinson GP (2003) Adrenocortical zonation and ACTH. *Microsc Res Tech* **61:** 227-239

Vokes SA, Ji H, McCuine S, Tenzen T, Giles S, Zhong S, Longabaugh WJ, Davidson EH, Wong WH, McMahon AP (2007) Genomic characterization of Gli-activator targets in sonic hedgehog-mediated neural patterning. *Development* **134:** 1977-1989

von Hofsten J, Larsson A, Olsson PE (2005) Novel steroidogenic factor-1 homolog (ff1d) is coexpressed with anti-Mullerian hormone (AMH) in zebrafish. *Dev Dyn* **233:** 595-604

Vortkamp A, Lee K, Lanske B, Segre GV, Kronenberg HM, Tabin CJ (1996) Regulation of rate of cartilage differentiation by Indian hedgehog and PTH-related protein. *Science* **273:** 613-622

Wake DJ, Strand M, Rask E, Westerbacka J, Livingstone DE, Soderberg S, Andrew R, Yki-Jarvinen H, Olsson T, Walker BR (2007) Intra-adipose sex steroid metabolism and body fat distribution in idiopathic human obesity. *Clin Endocrinol (Oxf)* **66:** 440-446

Wang B, Li Y (2006) Evidence for the direct involvement of Î²TrCP in Gli3 protein processing. *Proceedings of the National Academy of Sciences of the United States of America* **103:** 33-38

Wang T, Rainey WE (2012) Human adrenocortical carcinoma cell lines. *Mol Cell Endocrinol* **351:** 58-65

Wang Y (2009) Wnt/Planar cell polarity signaling: A new paradigm for cancer therapy. *Molecular Cancer Therapeutics* **8:** 2103-2109

Wang Y, Zhou Z, Walsh CT, McMahon AP (2009) Selective translocation of intracellular Smoothened to the primary cilium in response to Hedgehog pathway modulation. *Proceedings of the National Academy of Sciences* **106:** 2623-2628

Warnecke C, Sürder D, Curth R, Fleck E, Regitz-Zagrosek V (1999) Analysis and functional characterization of alternatively spliced angiotensin II type 1 and 2 receptor transcripts in the human heart. *Journal of Molecular Medicine* **77:** 718-727

Wehling M, Spes CH, Win N, Janson CP, Schmidt BM, Theisen K, Christ M (1998) Rapid cardiovascular action of aldosterone in man. *J Clin Endocrinol Metab* **83:** 3517-3522

Wendelaar Bonga SE (1997) The stress response in fish. *Physiol Rev* **77:** 591-625

Westfall TA, Brimeyer R, Twedt J, Gladon J, Olberding A, Furutani-Seiki M, Slusarski DC (2003) Wnt-5/pipetail functions in vertebrate axis formation as a negative regulator of Wnt/Î²-catenin activity. *The Journal of Cell Biology* **162:** 889-898

Wheeler R. (2010) Haemocytometer Grid. Vol. 2010.

White PC, Speiser PW (2000) Congenital Adrenal Hyperplasia due to 21-Hydroxylase Deficiency. *Endocrine Reviews* **21:** 245-291

Wilson CW, Chen MH, Chuang PT (2009) Smoothened adopts multiple active and inactive conformations capable of trafficking to the primary cilium. *PLoS ONE* **4:** e5182

Wojcikiewicz R, Nahorski S (1993) Modulation of signalling initiated by phosphoinositidase-C-linked receptors. *J Exp Biol* **184:** 145-159

Wolpert L (2007) *Principles of development*, 3rd ed. edn. Oxford: Oxford University Press.

Wu X, Ding S, Ding Q, Gray NS, Schultz PG (2002) A Small Molecule with Osteogenesis-Inducing Activity in Multipotent Mesenchymal Progenitor Cells. *Journal of the American Chemical Society* **124:** 14520-14521

Wu Y, Dai XQ, Li Q, Chen CX, Mai W, Hussain Z, Long W, Montalbetti N, Li G, Glynne R, Wang S, Cantiello HF, Wu G, Chen XZ (2006) Kinesin-2 mediates physical and functional interactions between polycystin-2 and fibrocystin. *Hum Mol Genet* **15:** 3280-3292

Yaguchi H, Tsutsumi K, Shimono K, Omura M, Sasano H, Nishikawa T (1998) Involvement of high density lipoprotein as substrate cholesterol for steroidogenesis by bovine adrenal fasciculo-reticularis cells. *Life Sci* **62:** 1387-1395

Yasumura Y, Buonassisi V, Sato G (1966) Clonal analysis of differentiated function in animal cell cultures. I. Possible correlated maintenance of differentiated function and the diploid karyotype. *Cancer Res* **26:** 529-535

Yaswen L, Diehl N, Brennan MB, Hochgeschwender U (1999) Obesity in the mouse model of pro-opiomelanocortin deficiency responds to peripheral melanocortin. *Nat Med* **5:** 1066-1070

Yauch RL, Dijkgraaf GJ, Alicke B, Januario T, Ahn CP, Holcomb T, Pujara K, Stinson J, Callahan CA, Tang T, Bazan JF, Kan Z, Seshagiri S, Hann CL, Gould SE, Low JA, Rudin CM, de Sauvage FJ (2009) Smoothened mutation confers resistance to a Hedgehog pathway inhibitor in medulloblastoma. *Science* **326:** 572-574

Yen H-J, Tayeh MK, Mullins RF, Stone EM, Sheffield VC, Slusarski DC (2006) Bardetâ€“Biedl syndrome genes are important in retrograde intracellular trafficking and Kupffer's vesicle cilia function. *Human Molecular Genetics* **15:** 667-677

Yu RN, Ito M, Jameson JL (1998) The murine Dax-1 promoter is stimulated by SF-1 (steroidogenic factor-1) and inhibited by COUP-TF (chicken ovalbumin upstream promoter-transcription factor) via a composite nuclear receptor-regulatory element. *Mol Endocrinol* **12:** 1010-1022

Yue S, Chen Y, Cheng SY (2008) Hedgehog signaling promotes the degradation of tumor suppressor Sufu through the ubiquitin-proteasome pathway. *Oncogene* **28:** 492-499

Zajicek G, Ariel I, Arber N (1986) The streaming adrenal cortex: direct evidence of centripetal migration of adrenocytes by estimation of cell turnover rate. *J Endocrinol* **111:** 477-482

Zanaria E, Muscatelli F, Bardoni B, Strom TM, Guioli S, Guo W, Lalli E, Moser C, Walker AP, McCabe ER (1994) An unusual member of the nuclear hormone receptor superfamily responsible for X-linked adrenal hypoplasia congenita. *Nature* **372:** 635-641

Zeng X, Goetz JA, Suber LM, Scott WJ, Schreiner CM, Robbins DJ (2001) A freely diffusible form of Sonic hedgehog mediates long-range signalling. *Nature* **411:** 716-720

Zhang J, Pratt RE (1996) The AT2 receptor selectively associates with Gialpha2 and Gialpha3 in the rat fetus. *J Biol Chem* **271:** 15026-15033

Zhang Q, Seo S, Bugge K, Stone EM, Sheffield VC (2012) BBS proteins interact genetically with the IFT pathway to influence SHH related phenotypes. *Hum Mol Genet*

Zhang YH, Guo W, Wagner RL, Huang BL, McCabe L, Vilain E, Burris TP, Anyane-Yeboa K, Burghes AH, Chitayat D, Chudley AE, Genel M, Gertner JM, Klingensmith GJ, Levine SN, Nakamoto J, New MI, Pagon RA, Pappas JG, Quigley CA, Rosenthal IM, Baxter JD, Fletterick RJ, McCabe ER (1998) DAX1 mutations map to putative structural domains in a deduced three-dimensional model. *Am J Hum Genet* **62:** 855-864

Zhao C, Chen A, Jamieson CH, Fereshteh M, Abrahamsson A, Blum J, Kwon HY, Kim J, Chute JP, Rizzieri D, Munchhof M, VanArsdale T, Beachy PA, Reya T (2009) Hedgehog signalling is essential for maintenance of cancer stem cells in myeloid leukaemia. *Nature* **458:** 776-779

Zhao Y, Tong C, Jiang J (2007) Hedgehog regulates smoothened activity by inducing a conformational switch. *Nature* **450:** 252-258

Zhao Y, Yang Z, Phelan JK, Wheeler DA, Lin S, McCabe ERB (2006) Zebrafish dax1 Is Required for Development of the Interrenal Organ, the Adrenal Cortex Equivalent. *Mol Endocrinol* **20:** 2630-2640

Zhou J, Ruan L, Li H, Wang Q, Zheng F, Wu F (2009) Addison's disease with pituitary hyperplasia: a case report and review of the literature. *Endocrine* **35:** 285-289

Zhou Z, Cironi P, Lin AJ, Xu Y, Hrvatin Sa, Golan DE, Silver PA, Walsh CT, Yin J (2007) Genetically Encoded Short Peptide Tags for Orthogonal Protein Labeling by Sfp and AcpS Phosphopantetheinyl Transferases. *ACS Chemical Biology* **2:** 337-346

LIST OF SUPPLIERS

Abcam	330 Cambridge Science Park, Cambridge CB4 0FL
Abnova	Boxbergring 107, 69126 Heidelberg, Germany
Ambion	Life Technologies, 3 Fountain Drive, Inchinnan Business Park, Paisley PA4 9RF
Applied Biosystems	Life Technologies, 3 Fountain Drive, Inchinnan Business Park, Paisley PA4 9RF
BDH Chemical	Merck Services, Wilberforce Court Alfred, Gelder Street, Hull, East Yorkshire HU1 1UY
Biosepra	Clarendon House, 125 Shenley Rd, Borehamwood, Hertfordshire WD6 1AG
Calbiochem	Merck Chemicals, Boulevard Industrial Park, Padge Road, Beeston, Nottingham NG9 2JR
Dako	Cambridge House, St Thomas Place, Ely, Cambridgeshire CB7 4EX
Demeditec Diagnostics	Lise-Meitner-Str. 2 24145 Kiel, Germany
Enzo Life Sciences	Palatine House, Matford Court, Exeter EX2 8NL
Eurogentec	Old Headmasters House, Unit 1, Building 1, Forest Business Centre, Fawley Road, Fawley, Southampton SO45 1FJ
Fermentas	Opelstrasse 9, 68789 St. Leon-Rot, Germany
Fisher Scientific	Bishop Meadow Road, Loughborough LE11 5RG
Fluka Biochemika	Sigma-Aldrich Company, The Old Brickyard, New Road, Gillingham, Dorset SP8 4XT
Gene Tools, LLC	1001 Summerton Way, Philomath, OR 97370 USA
Gibco	Life Technologies, 3 Fountain Drive, Inchinnan Business Park, Paisley PA4 9RF
Greiner Bio-One	Brunel Way, Stroudwater Business Park, Stonehouse GL10 3SX
Invitrogen	Life Technologies, 3 Fountain Drive, Inchinnan Business Park, Paisley PA4 9RF
Jackson ImmunoResearch	Unit 7, Acorn Business Centre, Oaks Drive, Newmarket, Suffolk CB8 7SY
Kapa Biosystems	Anachem House, 1 & 2 Titan Court, Laporte Way, Bedfordshire LU4 8EF
Lamb Laboratories	Fisher Scientific, Bishop Meadow Road, Loughborough LE11 5RG
LC Laboratories	165 New Boston Street, Woburn, MA 01801
Licor	St. John's Innovation Centre, Cowley Road, Cambridge CB4 0WS
Millipore	Suite 3 & 5, Building 6, Croxley Green Business Park, Watford WD18 8YH

National Diagnostics	Unit 4 Fleet Business Park, East Riding of Yorkshire, Itilngs Lane, Hessle HU13 9LX
Promega	Delta House, Southampton Science Park, Southampton SO16 7NS
ProteinTech Group	Manchester Science Park, Kilburn House, Lloyd Street North, Manchester M15 6SE
Qiagen	Fleming Way, Crawley, West Sussex RH10 9NQ
R&D Systems	19 Barton Lane, Abingdon Science Park, Arbingdon OX14 3NB
Santa Cruz Biotechnology	Bergheimer Str. 89-2, 69115 Heidelberg, Germany
Sigma-Aldrich	The Old Brickyard, New Road, Gillingham, Dorset SP8 4XT
Tocris Bioscience	R&D Systems, 19 Barton Lane, Abingdon Science Park, Arbington OX14 3NB
Vector Laboratories	3, Accent Park, Bakewell Road, Orton Southgate, Peterborough PE2 6XS
VWR	Hunter Boulevard, Magna Park, Lutterworth, Leicestershire LE17 4XN